

# Quantum entanglement in de Sitter space from Stringy Axion: An analysis using $\alpha$ vacua

Sayantana Choudhury,<sup>1a,b</sup> Sudhakar Panda<sup>c,d,e</sup>

<sup>a</sup>Quantum Gravity and Unified Theory and Theoretical Cosmology Group, Max Planck Institute for Gravitational Physics (Albert Einstein Institute), Am Mühlenberg 1, 14476 Potsdam-Golm, Germany.

<sup>b</sup>Inter-University Centre for Astronomy and Astrophysics, Post Bag 4, Ganeshkhind, Pune 411007, India.

<sup>c</sup>Institute of Physics, Sachivalaya Marg, Bhubaneswar, Odisha - 751005, India.

<sup>d</sup>National Institute of Science Education and Research, Jatni, Bhubaneswar, Odisha - 752050, India.

<sup>e</sup>Homi Bhabha National Institute, Training School Complex, Anushakti Nagar, Mumbai-400085, India.

E-mail: [sayantana@aei.mpg.de](mailto:sayantana@aei.mpg.de), [sayantana.choudhury@aei.mpg.de](mailto:sayantana.choudhury@aei.mpg.de),  
[panda@iopb.res.in](mailto:panda@iopb.res.in)

**ABSTRACT:** In this work, we study the phenomena of quantum entanglement by computing de Sitter entanglement entropy from von Neumann measure. For this purpose we consider a bipartite quantum field theoretic setup in presence of axion originating from **Type II B** string theory. We consider the initial vacuum to be CPT invariant non-adiabatic  $\alpha$  vacua state under **SO(1,4)** isometry, which is characterized by a real one-parameter family. To implement this technique we use a **S<sup>2</sup>** which divide the de Sitter into two exterior and interior sub-regions. First, we derive the wave function of axion in an open chart for  $\alpha$  vacua by applying Bogoliubov transformation on the solution for Bunch-Davies vacuum state. Further, we quantify the density matrix by tracing over the contribution from the exterior region. Using this result we derive entanglement entropy, Rényi entropy and explain the long-range quantum effects in primordial cosmological correlations. We also provide a comparison between the results obtained from Bunch-Davies vacuum and the generalized  $\alpha$  vacua, which implies that the amount of quantum entanglement and the long-range effects are larger for non zero value of the parameter  $\alpha$ . Most significantly, our derived results for  $\alpha$  vacua provides the necessary condition for generating non zero entanglement entropy in primordial cosmology.

**KEYWORDS:** De-Sitter space,  $\alpha$  vacua, Quantum Entanglement, Cosmology of Theories beyond the SM, Axion, String Cosmology.

<sup>1</sup>Alternative E-mail: [sayanphysicsisi@gmail.com](mailto:sayanphysicsisi@gmail.com).

---

## Contents

<b>1</b>	<b>Introduction</b>	<b>1</b>
<b>2</b>	<b>Basic setup: Brief review</b>	<b>5</b>
<b>3</b>	<b>Quantum entanglement for axionic pair using <math>\alpha</math> vacua</b>	<b>6</b>
3.1	Wave function of axion in open chart	6
3.1.1	Model for axion effective potential	6
3.1.2	Wave function for Axion using Bunch Davies vacuum	7
3.1.3	Wave function for Axion using $\alpha$ vacua	8
3.2	Construction of density matrix using $\alpha$ vacua	24
3.3	Computation of entanglement entropy using $\alpha$ vacua	35
3.4	Computation of Rényi entropy using $\alpha$ vacua	47
<b>4</b>	<b>Summary</b>	<b>63</b>

---

## 1 Introduction

It is well accepted fact that von Neumann entropy is a measure of quantum entanglement to quantify long range correlation in condensed matter physics [1–3] and cosmology [4–21]. In condensed matter physics entanglement entropy exactly mimics the role of an order parameter and the corresponding phase transition phenomena can be characterized by correlation in quantum level. On the other hand in cosmology entanglement entropy is acting as a key ingredient to understand role of the quantum mechanics in observed correlations through hot and cold spots in Cosmic Microwave Background (CMB) maps. Also it is expected from the theoretical background that from this understanding of long range effects in quantum mechanical correlations one can able to understand the underlying physics of the theory of multiverse, bubble nucleation etc in de sitter space [22]. As a consequence a prompt response one may observe due to the local measurement in quantum mechanical theory by violating causal structure of the space-time. In quantum theory such causality violation is known as Einstein-Podolsky-Rosen (EPR) paradox [23]. But in such type of local measurement practically causality remains unaffected as the required quantum information (in the form of qubits) are not propagating. In this connection Schwinger effect in de Sitter space [24, 25] is one of the prominent examples of quantum entanglement. In Schwinger effect particle pair creation takes place with a finite separation in de Sitter space-time in presence of a constant electric field [15] and the quantum states show long range correlation.

To quantify entanglement entropy in the context of quantum field theory one need to have a bipartite system, which is not a straightforward computation. For strong coupling regime of a quantum field theory using the principles of gauge gravity duality in the bulk it is possible to compute entanglement entropy [26–35], which is till now treated as a remarkable result in this literature. Using this technique later various works have been done in the context of holographic entanglement entropy. Further, in ref. [10] the authors have constructed a completely different

computational algorithm to quantify entanglement entropy using Bunch Davies initial state <sup>1</sup> in de Sitter space-time. After that in ref. [15] the authors have extended the computation of entanglement entropy using  $\alpha$  vacua initial state in de Sitter space by following the techniques presented in ref. [10]. Next, using this prescribed technique in presence of a linear source term in the effective action we have computed entanglement entropy for stringy axion using the same Bunch Davies initial state in de Sitter space [14]. We have shown that this result for axion compliments the necessary condition for the violation of Bell's inequality in primordial cosmology.

In quantum field theory of de Sitter curved background one can further introduce CPT invariant under  $\mathbf{SO}(1, 4)$  isometry group one parameter infinite family of initial vacuum states [36, 37]. These class of non-thermal states are characterized by the real parameter  $\alpha$ , known as  $\alpha$  vacua. For  $\alpha = 0$  one can get back the usual Bunch Davies vacuum state for  $\Lambda \neq 0$  ( $\Lambda > 0$  for de Sitter and  $\Lambda < 0$  for anti de Sitter) and flat Minkowski vacuum for  $\Lambda = 0$  <sup>2</sup>. In a more technical ground the  $\alpha$  vacua can be treated a squeezed quantum state, which are created by an unitary operator acting the Bunch Davies vacuum state. This leads to the generalization of Wick's theorem in interacting quantum field theory, which allows us to describe any free quantum field theory Green's function computed in presence of  $\alpha$  vacua in terms of the products of the Green's functions computed from Bunch davies vacuum [38]. See other refs. [37, 39, 40] for more details on the quantum field theory of  $\alpha$  vacua. For a specified  $\alpha$  vacuum state as an quantum initial condition it is possible to describe the long range correlations within the framework of quantum field theory. As a consequence the non-local quantum phenomena can be associated with the long range effects, which is described by quantum entanglement of vacuum state provided as an initial condition. It is important to mention that, till date there is no such experiment available using which one can able to test the local behaviour of quantum field theory in cosmological scale (Hubble scale). However, it is expected that in near future it is possible to test such prescriptions in various ways. In this connection setting up the theory to test the violation of Bell's inequality in primordial cosmology and its experimental detection possibility in CMB observations plays significant role. Now in the technical side it is important to note that, propagators in free quantum field theory of de Sitter space computed in presence of adiabatic Bunch Davies vacuum state manifest Hadamard singularity which is consistent with the result obtained in the context of Minkowski flat space time limit [41, 42]. However in the context of interacting quantum field theory of de Sitter space such a singular propagators applicable for adiabatic Bunch Davies vacuum are dubious. In this connection  $\alpha$  vacuum state plays significant role using which one can express the propagators in interaction picture. In this context the singularity of the propagators appear in the anti-podal points. In the quantum field theory describe by the  $\alpha$  vacua state the real parameter  $\alpha$  plays the role of superselection number associated with a quantum state of a different bipartite Hilbert space. However, it is still a debatable issue that whether the interaction picture of the quantum field theory with any arbitrary  $\alpha$  vacua with any superselection rule are consistent with the physical requirements of quantum mechanics or not [39]. In general, one can treat the  $\alpha$  vacua as a family of quantum initial state where we have quantum fluctuation around an excited state. Here it might be possible that the Hilbert space corresponding to excited state (for  $\alpha$  vacua) and the adiabatic Bunch Davies vacuum coincides with each other. In such a situation it is perfectly consistent to describe quantum field theory of excited state in de Sitter space in terms of the adiabatic Bunch Davies vacuum in the ultraviolet regime <sup>3</sup>. As a result this specific identification allows us to write an effective

---

<sup>1</sup>It is important to mention that, Bunch Davies initial state is exactly equivalent to the Euclidean or adiabatic vacuum state in quantum field theory.

<sup>2</sup>Here  $\Lambda$  is the cosmological constant. Also it is important to note that, the radius of curvature of a space-time  $R \propto \Lambda^{-1}$ . As a result the signature and the magnitude of  $\Lambda$  will directly fix the curvature of the space-time.

<sup>3</sup>In the infrared regime due to the non removal of divergences appearing from various interaction in quantum

field theory description in the ultraviolet end. This implies that identifying the correct and more appropriate quantum  $\alpha$  vacuum state is fine tuned. However, this fine tuning only allows us to describe the quantum field theory with any excited states compared to ground state described by the adiabatic Bunch Davies vacuum. Using this prescription apart from inflationary paradigm, one may be able to explain a lot of unexplored late time physics phenomena using this type of non standard vacuum state. In this work, we further generalize the computational strategy of entanglement entropy for axion using  $\alpha$  vacua initial state in de Sitter space. This result will surely establish the generation of quantum entanglement entropy in early universe in a more generalized fashion. In this connection EPR pair creation from the present setup it is important to note that this procedure has an inherent correlation associated at the quantum level. When in this type of setup the possibility of EPR pair creation increases, it naturally appears that the quantum long range correlation will increase accordingly. As a consequence the amount of entanglement entropy increases with increase in the value of the parameter  $\alpha$ . We have investigated this possibility with a specific model of axion derived from **Type IIB** string theory [43–46] setup in this paper. In this work we will demonstrate the bell’s inequality violation from non zero entanglement entropy of axion. This connection also will be helpful in future to provide an theoretical tool to compare various models of inflation [47–50]. In the same line we have also commented on Rényi entropy using the same setup which will finally give rise to a complete new interpretation to long range quantum correlation in presence of  $\alpha$  vacua. In table (1) we present a comparison between the features and results obtained from Bunch Davies vacuum and  $\alpha$  vacua in presence of axion field studied in this paper. The prime physical motivations for doing computation with  $\alpha$  vacua initial state are appended below:

1. The computation of entanglement entropy with de Sitter invariant one parameter family  $\alpha$  vacua allows us to understand the underlying physics of long range effects of quantum correlation for axion in a non-trivial fashion.
2. From the holographic perspective it is important to know about the changes in the computational scheme of entanglement entropy for axion with  $\alpha$  vacua.
3. From the point of view of cosmology it is crucial to know about the observational constraints on the  $\alpha$  (non- Bunch Davies) vacua from CMB maps [19, 51, 52]. In the presence of  $\alpha$  vacua it is expected that the (auto and cross) correlation functions of primordial fluctuations get modified significantly, which is obviously an important information to understand the underlying new physics of  $\alpha$  vacua. Also this will help us to discriminate between the physical outcomes of  $\alpha$  vacua and the adiabatic Bunch Davies vacuum state.
4. From the point of view of gravity it is also significant to understand the physical implications of the new physics originated from  $\alpha$  vacua described in a specific curved gravitational background. It is a very well established fact that the Einstein General Theory of relativity is a classical field theoretic description, which describes the interactions in astrophysical scales and constrained by galaxy rotation curves, dynamics of clusters etc. [39, 53]. However, in the infrared regime of the gravity sector till date is no observational probe exists using which one can be able to test the infrared correction to the classical field theory of gravity. Now from the theoretical perspective if we describe the fluctuation in the metric in terms of spin 2 transverse, traceless degrees of freedom <sup>4</sup> in the background de Sitter space-time, then in

---

field theory explaining the physics of excited states with the adiabatic vacuum is not a good approximation.

<sup>4</sup>Here it is important to note that in the quantum version such spin 2 degrees of freedom is identified with graviton.

<b>Featuures</b>	<b>Bunch-Davies vacuum</b>	<b><math>\alpha</math> vacua</b>
<b>I</b>	It describes an adiabatic and thermal quantum state.	It describe an non-adiabatic and non-thermal class of quantum state.
<b>II</b>	This describes quantum fluctuation around a ground state with a special choice $\alpha = 0$ .	This describe quantum fluctuation around a class of excited states, characterized by superselection (real) parameter $\alpha$ .
<b>III</b>	This is not CPT invariant.	This is CPT invariant.
<b>IV</b>	Fine tuning is small.	Fine tuning is large compared to BD vacuum.
<b>V</b>	This preserves <b>SO(1,4)</b> isometry in de Sitter space.	It also preserves <b>SO(1,4)</b> isometry in de Sitter space.
<b>VI</b>	von Neumann measure of entanglement entropy is non vanishing for axion.	von Neumann measure of entanglement entropy is significantly large for $\alpha$ vacua compared to BD vacuum for axion.
<b>VII</b>	Rényi entropy is considerably large for axion.	Rényi entropy is significantly large for $\alpha$ vacua compared to BD vacuum for axion.
<b>VIII</b>	For axion long range effects of quantum correlation is prominent.	For axion long range effects of quantum correlation is more significant than BD vacuum.
<b>IX</b>	Provides the necessary condition for generating non vanishing entanglement in primordial cosmology.	Provide more strongest necessary condition for generating non vanishing entanglement in primordial cosmology.

**Table 1.** Comparison between Bunch Davies vacuum and  $\alpha$  vacua in the light of axion.

presence of  $\alpha$  vacua using the non local field redefinition in metric one can express the scalar degrees of freedom. Testing this mechanism in presence of  $\alpha$  vacua is also an important work in this area.

This paper is organized as follows. In [section 2](#), we briefly review the basic setup using which we

will compute the entanglement entropy and Rényi entropy using  $\alpha$  vacua. In [section 3.1.1](#), we introduce the axion model from string theory. Then using this model we compute the expression for the wave function in a de Sitter hyperbolic open chart in presence of Bunch Davies vacuum in [section 3.1.2](#). Further using Bogoliubov transformation we express the solution in terms of new basis, called  $\alpha$  vacua in [section 3.1.3](#). After that in [section 3.2](#), we construct the density matrix in presence of  $\alpha$  vacua. Using this result further in [section 3.3](#), we derive the expression for the von Neumann entropy which is the measure of entanglement entropy in presence of  $\alpha$  vacua. Next in [section 3.3](#), we compute Rényi entropy using the result of density matrix as derived in [section 3.2](#). Finally we conclude in [section 4](#) with some future prospects of the present work.

## 2 Basic setup: Brief review

In this section we briefly review the computational method to derive entanglement entropy in de Sitter space following the work performed in ref. [10] and ref. [14]. We consider a time preserving space-like hypersurface  $\mathbf{S}^2$  for this purpose. As a result  $\mathbf{S}^2$  is divided into two sub regions-interior and exterior which are characterized by **RI** ( $\equiv \mathbf{L}$ ) and **RII** ( $\equiv \mathbf{R}$ ). In terms of the Lorentzian signature an open chart in de Sitter space is described by three different subregions regions [10, 14]:

$$\mathbf{R}(=\mathbf{RII}) : \begin{cases} \tau_{\mathbf{E}} = \frac{\pi}{2} - it_{\mathbf{R}} & \text{for } t_{\mathbf{R}} \geq 0 \\ \rho_{\mathbf{E}} = -ir_{\mathbf{R}} & \text{for } r_{\mathbf{R}} \geq 0. \end{cases} \quad (2.1)$$

$$\mathbf{C} : \begin{cases} \tau_{\mathbf{E}} = t_{\mathbf{C}} & \text{for } -\frac{\pi}{2} \leq t_{\mathbf{C}} \leq \frac{\pi}{2} \\ \rho_{\mathbf{E}} = \frac{\pi}{2} - ir_{\mathbf{C}} & \text{for } -\infty < r_{\mathbf{C}} < \infty. \end{cases} \quad (2.2)$$

$$\mathbf{L}(=\mathbf{RI}) : \begin{cases} \tau_{\mathbf{E}} = -\frac{\pi}{2} + it_{\mathbf{L}} & \text{for } t_{\mathbf{L}} \geq 0 \\ \rho_{\mathbf{E}} = -ir_{\mathbf{L}} & \text{for } r_{\mathbf{L}} \geq 0. \end{cases} \quad (2.3)$$

Also in open chart the metric with Lorentzian signature can be written as [10, 14]:

$$\mathbf{R}(=\mathbf{RII}) : \left\{ ds_{\mathbf{R}}^2 = \frac{1}{H^2} [-dt_{\mathbf{R}}^2 + \sinh^2 t_{\mathbf{R}} (dr_{\mathbf{R}}^2 + \sinh^2 r_{\mathbf{R}} d\Omega_2^2)] \right\}, \quad (2.4)$$

$$\mathbf{C} : \left\{ ds_{\mathbf{C}}^2 = \frac{1}{H^2} [dt_{\mathbf{C}}^2 + \cos^2 t_{\mathbf{C}} (-dr_{\mathbf{C}}^2 + \cosh^2 r_{\mathbf{C}} d\Omega_2^2)] \right\}, \quad (2.5)$$

$$\mathbf{L} = (\mathbf{RI}) : \left\{ ds_{\mathbf{L}}^2 = \frac{1}{H^2} [-dt_{\mathbf{L}}^2 + \sinh^2 t_{\mathbf{L}} (dr_{\mathbf{L}}^2 + \sinh^2 r_{\mathbf{L}} d\Omega_2^2)] \right\}. \quad (2.6)$$

where  $H = \dot{a}/a$  is the Hubble parameter and  $d\Omega_2^2$  represents angular part of the metric on  $\mathbf{S}^2$ .

Now let us assume that the total Hilbert space of the local quantum mechanical system is described by  $\mathcal{H}$ , which can be written using bipartite decomposition in a direct product space [54] as,  $\mathcal{H} = \mathcal{H}_{\mathbf{INT}} \otimes \mathcal{H}_{\mathbf{EXT}}$ . Here  $\mathcal{H}_{\mathbf{INT}}$  and  $\mathcal{H}_{\mathbf{EXT}}$  are the Hilbert space associated with interior and exterior region and describe the localized modes in **RI** and **RII** respectively. Consequently, one can construct the reduced density matrix for the internal **RI** region by tracing over the external **RII** region as:

$$\rho(\alpha) = \mathbf{Tr}_{\mathbf{R}} |\alpha\rangle \langle \alpha|. \quad (2.7)$$

Here the vacuum state  $|\alpha\rangle$  is the  $\alpha$  vacuum. Further using the Von Neumann entropy measure, the entanglement entropy in de Sitter space can be expressed as:

$$S(\alpha) = -\text{Tr} [\rho(\alpha) \ln \rho(\alpha)]. \quad (2.8)$$

Using this result we establish its connection with Bell's inequality violation in cosmology [11–13].

The reduced density matrix, which is a key ingredient for computing entanglement entropy, is obtained by tracing over the exterior (**R**) region. Also it is important to note that the total entanglement entropy can be expressed as a sum of UV divergent and finite contribution as:

$$S = S_{\text{UV-divergent}} + S_{\text{UV-finite}}. \quad (2.9)$$

In 3 + 1 D, the UV-divergent part of the entropy can be written as [10, 14, 15]:

$$S_{\text{UV-divergent}} = \mathbf{c}_1 \frac{\mathcal{A}_{\text{ENT}}}{\epsilon_{\text{UV}}^2} + [\mathbf{c}_2 + (\mathbf{c}_3 m^2 + \mathbf{c}_4 H^2) \mathcal{A}_{\text{ENT}}] \ln(\epsilon_{\text{UV}} H), \quad (2.10)$$

where  $\epsilon_{\text{UV}}$  is the short distance lattice UV cut-off,  $\mathcal{A}_{\text{ENT}}$  is the proper area of the entangling region of  $\mathbf{S}^2$  and  $\mathbf{c}_i \forall i = 1, 2, 3, 4$  are the coefficients.

However we restrict ourself only within the UV-finite part which contain the information of long range effects of quantum state. At late time ( $\eta \rightarrow 0$ ), the UV-finite part of the entanglement entropy can be expressed as [10, 14, 15]:

$$S_{\text{UV-finite}} = \mathbf{c}_5 \mathcal{A}_{\text{ENT}} H^2 - \frac{\mathbf{c}_6}{2} \ln(\mathcal{A}_{\text{ENT}} H^2) + \text{finite terms}. \quad (2.11)$$

Here  $\mathbf{c}_6$  quantify the long range effect. In general,  $\mathbf{c}_6$  can be expressed as [10, 14, 15],  $\mathbf{c}_6 \equiv S_{\text{intr}}$ , where  $S_{\text{intr}}$  is the UV-finite relevant part which we quantify in later sections.

### 3 Quantum entanglement for axionic pair using $\alpha$ vacua

#### 3.1 Wave function of axion in open chart

##### 3.1.1 Model for axion effective potential

In this section our prime objective is to compute de Sitter entanglement entropy in for axion. Such axion is appearing from RR sector of **Type IIB** string theory compactified on **CY<sup>3</sup>** in presence of **NS 5** brane. For details see refs. [43–46, 55]. Let us start with the following effective action for axion field:

$$S_{\text{axion}} = \int d^4x \sqrt{-g} \left[ -\frac{1}{2} (\partial\phi)^2 + V(\phi) \right], \quad (3.1)$$

where  $\phi$  is the axion and the effective potential can be written as:

$$V(\phi) = \mu^3 \phi + \Lambda_G^4 \cos\left(\frac{\phi}{f_a}\right) = \mu^3 \left[ \phi + b f_a \cos\left(\frac{\phi}{f_a}\right) \right], \quad (3.2)$$

where  $\mu^3$  is the mass scale,  $f_a$  is the decay constant of axion and we introduce a parameter  $b$ , is defined as,  $b = \frac{\Lambda_G^4}{\mu^3 f_a}$ . Here  $\Lambda_G$  can be expressed as,  $\Lambda_G = \sqrt{\frac{m_{\text{SUSY}} L^3}{\sqrt{\alpha'} g_s}} e^{-c S_{\text{inst}}}$ , where  $S_{\text{inst}}$  is the instanton action, factor  $c \sim \mathcal{O}(1)$ ,  $m_{\text{SUSY}}$  is SUSY breaking scale,  $\alpha'$  represents Regge slope parameter,  $g_s$  characterizes the string coupling constant and  $L^6$  is the world volume factor.

For further analysis we consider the following two cases which will be helpful to interpret the results:

1. **Case I:**

Here we restrict up to the linear term of the effective potential as given by:

$$V(\phi) \approx \mu^3 \phi, \quad (3.3)$$

which can be interpreted as a massless source in the equation of motion.

2. **Case II:**

In the limit  $\phi \ll f_a$ , the total effective potential for axion can be approximated as:

$$V(\phi) \approx \Lambda_C^4 + \mu^3 \phi - \frac{\Lambda_C^4}{2} \left( \frac{\phi}{f_a} \right)^2 = \mu^3 (bf_a + \phi) - \frac{m_{axion}^2}{2} \phi^2, \quad (3.4)$$

where we introduce the effective mass of the axion as <sup>5</sup>,

$$m_{axion}^2 = \frac{\mu^3 b}{f_a} = \frac{\Lambda_G^4}{f_a^2}. \quad (3.5)$$

### 3.1.2 Wave function for Axion using Bunch Davies vacuum

Further using Eqn (3.1) the field equation of motion for the axion caan be written as [14]:

$$\text{For Case I:} \quad \left[ \frac{1}{a^3(t)} \partial_t (a^3(t) \partial_t) - \frac{1}{H^2 a^2(t)} \hat{\mathbf{L}}_{\mathbf{H}^3}^2 \right] \phi = \mu^3, \quad (3.6)$$

$$\text{For Case II:} \quad \left[ \frac{1}{a^3(t)} \partial_t (a^3(t) \partial_t) - \frac{1}{H^2 a^2(t)} \hat{\mathbf{L}}_{\mathbf{H}^3}^2 + m_{axion}^2 \right] \phi = \mu^3, \quad (3.7)$$

where the scale factor  $a(t)$  in de Sitter open chart is given by,  $a(t) = \sinh t/H$ . Here the Laplacian operator  $\hat{\mathbf{L}}_{\mathbf{H}^3}^2$  in  $\mathbf{H}^3$  can be written as [56]:

$$\hat{\mathbf{L}}_{\mathbf{H}^3}^2 = \frac{1}{\sinh^2 r} \left[ \partial_r (\sinh^2 r \partial_r) + \frac{1}{\sin \theta} \partial_\theta (\sin \theta \partial_\theta) + \frac{1}{\sin^2 \theta} \partial_\phi^2 \right], \quad (3.8)$$

which satisfy the follwoing eigenvalue equation:

$$\hat{\mathbf{L}}_{\mathbf{H}^3}^2 \mathcal{Y}_{plm}(r, \theta, \phi) = -(1 + p^2) \mathcal{Y}_{plm}(r, \theta, \phi). \quad (3.9)$$

Here  $\mathcal{Y}_{plm}(r, \theta, \phi)$  represents orthonormal eigenfunctions which can be written in terms of a radial and angular part as:

$$\mathcal{Y}_{plm}(r, \theta, \phi) = \Psi_{pl}(r) Y_{lm}(\theta, \phi), \quad (3.10)$$

where the angular part  $Y_{lm}(\theta, \phi)$  and the radial part  $\Psi_{pl}(r)$  can be written as:

$$Y_{lm}(\theta, \phi) = (-1)^m \sqrt{\frac{2l+1}{4\pi}} \sqrt{\frac{(l-m)!}{(l+m)!}} \mathcal{P}_l^m(\cos \theta) e^{im\phi}, \quad (3.11)$$

$$\Psi_{pl}(r) = \frac{\Gamma(ip+l+1)}{\Gamma(ip+1)} \frac{p}{\sqrt{\sinh r}} \mathcal{P}_{(ip-\frac{1}{2})}^{-(l+\frac{1}{2})}(\cosh r). \quad (3.12)$$

---

<sup>5</sup>Axion decay consatnt follow a (conformal) time dependent profile which we choose to be,  $f_a^2/H^2 = 100 - \frac{80}{1+(\ln \frac{r}{r_c})^2}$ , to demonstrate Bell's inequality [11–14].



where  $\mathcal{P}_l^m(\cos \theta)$  and  $\mathcal{P}_{(ip-\frac{1}{2})}^{-(l+\frac{1}{2})}(\cosh r)$  represent associated Legendre polynomial.

The total solution of the equations of motion for the **Case I** and **Case II** can be written as:

$$\Phi(t, r, \theta, \phi) = \sum_{Q=p,l,m,\sigma} \left[ a_Q \mathcal{U}_Q(t, r, \theta, \phi) + a_Q^\dagger \mathcal{U}_Q^*(t, r, \theta, \phi) \right], \quad (3.13)$$

where  $\mathcal{U}_Q(t, r, \theta, \phi)$  forms complete basis of mode function labeled by index  $Q$ . Here  $\sigma = \pm 1$  for **R** and **L** hyperboloid and given by [14]:

$$\mathcal{U}_Q(t, r, \theta, \phi) = \frac{1}{a(t)} \chi_{p,\sigma}(t) \mathcal{Y}_{plm}(r, \theta, \phi) = \frac{H}{\sinh t} \chi_{p,\sigma}(t) \mathcal{Y}_{plm}(r, \theta, \phi), \quad (3.14)$$

where  $\chi_{p,\sigma}(t)$  forms a complete set of positive frequency function. Also this can be written as a sum of complementary ( $\chi_{p,\sigma}^{(c)}(t)$ ) and particular integral ( $\chi_{p,\sigma}^{(p)}(t)$ ) part, as given by [14]:

$$\chi_{p,\sigma}(t) = \chi_{p,\sigma}^{(c)}(t) + \chi_{p,\sigma}^{(p)}(t). \quad (3.15)$$

Explicitly the complementary part for **Case I** and **Case II** can be expressed as [14]:

**Case I :**

$$\chi_{p,\sigma}^{(c)}(t) = \begin{cases} \frac{1}{2 \sinh \pi p} \left[ \frac{(e^{\pi p} + \sigma)}{\Gamma(2 + ip)} \mathcal{P}_1^{ip}(\cosh t_{\mathbf{R}}) - \frac{(e^{-\pi p} + \sigma)}{\Gamma(2 - ip)} \mathcal{P}_1^{-ip}(\cosh t_{\mathbf{R}}) \right] & \text{for } \mathbf{R} \\ \frac{\sigma}{2 \sinh \pi p} \left[ \frac{(e^{\pi p} + \sigma)}{\Gamma(2 + ip)} \mathcal{P}_1^{ip}(\cosh t_{\mathbf{L}}) - \frac{(e^{-\pi p} + \sigma)}{\Gamma(2 - ip)} \mathcal{P}_1^{-ip}(\cosh t_{\mathbf{L}}) \right] & \text{for } \mathbf{L}. \end{cases} \quad (3.16)$$

**Case II :**

$$\chi_{p,\sigma}^{(c)}(t) = \begin{cases} \frac{1}{2 \sinh \pi p} \left[ \frac{(e^{\pi p} - i\sigma e^{-i\pi\nu})}{\Gamma(\nu + \frac{1}{2} + ip)} \mathcal{P}_{(\nu-\frac{1}{2})}^{ip}(\cosh t_{\mathbf{R}}) - \frac{(e^{-\pi p} - i\sigma e^{-i\pi\nu})}{\Gamma(\nu + \frac{1}{2} - ip)} \mathcal{P}_{(\nu-\frac{1}{2})}^{-ip}(\cosh t_{\mathbf{R}}) \right] & \text{for } \mathbf{R} \\ \frac{\sigma}{2 \sinh \pi p} \left[ \frac{(e^{\pi p} - i\sigma e^{-i\pi\nu})}{\Gamma(\nu + \frac{1}{2} + ip)} \mathcal{P}_{(\nu-\frac{1}{2})}^{ip}(\cosh t_{\mathbf{L}}) - \frac{(e^{-\pi p} - i\sigma e^{-i\pi\nu})}{\Gamma(\nu + \frac{1}{2} - ip)} \mathcal{P}_{(\nu-\frac{1}{2})}^{-ip}(\cosh t_{\mathbf{L}}) \right] & \text{for } \mathbf{L}, \end{cases} \quad (3.17)$$

where in **Case II** the parameter  $\nu$  is defined as [14]:

$$\nu = \sqrt{\frac{9}{4} - \frac{m_{axion}^2}{H^2}} = \sqrt{\frac{9}{4} - \frac{\mu^3 b}{f_a H^2}} = \sqrt{\frac{9}{4} - \frac{\Lambda_G^4}{f_a^2 H^2}}. \quad (3.18)$$

This solution is symmetric under the exchange of the signature of quantum number  $p$  i.e.  $\chi_{p,\sigma}^{(c)}(t) = \chi_{-p,\sigma}^{(c)}(t)$ . In this context the overall normalization constant of the time dependent complementary part of the solution is fixed by the Klein Gordon inner product.

The solution for the particular integral part for **Case I** and **Case II** can be expressed as [14]:

$$\chi_{p,\sigma}^{(p)}(t) = \sinh^2 t \sum_{n=0}^{\infty} \frac{1}{(p^2 - p_n^2)} \chi_{p_n,\sigma}^{(c)}(t) \int dt' \chi_{p_n,\sigma}^{(c)}(t') \mathcal{J}(t'), \quad (3.19)$$

where the source for axion is  $\mathcal{J} = \mu^3$ .

### 3.1.3 Wave function for Axion using $\alpha$ vacua

Here our prime objective is to derive results for  $\alpha$ -vacua, which can be interpreted as a quantum state filled with particles defined by some hypothetical observer who belongs to the Bunch Davies

vacuum state originally. Here the  $\alpha$  vacua are invariant under  $\mathbf{SO}(1, 4)$  isometry group of de Sitter space. Consequently we use the equivalent prescription followed in case of Bunch Davies vacuum by defining two subspaces in de Sitter space, which is identified as **RI** and **RII** respectively. Additionally, it is important to note that, in general  $\alpha$ -vacua is CPT invariant, which is parameterized by a single real positive parameter  $\alpha$  which plays the role of superselection quantum number. Bunch Davies vacuum is the special case of  $\alpha$  vacua, where we set  $\alpha = 0$  in the final solutions. In this section we will explicitly investigate that how the long range effects in quantum entanglement is improved by the choice of the  $\alpha$ -vacua. To serve this purpose, we use the results obtained for the solution of the EOM where we expand the field in terms of creation and annihilation operators in Bunch Davies vacuum, and further using Bogoliubov transformation the mode functions for the  $\alpha$ -vacua can be written as:

$$\Phi(r, t, \theta, \phi) = \int_0^\infty dp \sum_{\sigma=\pm 1} \sum_{l=0}^\infty \sum_{m=-l}^{+l} \left[ d_{\sigma plm} \mathcal{E}_{\sigma plm}^{(\alpha)}(r, t, \theta, \phi) + d_{\sigma plm}^\dagger (\mathcal{E}_{\sigma plm}^{(\alpha)})^*(r, t, \theta, \phi) \right], \quad (3.20)$$

where the  $\alpha$ -vacua state are defined as:

$$d_{\sigma plm} |\alpha\rangle = 0 \quad \forall \sigma = (+1, -1); 0 < p < \infty; l = 0, \dots, \infty, m = -l, \dots, +l. \quad (3.21)$$

In this context, the  $\alpha$ -vacua mode function  $\mathcal{E}_{\sigma plm}^{(\alpha)}$  can be expressed in terms of Bunch Davies mode function  $\mathcal{U}_{\sigma plm}(r, t, \theta, \phi)$  using Bogoliubov transformation as:

$$\mathcal{E}_{\sigma plm}^{(\alpha)} = [\cosh \alpha \mathcal{U}_{\sigma plm}(r, t, \theta, \phi) + \sinh \alpha \mathcal{U}_{\sigma plm}^*(r, t, \theta, \phi)]. \quad (3.22)$$

Here  $\mathcal{U}_{\sigma plm}(r, t, \theta, \phi)$  is the Bunch Davies vacuum states, which is defined as [14]:

$$\mathcal{U}_{\sigma plm}(r, t, \theta, \phi) = \frac{H}{\sinh t} \chi_{p,\sigma}(t) \mathcal{Y}_{plm}(r, \theta, \phi). \quad (3.23)$$

After substituting Eq (3.22) and Eq (3.23) in Eq (3.20) we get the following expression for the wave function:

$$\Phi(r, t, \theta, \phi) = \int_0^\infty dp \sum_{l=0}^\infty \sum_{m=-l}^{+l} \mathcal{Z}_{plm}^{(\alpha)}(t) \mathcal{Y}_{plm}(r, \theta, \phi), \quad (3.24)$$

where we introduce a new function  $\mathcal{W}_{plm}(t)$ , which is defined as:

$$\mathcal{Z}_{plm}^{(\alpha)}(t) = \frac{H}{\sinh t} \sum_{\sigma=\pm 1} \left[ d_{\sigma plm} \cosh \alpha \chi_{p,\sigma}(t) + d_{\sigma plm}^\dagger \sinh \alpha \chi_{p,\sigma}^*(t) \right]. \quad (3.25)$$

Finally, the solution of the time dependent part of the wave function can be recast as [14]:

$$\chi_{p,\sigma}(t) = \sum_{q=\mathbf{R}, \mathbf{L}} \left\{ \underbrace{\frac{1}{\mathcal{N}_p} [\alpha_q^\sigma \mathcal{P}^q + \beta_q^\sigma \mathcal{P}^{q*}]}_{\text{Complementary solution}} + \underbrace{\sum_{n=0}^\infty \frac{1}{\mathcal{N}_{p_n} (p_n^2 - p^2)} [\bar{\alpha}_{q,n}^\sigma \bar{\mathcal{P}}^{q,n} + \bar{\beta}_{q,n}^\sigma \bar{\mathcal{P}}^{q*,n}]}_{\text{Particular solution}} \right\}, \quad (3.26)$$

where we use the following shorthand notation:

$$\bar{\mathcal{P}}^{q,n} = \sinh^2 t \int dt' \chi_{p_n,\sigma,q}^{(c)}(t') \mathcal{J}(t') \mathcal{P}^{q,n}. \quad (3.27)$$

Additionally, here we use the shorthand notations  $\mathcal{P}^q$ ,  $\mathcal{P}^{*q}$ ,  $\mathcal{P}^{q,n}$ ,  $\mathcal{P}^{*q,n}$  for the Legendre polynomial and for its complex conjugate counterpart, which is defined in ref. [14]. Also the coefficient functions  $(\alpha_q^\sigma, \beta_q^\sigma)$  and  $(\alpha_{q,n}^\sigma, \beta_{q,n}^\sigma)$  (where  $\sigma = \pm 1$ ), normalization constants  $\mathcal{N}_p$ ,  $\mathcal{N}_{p_n}$  for the complementary and particular part of the solution are explicitly mentioned in ref. [14] for **Case I** and **Case II**.

For further computation  $\alpha$ -vacua are defined in terms of Bunch Davies vacuum state as:

$$|\alpha\rangle = \exp\left(\frac{1}{2} \tanh \alpha \sum_{\sigma=\pm 1} a_\sigma^\dagger a_\sigma\right) |\mathbf{BD}\rangle. \quad (3.28)$$

Here it is important to note that for  $\alpha = 0$  we get,  $|\alpha = 0\rangle = |0\rangle = |\mathbf{BD}\rangle$ . Further one can also write the the **R** and **L** vacua as [14]:

$$|\mathbf{R}\rangle = |\mathbf{R}\rangle_{(c)} + \sum_{n=0}^{\infty} |\mathbf{R}\rangle_{(p),n}, \quad |\mathbf{L}\rangle = |\mathbf{L}\rangle_{(c)} + \sum_{n=0}^{\infty} |\mathbf{L}\rangle_{(p),n}, \quad (3.29)$$

with  $(c)$  and  $(p)$  representing the complementary and particular part respectively.

Further assuming the bipartite Hilbert space ( $\mathcal{H}_\alpha := \mathcal{H}_{\mathbf{R}} \otimes \mathcal{H}_{\mathbf{L}}$ ) one can also write the  $\alpha$ -vacua in terms of the **R** and **L** vacuum as:

$$|\alpha\rangle = \exp\left(\frac{1}{2} \tanh \alpha \sum_{\sigma=\pm 1} a_\sigma^\dagger a_\sigma\right) e^{\hat{O}}(|\mathbf{R}\rangle \otimes |\mathbf{L}\rangle), \quad (3.30)$$

where the creation and annihilation operators  $a_\sigma^\dagger$  and  $a_\sigma$  for the **R** and **L** vacuum are defined as [14]:

$$a_\sigma = \sum_{q=\mathbf{R},\mathbf{L}} \left\{ \left[ \gamma_{q\sigma} b_q + \delta_{q\sigma}^* b_q^\dagger \right] + \sum_{n=0}^{\infty} \left[ \bar{\gamma}_{q\sigma,n} \bar{b}_{q,n} + \bar{\delta}_{q\sigma,n}^* \bar{b}_{q,n}^\dagger \right] \right\}, \quad (3.31)$$

$$a_\sigma^\dagger = \sum_{q=\mathbf{R},\mathbf{L}} \left\{ \left[ \gamma_{q\sigma}^* b_q^\dagger + \delta_{q\sigma} b_q \right] + \sum_{n=0}^{\infty} \left[ \bar{\gamma}_{q\sigma,n}^* \bar{b}_{q,n}^\dagger + \bar{\delta}_{q\sigma,n} \bar{b}_{q,n} \right] \right\}, \quad (3.32)$$

with  $\sigma = \pm 1$ . Here it is important to note that, the coefficient matrices for the Bogoliubov transformation  $\gamma_{q\sigma}$ ,  $\delta_{q\sigma}$ ,  $\bar{\gamma}_{q\sigma,n}$  and  $\bar{\delta}_{q\sigma,n}$  helps us to write the  $a$  type of oscillators in terms of a new  $b$  type of oscillators. For more details see ref. [14] where all the symbols are explicitly defined. Here it is important to note that, the newly introduced  $b$  type of oscillators exactly satisfy the harmonic oscillator algebra, provided the oscillators corresponding to the solution of complementary and particular part of the time dependent solution of the wave function are not interacting with each other. This surely helps us to set up the rules for the operation of creation and annihilation operators of these oscillators in this context [14].

Also in Eq (3.30), the composite operator  $\hat{O}$  which acts on the direct product of **R** and **L** state is defined as [14]:

$$\hat{O} = \frac{1}{2} \sum_{i,j=\mathbf{R},\mathbf{L}} m_{ij} b_i^\dagger b_j^\dagger + \frac{1}{2} \sum_{i,j=\mathbf{R},\mathbf{L}} \sum_{n=0}^{\infty} \bar{m}_{ij,n} \bar{b}_{i,n}^\dagger \bar{b}_{j,n}^\dagger, \quad (3.33)$$

where the matrices  $m_{ij}$  and  $\bar{m}_{ij,n}$  corresponding to complementary and particular part of the solution are explicitly computed in ref. [14] for Bunch Davies vacuum.

For our further computation we use the definition of  $\alpha$ -vacuum state as given in Eq (3.30), which is very useful to compute entanglement entropy in de Sitter space. However, it is important to note that the technical steps for the computation of the entanglement entropy in de Sitter space from  $\alpha$ -vacua are exactly similar to the steps followed for Bunch Davies vacuum. Only difference will appear when we use the creation and annihilation operators in the context of  $\alpha$ -vacua, which can be written in terms of the creation and annihilation operators defined for  $\mathbf{R}$  or  $\mathbf{L}$  vacuum state as:

$$d_\sigma = \sum_{q=\mathbf{R},\mathbf{L}} \left\{ \left[ (\cosh \alpha \gamma_{q\sigma} - \sinh \alpha \delta_{q\sigma}) b_q + (\cosh \alpha \delta_{q\sigma}^* - \sinh \alpha \gamma_{q\sigma}^*) b_q^\dagger \right] + \left[ \left( \cosh \alpha \sum_{n=0}^{\infty} \bar{\gamma}_{q\sigma,n} \bar{b}_{q,n} - \sinh \alpha \sum_{n=0}^{\infty} \bar{\delta}_{q\sigma,n} \bar{b}_{q,n} \right) + \left( \cosh \alpha \sum_{n=0}^{\infty} \bar{\delta}_{q\sigma,n}^* \bar{b}_{q,n}^\dagger - \sinh \alpha \sum_{n=0}^{\infty} \bar{\gamma}_{q\sigma,n}^* \bar{b}_{q,n}^\dagger \right) \right] \right\}, \quad (3.34)$$

$$d_\sigma^\dagger = \sum_{q=\mathbf{R},\mathbf{L}} \left\{ \left[ (\cosh \alpha \gamma_{q\sigma}^* - \sinh \alpha \delta_{q\sigma}^*) b_q^\dagger + (\cosh \alpha \delta_{q\sigma} - \sinh \alpha \gamma_{q\sigma}) b_q \right] + \left[ \left( \cosh \alpha \sum_{n=0}^{\infty} \bar{\gamma}_{q\sigma,n}^* \bar{b}_{q,n}^\dagger - \sinh \alpha \sum_{n=0}^{\infty} \bar{\delta}_{q\sigma,n}^* \bar{b}_{q,n}^\dagger \right) + \left( \cosh \alpha \sum_{n=0}^{\infty} \bar{\delta}_{q\sigma,n} \bar{b}_{q,n} - \sinh \alpha \sum_{n=0}^{\infty} \bar{\gamma}_{q\sigma,n} \bar{b}_{q,n} \right) \right] \right\}, \quad (3.35)$$

where we use the definition of creation and annihilation operators in Bunch Davies vacuum as mentioned in Eq (3.32) and Eq (3.31). In this computation it is important to note that, under Bogoliubov transformation the original matrix  $\gamma_{q\sigma}$ ,  $\delta_{q\sigma}$ ,  $\bar{\gamma}_{q\sigma,n}$  and  $\bar{\delta}_{q\sigma,n}$  used for Bunch Davies vacuum are transformed in the context of  $\alpha$ -vacua as:

$$\begin{aligned} \gamma_{q\sigma} &\longrightarrow (\cosh \alpha \gamma_{q\sigma} - \sinh \alpha \delta_{q\sigma}), & \delta_{q\sigma} &\longrightarrow (\cosh \alpha \delta_{q\sigma} - \sinh \alpha \gamma_{q\sigma}), \\ \bar{\gamma}_{q\sigma,n} &\longrightarrow (\cosh \alpha \bar{\gamma}_{q\sigma,n} - \sinh \alpha \bar{\delta}_{q\sigma,n}), & \bar{\delta}_{q\sigma,n} &\longrightarrow (\cosh \alpha \bar{\delta}_{q\sigma,n} - \sinh \alpha \bar{\gamma}_{q\sigma,n}). \end{aligned} \quad (3.36)$$

Considering this fact, after Bogoliubov transformation  $\alpha$ -vacua state can be written in terms of  $\mathbf{R}$  and  $\mathbf{L}$  vacua as:

$$|\alpha\rangle = e^{\hat{\mathcal{O}}}(|\mathbf{R}\rangle \otimes |\mathbf{L}\rangle), \quad (3.37)$$

where the new operator  $\hat{\mathcal{O}}$  is defined as:

$$\hat{\mathcal{O}} = \frac{1}{2} \sum_{i,j=\mathbf{R},\mathbf{L}} \tilde{m}_{ij} b_i^\dagger b_j^\dagger + \frac{1}{2} \sum_{i,j=\mathbf{R},\mathbf{L}} \sum_{n=0}^{\infty} \tilde{\bar{m}}_{ij,n} \bar{b}_{i,n}^\dagger \bar{b}_{j,n}^\dagger. \quad (3.38)$$

Here  $\tilde{m}_{ij}$  and  $\tilde{\bar{m}}_{ij,n}$  represents the entries of the matrices corresponding to the complementary and particular solution in presence of  $\alpha$  vacuum which we will compute in this paper.

Further one can write the annihilation of  $\alpha$  vacuum in terms of the annihilations of the direct product state of  $\mathbf{R}$  and  $\mathbf{L}$  vacuum as:

$$d_\sigma |\alpha\rangle = \sum_{q=\mathbf{R},\mathbf{L}} \sum_{s=1}^4 \mathcal{J}_s^{(q)} = 0, \quad (3.39)$$

where neglecting contribution from the powers of creation operators,  $\mathcal{J}_s^{(q)} \forall s = 1, 2, 3, 4, q = \mathbf{R}, \mathbf{L}$  are defined as:

$$\begin{aligned} \sum_{q=\mathbf{R},\mathbf{L}} \mathcal{J}_1^{(q)} &= \sum_{q=\mathbf{R},\mathbf{L}} (\cosh \alpha \gamma_{q\sigma} - \sinh \alpha \delta_{q\sigma}) b_q e^{\hat{\mathcal{O}}} (|\mathbf{R}\rangle \otimes |\mathbf{L}\rangle) \\ &\approx \sum_{i,j=\mathbf{R},\mathbf{L}} \tilde{m}_{ij} (\cosh \alpha \gamma_{j\sigma} - \sinh \alpha \delta_{j\sigma}) b_i^\dagger (|\mathbf{R}\rangle \otimes |\mathbf{L}\rangle), \end{aligned} \quad (3.40)$$

$$\begin{aligned} \sum_{q=\mathbf{R},\mathbf{L}} \mathcal{J}_2^{(q)} &= \sum_{q=\mathbf{R},\mathbf{L}} (\cosh \alpha \delta_{q\sigma}^* - \sinh \alpha \gamma_{q\sigma}^*) b_q^\dagger e^{\hat{\mathcal{O}}} (|\mathbf{R}\rangle \otimes |\mathbf{L}\rangle) \\ &\approx \sum_{q=\mathbf{R},\mathbf{L}} (\cosh \alpha \delta_{q\sigma}^* - \sinh \alpha \gamma_{q\sigma}^*) b_q^\dagger (|\mathbf{R}\rangle \otimes |\mathbf{L}\rangle), \end{aligned} \quad (3.41)$$

$$\begin{aligned} \sum_{q=\mathbf{R},\mathbf{L}} \mathcal{J}_3^{(q)} &= \sum_{q=\mathbf{R},\mathbf{L}} \left( \cosh \alpha \sum_{n=0}^{\infty} \bar{\gamma}_{q\sigma,n} \bar{b}_{q,n} - \sinh \alpha \sum_{n=0}^{\infty} \bar{\delta}_{q\sigma,n} \bar{b}_{q,n} \right) e^{\hat{\mathcal{O}}} (|\mathbf{R}\rangle \otimes |\mathbf{L}\rangle) \\ &\approx \sum_{i,j=\mathbf{R},\mathbf{L}} \left( \cosh \alpha \sum_{n=0}^{\infty} \bar{\tilde{m}}_{ij,n} \bar{\gamma}_{j\sigma,n} \bar{b}_{i,n}^\dagger - \sinh \alpha \sum_{n=0}^{\infty} \bar{\tilde{m}}_{ij,n} \bar{\delta}_{j\sigma,n} \bar{b}_{i,n}^\dagger \right) (|\mathbf{R}\rangle \otimes |\mathbf{L}\rangle), \end{aligned} \quad (3.42)$$

$$\begin{aligned} \sum_{q=\mathbf{R},\mathbf{L}} \mathcal{J}_4^{(q)} &= \sum_{q=\mathbf{R},\mathbf{L}} \left( \cosh \alpha \sum_{n=0}^{\infty} \bar{\delta}_{q\sigma,n}^* \bar{b}_{q,n}^\dagger - \sinh \alpha \sum_{n=0}^{\infty} \bar{\gamma}_{q\sigma,n}^* \bar{b}_{q,n}^\dagger \right) e^{\hat{\mathcal{O}}} (|\mathbf{R}\rangle \otimes |\mathbf{L}\rangle) \\ &\approx \sum_{q=\mathbf{R},\mathbf{L}} \sum_{n=0}^{\infty} \left( \cosh \alpha \bar{\delta}_{q\sigma,n}^* \bar{b}_{q,n}^\dagger - \sinh \alpha \bar{\gamma}_{q\sigma,n}^* \bar{b}_{q,n}^\dagger \right) (|\mathbf{R}\rangle \otimes |\mathbf{L}\rangle). \end{aligned} \quad (3.43)$$

This directly implies that:

$$\begin{aligned} &[\tilde{m}_{ij} (\cosh \alpha \gamma_{j\sigma} - \sinh \alpha \delta_{j\sigma}) + (\cosh \alpha \delta_{i\sigma}^* - \sinh \alpha \gamma_{i\sigma}^*)] b_i^\dagger \\ &+ \left[ \left( \cosh \alpha \sum_{n=0}^{\infty} \bar{\tilde{m}}_{ij,n} \bar{\gamma}_{j\sigma,n} \bar{b}_{i,n}^\dagger - \sinh \alpha \sum_{n=0}^{\infty} \bar{\tilde{m}}_{ij,n} \bar{\delta}_{j\sigma,n} \bar{b}_{i,n}^\dagger \right) \right. \\ &\quad \left. + \left( \cosh \alpha \sum_{n=0}^{\infty} \bar{\delta}_{i\sigma,n}^* \bar{b}_{i,n}^\dagger - \sinh \alpha \sum_{n=0}^{\infty} \bar{\gamma}_{i\sigma,n}^* \bar{b}_{i,n}^\dagger \right) \right] = 0. \end{aligned} \quad (3.44)$$

As we have already mentioned that the complementary and particular part of the solutions are completely independent of each other and hence vanish individually. Consequently, we get the following constraints in case of  $\alpha$  vacuum:

$$[\tilde{m}_{ij} (\cosh \alpha \gamma_{j\sigma} - \sinh \alpha \delta_{j\sigma}) + (\cosh \alpha \delta_{i\sigma}^* - \sinh \alpha \gamma_{i\sigma}^*)] = 0, \quad (3.45)$$

$$[(\cosh \alpha \bar{\tilde{m}}_{ij,n} \bar{\gamma}_{j\sigma,n} - \sinh \alpha \bar{\tilde{m}}_{ij,n} \bar{\delta}_{j\sigma,n}) + (\cosh \alpha \bar{\delta}_{i\sigma,n}^* - \sinh \alpha \bar{\gamma}_{i\sigma,n}^*)] = 0 \forall n. \quad (3.46)$$

Further using Eq (3.45) and Eq (3.46), the matrices corresponding to the complementary and particular part of the solution can be expressed as:

$$\tilde{m}_{ij} = -(\cosh \alpha \delta_{i\sigma}^* - \sinh \alpha \gamma_{i\sigma}^*) (\cosh \alpha \gamma - \sinh \alpha \delta)_{\sigma j}^{-1} = \begin{pmatrix} \tilde{m}_{\mathbf{RR}} & \tilde{m}_{\mathbf{RL}} \\ \tilde{m}_{\mathbf{LR}} & \tilde{m}_{\mathbf{LL}} \end{pmatrix}, \quad (3.47)$$

$$\bar{\tilde{m}}_{ij,n} = -(\cosh \alpha \bar{\delta}_{i\sigma,n}^* - \sinh \alpha \bar{\gamma}_{i\sigma,n}^*) (\cosh \alpha \bar{\gamma} - \sinh \alpha \bar{\delta})_{\sigma j,n}^{-1} = \begin{pmatrix} \bar{\tilde{m}}_{\mathbf{RR},n} & \bar{\tilde{m}}_{\mathbf{RL},n} \\ \bar{\tilde{m}}_{\mathbf{LR},n} & \bar{\tilde{m}}_{\mathbf{LL},n} \end{pmatrix}. \quad (3.48)$$

Further substituting the expressions for  $\gamma$ ,  $\delta$ ,  $\gamma_n$  and  $\delta_n$  we finally get the following simplified expressions: Next substituting the right hand side of the above mentioned equations explicitly the entries of the mass matrices can be expressed for  $i, j = \mathbf{R}, \mathbf{L}$  as:

**For complementary solution :**

$$\tilde{m}_{ij} = \begin{cases} \frac{\Gamma(2-ip)}{\Gamma(2+ip)} \frac{2\mathcal{D}_{ij}^{(\frac{3}{2})}}{e^{2\pi p} (\cosh \alpha - \sinh \alpha e^{-2\pi p})^2 - (\cosh \alpha - \sinh \alpha)^2} & \text{for Case I} \\ -\frac{\Gamma(\nu + \frac{1}{2} - ip)}{\Gamma(\nu + \frac{1}{2} + ip)} \frac{2\mathcal{D}_{ij}^{(\nu)}}{e^{2\pi p} (\cosh \alpha - \sinh \alpha e^{-2\pi p})^2 + e^{2i\pi\nu} (\cosh \alpha + \sinh \alpha e^{-2i\pi\nu})^2} & \text{for Case II.} \end{cases} \quad (3.49)$$

**For particular solution :**

$$\bar{\tilde{m}}_{ij,n} = \begin{cases} \frac{\Gamma(2-ip_n)}{\Gamma(2+ip_n)} \frac{2\mathcal{D}_{ij}^{(\frac{3}{2},n)}}{e^{2\pi p_n} (\cosh \alpha - \sinh \alpha e^{-2\pi p_n})^2 - (\cosh \alpha - \sinh \alpha)^2} & \text{for Case I} \\ -\frac{\Gamma(\nu + \frac{1}{2} - ip_n)}{\Gamma(\nu + \frac{1}{2} + ip_n)} \frac{2\mathcal{D}_{ij}^{(\nu,n)}}{e^{2\pi p_n} (\cosh \alpha - \sinh \alpha e^{-2\pi p_n})^2 + e^{2i\pi\nu} (\cosh \alpha + \sinh \alpha e^{-2i\pi\nu})^2} & \text{for Case II.} \end{cases} \quad (3.50)$$

Here for **Case I** and **Case II**, we define the  $\mathcal{D}$  matrices as:

$$\text{Case I:} \quad \mathcal{D}_{ij}^{(\frac{3}{2})} = \begin{pmatrix} \mathcal{D}_{\mathbf{RR}}^{(\frac{3}{2})} & \mathcal{D}_{\mathbf{RL}}^{(\frac{3}{2})} \\ \mathcal{D}_{\mathbf{LR}}^{(\frac{3}{2})} & \mathcal{D}_{\mathbf{LL}}^{(\frac{3}{2})} \end{pmatrix}, \quad \mathcal{D}_{ij}^{(\frac{3}{2},n)} = \begin{pmatrix} \mathcal{D}_{\mathbf{RR}}^{(\frac{3}{2},n)} & \mathcal{D}_{\mathbf{RL}}^{(\frac{3}{2},n)} \\ \mathcal{D}_{\mathbf{LR}}^{(\frac{3}{2},n)} & \mathcal{D}_{\mathbf{LL}}^{(\frac{3}{2},n)} \end{pmatrix}, \quad (3.51)$$

$$\text{Case II:} \quad \mathcal{D}_{ij}^{(\nu)} = \begin{pmatrix} \mathcal{D}_{\mathbf{RR}}^{(\nu)} & \mathcal{D}_{\mathbf{RL}}^{(\nu)} \\ \mathcal{D}_{\mathbf{LR}}^{(\nu)} & \mathcal{D}_{\mathbf{LL}}^{(\nu)} \end{pmatrix}, \quad \mathcal{D}_{ij}^{(\nu,n)} = \begin{pmatrix} \mathcal{D}_{\mathbf{RR}}^{(\nu,n)} & \mathcal{D}_{\mathbf{RL}}^{(\nu,n)} \\ \mathcal{D}_{\mathbf{LR}}^{(\nu,n)} & \mathcal{D}_{\mathbf{LL}}^{(\nu,n)} \end{pmatrix}. \quad (3.52)$$

and the corresponding entries of the  $\mathcal{D}$  matrices are given by:

**Case I :**

$$\mathcal{D}_{\mathbf{RR}}^{(\frac{3}{2})} = \mathcal{D}_{\mathbf{LL}}^{(\frac{3}{2})} = -\sinh 2\alpha \sinh^2 \pi p, \quad (3.53)$$

$$\mathcal{D}_{\mathbf{RL}}^{(\frac{3}{2})} = \mathcal{D}_{\mathbf{LR}}^{(\frac{3}{2})} = i \sinh \pi p, \quad (3.54)$$

$$\mathcal{D}_{\mathbf{RR}}^{(\frac{3}{2},n)} = \mathcal{D}_{\mathbf{LL}}^{(\frac{3}{2},n)} = -\sinh 2\alpha \sinh^2 \pi p_n, \quad (3.55)$$

$$\mathcal{D}_{\mathbf{RL}}^{(\frac{3}{2},n)} = \mathcal{D}_{\mathbf{LR}}^{(\frac{3}{2},n)} = i \sinh \pi p_n, \quad (3.56)$$

**Case II :**

$$\mathcal{D}_{\mathbf{RR}}^{(\nu)} = \mathcal{D}_{\mathbf{LL}}^{(\nu)} = (\cosh^2 \alpha e^{i\pi\nu} + \sinh^2 \alpha e^{-i\pi\nu}) \cos \pi\nu - \sinh 2\alpha \sinh^2 \pi p, \quad (3.57)$$

$$\mathcal{D}_{\mathbf{RL}}^{(\nu)} = \mathcal{D}_{\mathbf{LR}}^{(\nu)} = i (\cosh^2 \alpha e^{i\pi\nu} + \sinh^2 \alpha e^{-i\pi\nu} + \sinh 2\alpha \cos \pi\nu) \sinh \pi p, \quad (3.58)$$

$$\mathcal{D}_{\mathbf{RR}}^{(\nu,n)} = \mathcal{D}_{\mathbf{LL}}^{(\nu,n)} = (\cosh^2 \alpha e^{i\pi\nu} + \sinh^2 \alpha e^{-i\pi\nu}) \cos \pi\nu - \sinh 2\alpha \sinh^2 \pi p_n, \quad (3.59)$$

$$\mathcal{D}_{\mathbf{RL}}^{(\nu,n)} = \mathcal{D}_{\mathbf{LR}}^{(\nu,n)} = i (\cosh^2 \alpha e^{i\pi\nu} + \sinh^2 \alpha e^{-i\pi\nu} + \sinh 2\alpha \cos \pi\nu) \sinh \pi p_n. \quad (3.60)$$

Before further discussion here we point out few important features from the obtained results:

- For the **Case I** we see that for the complementary and particular part of the solution

$$\tilde{m}_{\mathbf{RR}} = \tilde{m}_{\mathbf{LL}} = -\frac{\Gamma(2-ip)}{\Gamma(2+ip)} \frac{2 \sinh 2\alpha \sinh^2 \pi p}{e^{2\pi p} (\cosh \alpha - \sinh \alpha e^{-2\pi p})^2 - (\cosh \alpha - \sinh \alpha)^2}, \quad (3.61)$$

$$\tilde{\bar{m}}_{\mathbf{RR},n} = \tilde{\bar{m}}_{\mathbf{LL},n} = -\frac{\Gamma(2-ip_n)}{\Gamma(2+ip_n)} \frac{2 \sinh 2\alpha \sinh^2 \pi p_n}{e^{2\pi p_n} (\cosh \alpha - \sinh \alpha e^{-2\pi p_n})^2 - (\cosh \alpha - \sinh \alpha)^2}. \quad (3.62)$$

But for **Case II** we find that

$$\begin{aligned} \tilde{m}_{\mathbf{RR}} = \tilde{m}_{\mathbf{LL}} &= -\frac{\Gamma(\nu + \frac{1}{2} - ip)}{\Gamma(\nu + \frac{1}{2} + ip)} \\ &\times \frac{2 [(\cosh^2 \alpha e^{i\pi\nu} + \sinh^2 \alpha e^{-i\pi\nu}) \cos \pi\nu - \sinh 2\alpha \sinh^2 \pi p]}{e^{2\pi p} (\cosh \alpha - \sinh \alpha e^{-2\pi p})^2 + e^{2i\pi\nu} (\cosh \alpha + \sinh \alpha e^{-2i\pi\nu})^2}, \end{aligned} \quad (3.63)$$

$$\begin{aligned} \tilde{\bar{m}}_{\mathbf{RR},n} = \tilde{\bar{m}}_{\mathbf{LL},n} &= -\frac{\Gamma(\nu + \frac{1}{2} - ip_n)}{\Gamma(\nu + \frac{1}{2} + ip_n)} \\ &\times \frac{2 [(\cosh^2 \alpha e^{i\pi\nu} + \sinh^2 \alpha e^{-i\pi\nu}) \cos \pi\nu - \sinh 2\alpha \sinh^2 \pi p_n]}{e^{2\pi p_n} (\cosh \alpha - \sinh \alpha e^{-2\pi p_n})^2 + e^{2i\pi\nu} (\cosh \alpha + \sinh \alpha e^{-2i\pi\nu})^2}. \end{aligned} \quad (3.64)$$

which is non vanishing for  $0 < \nu \leq 3/2$  and  $\nu > 3/2$ . For  $\nu = 3/2$  we get the non vanishing result from **Case I** using  $\alpha$ -vacuum and this result is significantly different from the result obtained for Bunch Davies vacuum state. Here by setting  $\alpha = 0$  and  $\nu = 3/2$  in **Case I** one can check that the entries of the matrices vanish for Bunch Davies vacuum.

Finally to implement numerical analysis we use the following approximated expressions for the entries of the coefficient matrices as given by:

**Case I:**

$$\tilde{m}_{\mathbf{RR}} = e^{i(\theta + \frac{\pi}{2})} \frac{\sqrt{2} e^{-p\pi}}{\sqrt{\cosh 2\pi p - 1}} \frac{\sinh 2\alpha \sinh^2 \pi p}{(\cosh^2 \alpha - \sinh^2 \alpha e^{-2\pi p})}, \quad (3.65)$$

$$\tilde{\bar{m}}_{\mathbf{RR},n} = e^{i(\theta + \frac{\pi}{2})} \frac{\sqrt{2} e^{-p_n\pi}}{\sqrt{\cosh 2\pi p_n - 1}} \frac{\sinh 2\alpha \sinh^2 \pi p_n}{(\cosh^2 \alpha - \sinh^2 \alpha e^{-2\pi p_n})}, \quad (3.66)$$

which vanishes for Bunch Davies vacuum with  $\alpha = 0$ . On the other hand for a most generalized situation we get:

**Case II:**

$$\tilde{m}_{\mathbf{RR}} = m_{\mathbf{RR}} \times \frac{[(\cosh^2 \alpha + \sinh^2 \alpha e^{-2i\pi\nu}) - \sinh 2\alpha \sinh^2 \pi p e^{-i\pi\nu} \sec \pi\nu]}{(\cosh^2 \alpha + \sinh^2 \alpha e^{-2\pi(p+i\nu)})}, \quad (3.67)$$

$$\tilde{\bar{m}}_{\mathbf{RR},n} = m_{\mathbf{RR},n} \times \frac{[(\cosh^2 \alpha + \sinh^2 \alpha e^{-2i\pi\nu}) - \sinh 2\alpha \sinh^2 \pi p_n e^{-i\pi\nu} \sec \pi\nu]}{(\cosh^2 \alpha + \sinh^2 \alpha e^{-2\pi(p_n+i\nu)})}, \quad (3.68)$$

where for **Case II**,  $m_{\mathbf{RR}}$  and  $m_{\mathbf{RR},n}$  represent the contributions for the coefficient matrices from its Bunch Davies vacuum counterpart as given by <sup>6</sup>:

$$m_{\mathbf{RR}} = e^{i\theta} \frac{\sqrt{2} e^{-p\pi} \cos \pi\nu}{\sqrt{\cosh 2\pi p + \cos 2\pi\nu}}, \quad (3.69)$$

$$m_{\mathbf{RR},n} = e^{i\theta} \frac{\sqrt{2} e^{-p_n\pi} \cos \pi\nu}{\sqrt{\cosh 2\pi p_n + \cos 2\pi\nu}}. \quad (3.70)$$

---

<sup>6</sup>For rest of the analysis we absorb this overall phase factor  $e^{i\theta}$ .

- For the **Case I** we see that for the complementary and particular part of the solution:

$$\tilde{m}_{\mathbf{RL}} = \tilde{m}_{\mathbf{LR}} = -\frac{\Gamma(2-ip)}{\Gamma(2+ip)} \frac{2 \sinh \pi p}{e^{2\pi p} (\cosh \alpha - \sinh \alpha e^{-2\pi p})^2 - (\cosh \alpha - \sinh \alpha)^2}, \quad (3.71)$$

$$\bar{\tilde{m}}_{\mathbf{RL},n} = \bar{\tilde{m}}_{\mathbf{LR},n} = -\frac{\Gamma(2-ip_n)}{\Gamma(2+ip_n)} \frac{2 \sinh \pi p}{e^{2\pi p_n} (\cosh \alpha - \sinh \alpha e^{-2\pi p_n})^2 - (\cosh \alpha - \sinh \alpha)^2}. \quad (3.72)$$

But for **Case II** we find that

$$\begin{aligned} \tilde{m}_{\mathbf{RL}} = \tilde{m}_{\mathbf{LR}} &= -\frac{\Gamma(\nu + \frac{1}{2} - ip)}{\Gamma(\nu + \frac{1}{2} + ip)} \\ &\times \frac{2i [(\cosh^2 \alpha e^{i\pi\nu} + \sinh^2 \alpha e^{-i\pi\nu} + \sinh 2\alpha \cos \pi\nu) \sinh \pi p]}{e^{2\pi p} (\cosh \alpha - \sinh \alpha e^{-2\pi p})^2 + e^{2i\pi\nu} (\cosh \alpha + \sinh \alpha e^{-2i\pi\nu})^2}, \end{aligned} \quad (3.73)$$

$$\begin{aligned} \bar{\tilde{m}}_{\mathbf{RL},n} = \bar{\tilde{m}}_{\mathbf{LR},n} &= -\frac{\Gamma(\nu + \frac{1}{2} - ip)}{\Gamma(\nu + \frac{1}{2} + ip)} \\ &\times \frac{2i [(\cosh^2 \alpha e^{i\pi\nu} + \sinh^2 \alpha e^{-i\pi\nu} + \sinh 2\alpha \cos \pi\nu) \sinh \pi p_n]}{e^{2\pi p_n} (\cosh \alpha - \sinh \alpha e^{-2\pi p_n})^2 + e^{2i\pi\nu} (\cosh \alpha + \sinh \alpha e^{-2i\pi\nu})^2}. \end{aligned} \quad (3.74)$$

Here a special case appear for  $\nu = 3/2$ , where the result reduces to the result of **Case I**. Additionally, the non vanishing entries of the off diagonal components of the coefficient matrix for both of the cases in presence of  $\alpha$ -vacuum indicates the existence of quantum entanglement in the present computation, which we will explicitly show that finally give rise to a non vanishing entanglement entropy.

Finally to implement numerical analysis we use the following approximated expressions for the entries of the coefficient matrices as given by:

**Case I:**

$$\tilde{m}_{\mathbf{RL}} = e^{i(\theta+\frac{\pi}{2})} \frac{\sqrt{2} e^{-p\pi}}{\sqrt{\cosh 2\pi p - 1}} \frac{\sinh \pi p}{(\cosh^2 \alpha - \sinh^2 \alpha e^{-2\pi p})}, \quad (3.75)$$

$$\bar{\tilde{m}}_{\mathbf{RL},n} = e^{i(\theta+\frac{\pi}{2})} \frac{\sqrt{2} e^{-p_n\pi}}{\sqrt{\cosh 2\pi p_n - 1}} \frac{\sinh \pi p_n}{(\cosh^2 \alpha - \sinh^2 \alpha e^{-2\pi p_n})}, \quad (3.76)$$

which vanishes for Bunch Davies vacuum with  $\alpha = 0$ . On the other hand for a most generalized situation we get:

**Case II:**

$$\tilde{m}_{\mathbf{RL}} = m_{\mathbf{RL}} \times \frac{[\cosh^2 \alpha + \sinh^2 \alpha e^{-2i\pi\nu} + \sinh 2\alpha \cos \pi\nu e^{-i\pi\nu}]}{(\cosh^2 \alpha + \sinh^2 \alpha e^{-2\pi(p+i\nu)})}, \quad (3.77)$$

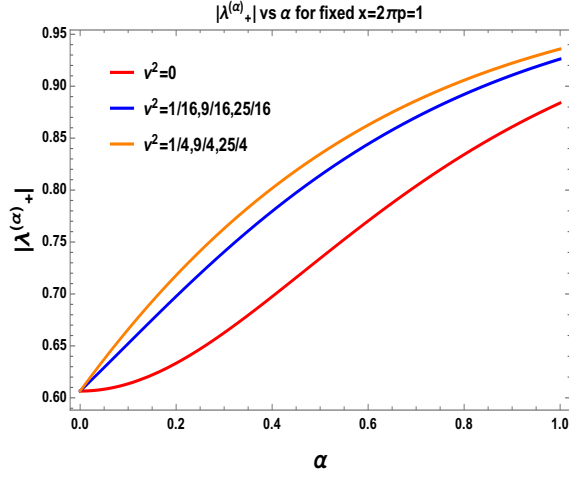
$$\bar{\tilde{m}}_{\mathbf{RL},n} = m_{\mathbf{RL},n} \times \frac{[\cosh^2 \alpha + \sinh^2 \alpha e^{-2i\pi\nu} + \sinh 2\alpha \cos \pi\nu e^{-i\pi\nu}]}{(\cosh^2 \alpha + \sinh^2 \alpha e^{-2\pi(p_n+i\nu)})}, \quad (3.78)$$

where for **Case II**,  $m_{\mathbf{RL}}$  and  $m_{\mathbf{RL},n}$  represent the contributions for the coefficient matrices from its Bunch Davies vacuum counterpart as given by <sup>7</sup>:

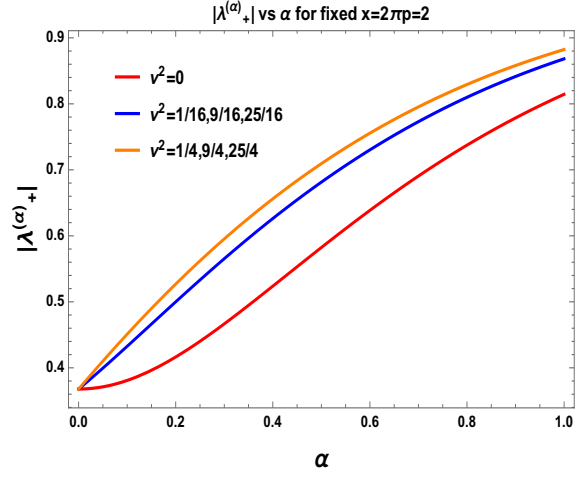
$$m_{\mathbf{RL}} = e^{i(\theta+\frac{\pi}{2})} \frac{\sqrt{2} e^{-p\pi} \sinh \pi p}{\sqrt{\cosh 2\pi p + \cos 2\pi\nu}}, \quad (3.79)$$

$$m_{\mathbf{RL},n} = e^{i(\theta+\frac{\pi}{2})} \frac{\sqrt{2} e^{-p_n\pi} \sinh \pi p_n}{\sqrt{\cosh 2\pi p_n + \cos 2\pi\nu}}. \quad (3.80)$$

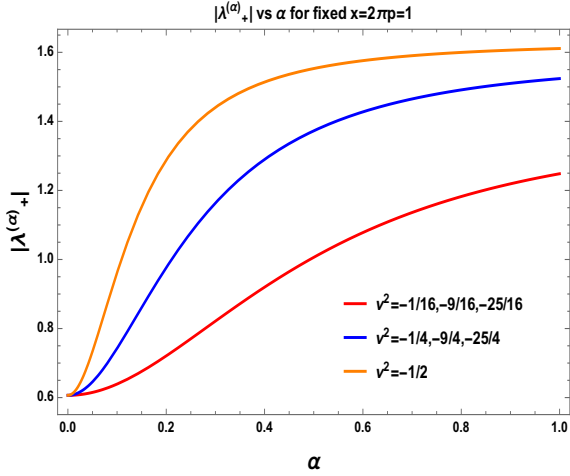




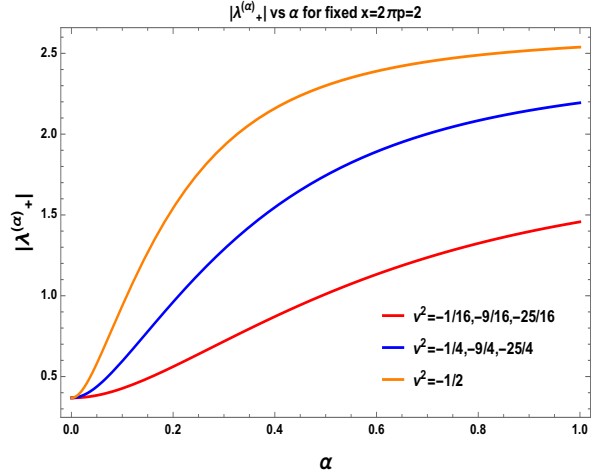
(a)  $|\lambda_+^{(\alpha)}|$  vs  $\alpha$  plot for  $x = 1$  and  $\nu^2 > 0$ .



(b)  $|\lambda_+^{(\alpha)}|$  vs  $\alpha$  plot for  $x = 2$  and  $\nu^2 > 0$ .



(c)  $|\lambda_+^{(\alpha)}|$  vs  $\alpha$  plot for  $x = 1$  and  $\nu^2 < 0$ .



(d)  $|\lambda_+^{(\alpha)}|$  vs  $\alpha$  plot for  $x = 2$  and  $\nu^2 < 0$ .

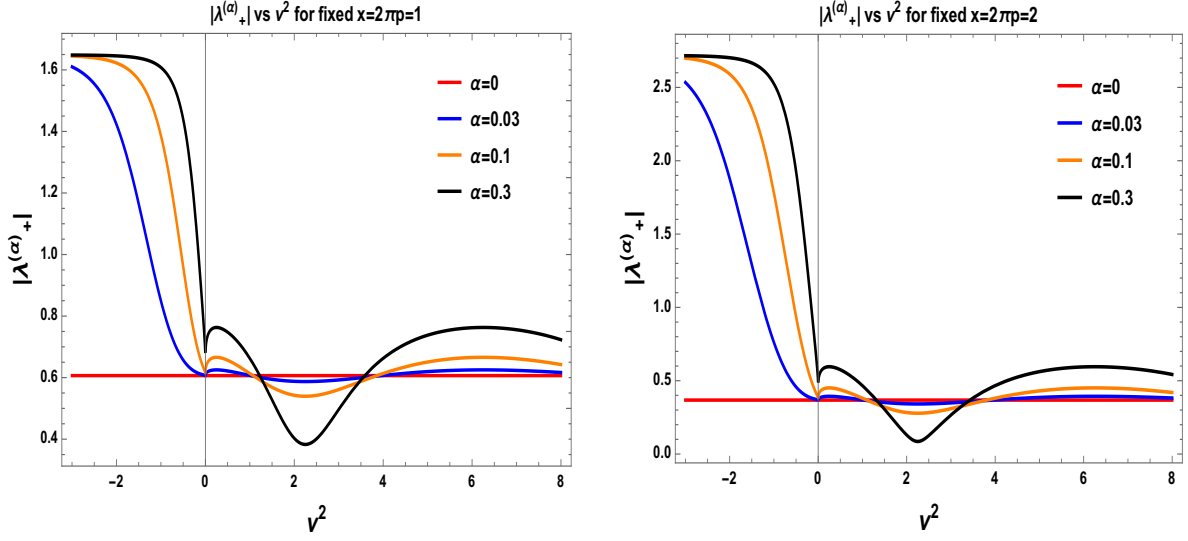
**Figure 1.** Behaviour of  $|\lambda_+^{(\alpha)}|$  in de Sitter space with respect to the parameter  $\alpha$ .

- In this context the eigenvalues of the coefficient matrix are given by from the complementary and particular part of the solution as:

$$\lambda_{\pm}^{(\alpha)} = \frac{1}{2} \left[ (\tilde{m}_{\mathbf{LL}} + \tilde{m}_{\mathbf{RR}}) \pm \sqrt{(\tilde{m}_{\mathbf{LL}} - \tilde{m}_{\mathbf{RR}})^2 + 4\tilde{m}_{\mathbf{RL}}\tilde{m}_{\mathbf{LR}}} \right], \quad (3.81)$$

$$\bar{\lambda}_{\pm, n}^{(\alpha)} = \frac{1}{2} \left[ (\tilde{m}_{\mathbf{LL}, n} + \tilde{m}_{\mathbf{RR}, n}) \pm \sqrt{(\tilde{m}_{\mathbf{LL}, n} - \tilde{m}_{\mathbf{RR}, n})^2 + 4\tilde{m}_{\mathbf{RL}, n}\tilde{m}_{\mathbf{LR}, n}} \right]. \quad (3.82)$$

<sup>7</sup>For rest of the analysis we absorb this overall phase factor  $e^{i\theta}$ .



(a)  $|\lambda_+^{(\alpha)}|$  vs  $\nu^2$  plot for  $x = 1$  and  $\alpha = 0, 0.03, 0.1, 0.3$ . (b)  $|\lambda_+^{(\alpha)}|$  vs  $\nu^2$  plot for  $x = 2$  and  $\alpha = 0, 0.03, 0.1, 0.3$ .

**Figure 2.** Behaviour of  $|\lambda_+^{(\alpha)}|$  in de Sitter space with respect to mass parameter  $\nu^2$  for  $x = 1$  and  $x = 2$ . Here it is important to note that,  $|\lambda_+^{(\alpha)}| = |\lambda_-^{(\alpha)}|$ .

In terms of the result obtained for the coefficient matrices for **Case I** and **Case II** we get:

**Case I :**

$$\lambda_{\pm}^{(\alpha)} = \tilde{m}_{\mathbf{RR}} \pm \tilde{m}_{\mathbf{RL}} = e^{i(\theta + \frac{\pi}{2})} e^{-p\pi} \frac{[\sinh 2\alpha \sinh \pi p \pm 1]}{(\cosh^2 \alpha - \sinh^2 \alpha e^{-2\pi p})}, \quad (3.83)$$

$$\lambda_{\pm, n}^{(\alpha)} = \tilde{m}_{\mathbf{RR}, n} \pm \tilde{m}_{\mathbf{RL}, n} = e^{i(\theta + \frac{\pi}{2})} e^{-p_n \pi} \frac{[\sinh 2\alpha \sinh \pi p_n \pm 1]}{(\cosh^2 \alpha - \sinh^2 \alpha e^{-2\pi p_n})}. \quad (3.84)$$

**Case II :**

$$\begin{aligned} \lambda_{\pm}^{(\alpha)} &= \tilde{m}_{\mathbf{RR}} \pm \tilde{m}_{\mathbf{RL}} \\ &= e^{i\theta} \frac{\sqrt{2} e^{-p\pi} (\cos \pi \nu \pm i \sinh \pi p)}{\sqrt{\cosh 2\pi p + \cos 2\pi \nu}} \frac{[\cosh^2 \alpha + \sinh^2 \alpha e^{-2i\pi \nu} \pm i \sinh 2\alpha \sinh \pi p e^{-i\pi \nu}]}{(\cosh^2 \alpha + \sinh^2 \alpha e^{-2\pi(p+i\nu)})}, \end{aligned} \quad (3.85)$$

$$\begin{aligned} \lambda_{\pm, n}^{(\alpha)} &= \tilde{m}_{\mathbf{RR}, n} \pm \tilde{m}_{\mathbf{RL}, n} \\ &= e^{i\theta} \frac{\sqrt{2} e^{-p_n \pi} (\cos \pi \nu \pm i \sinh \pi p_n)}{\sqrt{\cosh 2\pi p_n + \cos 2\pi \nu}} \frac{[\cosh^2 \alpha + \sinh^2 \alpha e^{-2i\pi \nu} \pm i \sinh 2\alpha \sinh \pi p_n e^{-i\pi \nu}]}{(\cosh^2 \alpha + \sinh^2 \alpha e^{-2\pi(p_n+i\nu)})}. \end{aligned} \quad (3.86)$$

In fig. (1) we have shown the behaviour of the magnitude of the eigenvalue  $|\lambda_+^{(\alpha)}|$  with the variation of the parameter  $\alpha$  for mass parameter  $\nu^2 \geq 0$  with  $x = 1$  (fig. (1(a))) and  $x = 2$  (fig. (1(a))),  $\nu^2 < 0$  with  $x = 1$  (fig. (1(c))) and  $x = 2$  (fig. (1(d))) respectively. In both fig. (1(a)) and fig. (1(b)) magnitude of the eigenvalue  $|\lambda_+^{(\alpha)}|$  increase with the increase in the parameter  $\alpha$ . In fig. (1(c)) and fig. (1(d)) magnitude of the eigenvalue  $|\lambda_+^{(\alpha)}|$  also increase with the increase in the parameter  $\alpha$  in a different fashion.

Further, in fig. (2) we have shown the behaviour of the magnitude of the eigenvalue  $|\lambda_+^{(\alpha)}|$  with the respect mass parameter  $\nu^2$  for fixed value of the rescaled **SO(3, 1)** quantum number  $x = 1$  (fig. (2(a))) and  $x = 2$  (fig. (2(b))). In fig. (2(a)) and fig. (2(b)) we also fix the parameter

$\alpha$  at,  $\alpha = 0$  (**red**),  $\alpha = 0.03$  (**blue**),  $\alpha = 0.1$  (**orange**) and  $\alpha = 0.3$  (**black**) respectively. For  $x = 1$  and  $x = 2$  comparing the behaviour obtained for different values of  $\alpha$  in  $\nu^2 > 0$  region, it is observed that the amplitude of the aperiodic oscillations are larger for  $\alpha = 0.3$  compared to the results obtained for  $\alpha = 0, \alpha = 0.03$  and  $\alpha = 0.1$ . For  $\nu^2 < 0$  region both the plots show identical behaviour for all values of the parameter  $\alpha$ .

To find a suitable basis first of all we trace over all possible contributions from  $\mathbf{R}$  and  $\mathbf{L}$  region. To implement this we need to perform another Bogoliubov transformation introducing new sets of operators as given by:

$$\tilde{c}_{\mathbf{R}} = \tilde{u} b_{\mathbf{R}} + \tilde{v} b_{\mathbf{R}}^\dagger, \quad \tilde{c}_{\mathbf{L}} = \bar{\tilde{u}} b_{\mathbf{L}} + \bar{\tilde{v}} b_{\mathbf{L}}^\dagger, \quad (3.87)$$

$$\tilde{C}_{\mathbf{R},n} = \tilde{U}_n b_{\mathbf{R},n} + \tilde{V}_n b_{\mathbf{R},n}^\dagger, \quad \tilde{C}_{\mathbf{L},n} = \bar{\tilde{U}}_n b_{\mathbf{L},n} + \bar{\tilde{V}}_n b_{\mathbf{L},n}^\dagger, \quad (3.88)$$

where following conditions are satisfied:

$$|\tilde{u}|^2 - |\tilde{v}|^2 = 1, \quad |\bar{\tilde{u}}|^2 - |\bar{\tilde{v}}|^2 = 1, \quad |\tilde{U}_n|^2 - |\tilde{V}_n|^2 = 1, \quad |\bar{\tilde{U}}_n|^2 - |\bar{\tilde{V}}_n|^2 = 1. \quad (3.89)$$

Here using these new sets of operators one can write the  $\alpha$ -vacuum state in terms of new basis represented by the direct product of  $\mathbf{R}'$  and  $\mathbf{L}'$  vacuum state as:

$$|\alpha\rangle = e^{\hat{Q}} (|\mathbf{R}\rangle \otimes |\mathbf{L}\rangle) = \frac{1}{\tilde{\mathcal{N}}_p^{(\alpha)}} e^{\hat{Q}} (|\mathbf{R}'\rangle \otimes |\mathbf{L}'\rangle)^{(\alpha)}, \quad (3.90)$$

where we introduce a new composite operator  $\hat{Q}$  which is defined in the new transformed basis as:

$$\hat{Q} = \gamma_p^{(\alpha)} \tilde{c}_{\mathbf{R}}^\dagger \tilde{c}_{\mathbf{L}}^\dagger + \sum_{n=0}^{\infty} \Gamma_{p,n}^{(\alpha)} \tilde{C}_{\mathbf{R},n}^\dagger \tilde{C}_{\mathbf{L},n}^\dagger, \quad (3.91)$$

where  $\gamma_p^{(\alpha)}$  and  $\Gamma_{p,n}^{(\alpha)}$  are defined corresponding to the complementary and particular solution, which we will explicitly compute further for  $\alpha$  vacuum. Additionally, it is important to note that the overall normalization factor  $\tilde{\mathcal{N}}_p^{(\alpha)}$  is defined as:

$$\tilde{\mathcal{N}}_p^{(\alpha)} = \left| e^{\hat{Q}} (|\mathbf{R}'\rangle \otimes |\mathbf{L}'\rangle)^{(\alpha)} \right| \approx \left[ 1 - \left( |\gamma_p^{(\alpha)}|^2 + \sum_{n=0}^{\infty} |\Gamma_{p,n}^{(\alpha)}|^2 \right) \right]^{-1/2}, \quad (3.92)$$

which reduces to the result obtained for Bunch Davies vacuum in ref. [14] for  $\alpha = 0$ . In this calculation due to the second Bogoliubov transformation the direct product of the  $\mathbf{R}$  and  $\mathbf{L}$  vacuum state is connected to the direct product of the new  $\mathbf{R}'$  and  $\mathbf{L}'$  vacuum state as:

$$(|\mathbf{R}\rangle \otimes |\mathbf{L}\rangle) \rightarrow (|\mathbf{R}'\rangle \otimes |\mathbf{L}'\rangle)^{(\alpha)} = \tilde{\mathcal{N}}_p^{(\alpha)} e^{-\hat{Q}} e^{\hat{Q}} (|\mathbf{R}\rangle \otimes |\mathbf{L}\rangle). \quad (3.93)$$

Let us now mention the commutation relations of the creation and annihilation operators corresponding to the new sets of oscillators describing the  $\mathbf{R}'$  and  $\mathbf{L}'$  vacuum state as:

$$[\tilde{c}_i, \tilde{c}_j^\dagger] = \delta_{ij}, \quad [\tilde{c}_i, \tilde{c}_j] = 0 = [\tilde{c}_i^\dagger, \tilde{c}_j^\dagger]. \quad (3.94)$$

$$[\tilde{C}_{i,n}, \tilde{C}_{j,m}^\dagger] = \delta_{ij} \delta_{nm}, \quad [\tilde{C}_{i,n}, \tilde{C}_{j,m}] = 0 = [\tilde{C}_{i,m}^\dagger, \tilde{C}_{j,m}^\dagger]. \quad (3.95)$$

Here for  $\alpha$  vacuum the oscillator algebra is exactly same as that obtained for Bunch Davies vacuum. However for  $\alpha$  vacuum the structure of these operators are completely different and also they are

acting in a different Hilbert space  $\mathcal{H}_\alpha$ , which is characterised by one parameter  $\alpha$ . Here it is important to note that for  $\alpha = 0$  these oscillators will act on Bunch Davies vacuum state where the corresponding Hilbert space,  $\mathcal{H}_{\mathbf{BD}}$  is the subclass of  $\mathcal{H}_\alpha$ .

In this context, the operations of creation and annihilation operators defined after on the  $\alpha$  vacuum state are appended below:

$$\tilde{c}_{\mathbf{R}}|\alpha\rangle = \gamma_p^{(\alpha)} \tilde{c}_{\mathbf{L}}^\dagger|\alpha\rangle, \quad \tilde{c}_{\mathbf{L}}|\alpha\rangle = \gamma_p^{(\alpha)} \tilde{c}_{\mathbf{R}}^\dagger|\alpha\rangle, \quad (3.96)$$

$$\tilde{C}_{\mathbf{R},n}|\alpha\rangle = \Gamma_{p,n}^{(\alpha)} \tilde{C}_{\mathbf{L},n}^\dagger|\alpha\rangle, \quad \tilde{C}_{\mathbf{L},n}|\alpha\rangle = \Gamma_{p,n}^{(\alpha)} \tilde{C}_{\mathbf{R},n}^\dagger|\alpha\rangle. \quad (3.97)$$

Further, one can express the new  $c$  type annihilation operators in terms of the old  $b$  type annihilation operators as:

$$\tilde{c}_J = b_I \tilde{\mathcal{G}}_J^I, \quad \tilde{C}_{J(n)} = \bar{b}_{J(n)} \left( \tilde{\mathcal{G}}_{(n)} \right)_J^I. \quad (3.98)$$

Here the matrices  $\tilde{\mathcal{G}}_J^I$  and  $\left( \tilde{\mathcal{G}}_{(n)} \right)_J^I$  for  $\alpha$  vacuum are defined as:

$$\tilde{\mathcal{G}}_J^I = \begin{pmatrix} \tilde{U}_q & \tilde{V}_q^* \\ \tilde{V}_q & \tilde{U}_q^* \end{pmatrix}, \quad \left( \tilde{\mathcal{G}}_{(n)} \right)_J^I = \begin{pmatrix} \tilde{\bar{U}}_{q,n} & \tilde{\bar{V}}_{\sigma q,n}^* \\ \tilde{\bar{V}}_{q,n} & \tilde{\bar{U}}_{q,n}^* \end{pmatrix}, \quad (3.99)$$

Here the entries of the matrices for  $\alpha$  vacuum are given by:

$$\tilde{U}_q \equiv \mathbf{diag}(\tilde{u}, \tilde{\bar{u}}), \quad \tilde{V}_q \equiv \mathbf{diag}(\tilde{v}, \tilde{\bar{v}}), \quad \tilde{\bar{U}}_{q,n} \equiv \mathbf{diag}(\tilde{U}_n, \tilde{\bar{U}}_n), \quad \tilde{\bar{V}}_{q,n} \equiv \mathbf{diag}(\tilde{V}_n, \tilde{\bar{V}}_n) \quad (3.100)$$

Further using Eq (3.87) and Eq (3.88), in Eq (3.96) and Eq (3.97), we get the following sets of homogeneous equations for **Case I** and **Case II**:

**For complementary solution :**

$$\tilde{m}_{\mathbf{RR}}\tilde{u} + \tilde{v} - \gamma_p^{(\alpha)}\tilde{m}_{\mathbf{RL}}\tilde{\bar{v}}^* = 0, \quad (3.101)$$

$$\tilde{m}_{\mathbf{RR}}\tilde{\bar{u}} + \tilde{\bar{v}} - \gamma_p^{(\alpha)}\tilde{m}_{\mathbf{RL}}\tilde{v}^* = 0, \quad (3.102)$$

$$\tilde{m}_{\mathbf{RL}}\tilde{u} - \gamma_p^{(\alpha)}\tilde{\bar{u}}^* - \gamma_p^{(\alpha)}\tilde{m}_{\mathbf{RR}}\tilde{\bar{v}}^* = 0, \quad (3.103)$$

$$\tilde{m}_{\mathbf{RL}}\tilde{\bar{u}} - \gamma_p^{(\alpha)}\tilde{u}^* - \gamma_p^{(\alpha)}\tilde{m}_{\mathbf{RR}}\tilde{v}^* = 0, \quad (3.104)$$

**For particular solution :**

$$\tilde{m}_{\mathbf{RR},n}\tilde{U}_n + \tilde{V}_n - \Gamma_{p,n}^{(\alpha)}\tilde{m}_{\mathbf{RL},n}\tilde{\bar{V}}_n^* = 0, \quad (3.105)$$

$$\tilde{m}_{\mathbf{RR},n}\tilde{\bar{U}}_n + \tilde{\bar{V}}_n - \Gamma_{p,n}^{(\alpha)}\tilde{m}_{\mathbf{RL},n}\tilde{V}_n^* = 0, \quad (3.106)$$

$$\tilde{m}_{\mathbf{RL},n}\tilde{U}_n - \Gamma_{p,n}^{(\alpha)}\tilde{\bar{U}}_n^* - \Gamma_{p,n}^{(\alpha)}\tilde{m}_{\mathbf{RR},n}\tilde{\bar{V}}_n^* = 0, \quad (3.107)$$

$$\tilde{m}_{\mathbf{RL},n}\tilde{\bar{U}}_n - \Gamma_{p,n}^{(\alpha)}\tilde{U}_n^* - \Gamma_{p,n}^{(\alpha)}\tilde{m}_{\mathbf{RR},n}\tilde{V}_n^* = 0, \quad (3.108)$$

In the **Case II** with  $\alpha$  vacuum it is not sufficient to use  $\tilde{v}^* = \tilde{\bar{v}}$ ,  $\tilde{u}^* = \tilde{\bar{u}}$  for particular part and also  $\tilde{V}_n^* = \tilde{\bar{V}}_n$ ,  $\tilde{U}_n^* = \tilde{\bar{U}}_n$  for the complementary part. In this case the system of four equations each for complementary and particular part will not be reduced to two sets of simplified equations. This is an outcome of the fact that in case of  $\alpha$  vacuum the entries of the coefficient matrices  $\tilde{m}_{ij}$  and

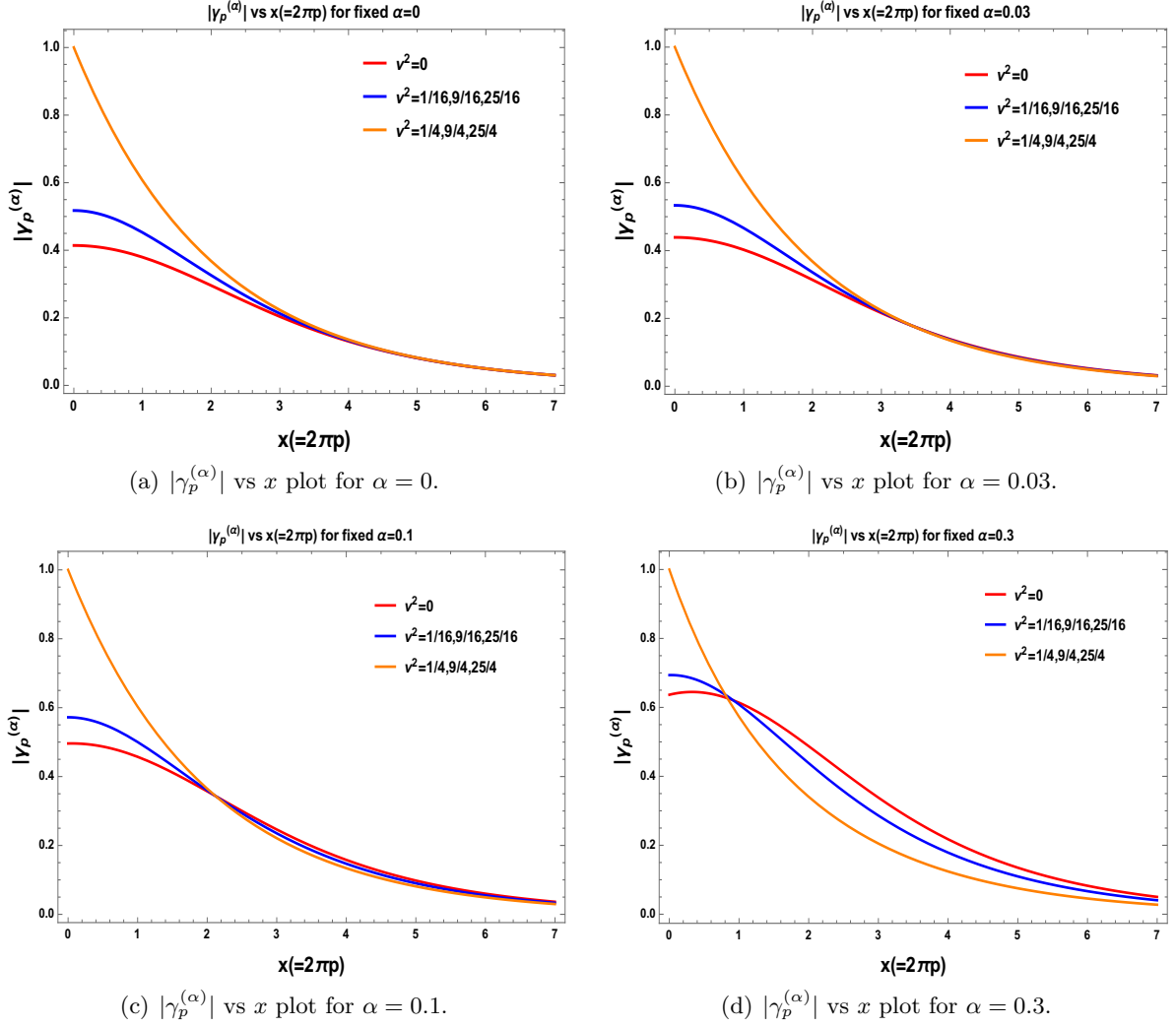


**Figure 3.** Behaviour of  $|\gamma_p^{(\alpha)}|$  in de Sitter space with respect to the rescaled  $\mathbf{SO}(1, 3)$  principal quantum number  $x$  for ‘+’ branch of solution.

$\tilde{m}_{ij,n}$  are complex in nature, which is either real or imaginary in case of Bunch Davies vacuum state consider all signatures of the mass parameter  $\nu^2$ . To solve these equations for  $\gamma_p^{(\alpha)}$  and  $\Gamma_{p,n}^{(\alpha)}$  here we need to use additionally the normalization conditions,  $|\tilde{u}|^2 - |\tilde{v}|^2 = 1$  and  $|\tilde{U}_n|^2 - |\tilde{V}_n|^2 = 1$ .

Finally, the non trivial solutions obtained from these system of equations for **Case I** and **Case II** can be expressed as:

$$\begin{aligned}
\gamma_p^{(\alpha)} = & \frac{1}{\sqrt{2}|\tilde{m}_{\mathbf{RL}}|} \left[ (1 + |\tilde{m}_{\mathbf{RL}}|^4 + |\tilde{m}_{\mathbf{RR}}|^4 \right. \\
& - 2|\tilde{m}_{\mathbf{RR}}|^2 - \tilde{m}_{\mathbf{RR}}^2(\tilde{m}_{\mathbf{RL}}^*)^2 - \tilde{m}_{\mathbf{RL}}^2(\tilde{m}_{\mathbf{RR}}^*)^2) \pm \left\{ (-1 - |\tilde{m}_{\mathbf{RL}}|^4 - |\tilde{m}_{\mathbf{RR}}|^4 \right. \\
& \left. \left. + 2|\tilde{m}_{\mathbf{RR}}|^2 + \tilde{m}_{\mathbf{RR}}^2(\tilde{m}_{\mathbf{RL}}^*)^2 + \tilde{m}_{\mathbf{RL}}^2(\tilde{m}_{\mathbf{RR}}^*)^2) - 4|\tilde{m}_{\mathbf{RL}}|^4 \right\}^{\frac{1}{2}} \right]^{\frac{1}{2}}, \quad (3.109)
\end{aligned}$$

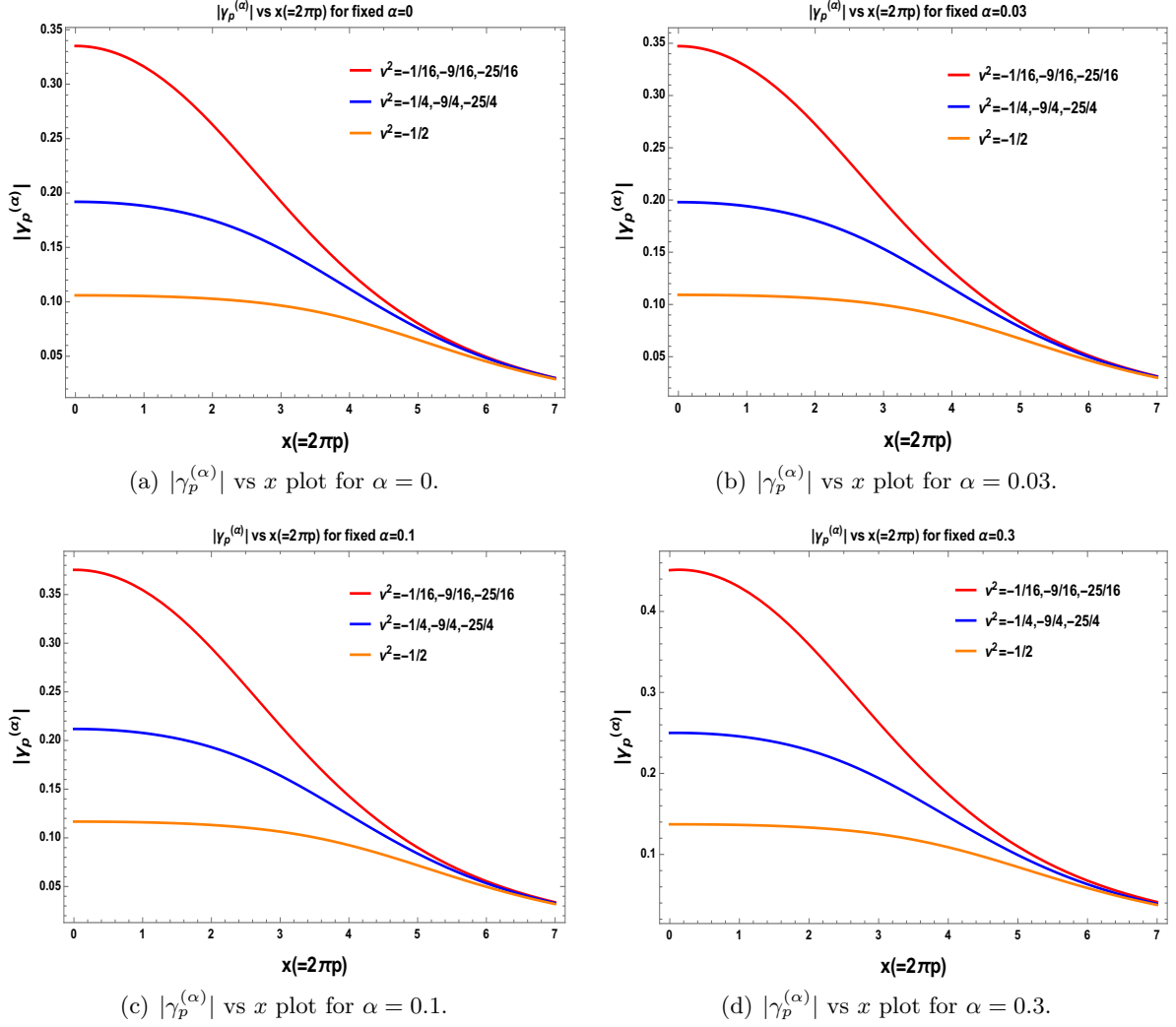


**Figure 4.** Behaviour of  $|\gamma_p^{(\alpha)}|$  in de Sitter space with respect to the rescaled  $\mathbf{SO}(1, 3)$  principal quantum number  $x$  for ‘+’ branch of solution.

$$\Gamma_{p,n}^{(\alpha)} = \frac{1}{\sqrt{2}|\tilde{m}_{\mathbf{RL},n}|} \left[ (1 + |\tilde{m}_{\mathbf{RL},n}|^4 + |\tilde{m}_{\mathbf{RR},n}|^4 - 2|\tilde{m}_{\mathbf{RR},n}|^2 - \tilde{m}_{\mathbf{RR},n}^2(\tilde{m}_{\mathbf{RL},n}^*)^2 - \tilde{m}_{\mathbf{RL},n}^2(\tilde{m}_{\mathbf{RR},n}^*)^2) \pm \{ (-1 - |\tilde{m}_{\mathbf{RL},n}|^4 - |\tilde{m}_{\mathbf{RR},n}|^4 + 2|\tilde{m}_{\mathbf{RR},n}|^2 + \tilde{m}_{\mathbf{RR},n}^2(\tilde{m}_{\mathbf{RL},n}^*)^2 + \tilde{m}_{\mathbf{RL},n}^2(\tilde{m}_{\mathbf{RR},n}^*)^2) - 4|\tilde{m}_{\mathbf{RL},n}|^4 \}^{\frac{1}{2}} \right]^{\frac{1}{2}}, \quad (3.110)$$

where the components  $\tilde{m}_{\mathbf{RR}} = \tilde{m}_{\mathbf{LL}}$ ,  $\tilde{m}_{\mathbf{RL}} = \tilde{m}_{\mathbf{LR}}$  and  $\tilde{m}_{\mathbf{RR},n} = \tilde{m}_{\mathbf{LL},n}$ ,  $\tilde{m}_{\mathbf{RL},n} = \tilde{m}_{\mathbf{LR},n}$  are defined for **Case I** and **Case II** in Eqn (3.61), Eqn (3.62), Eqn (3.63), Eqn (3.64) and Eqn (3.71), Eqn (3.72), Eqn (3.73), Eqn (3.74) respectively. Note that here in both the solutions for  $\gamma_p^{(\alpha)}$  and  $\Gamma_{p,n}^{(\alpha)}$  we absorb the overall phase factor.

After further simplification we get the following expressions for the non trivial solutions from

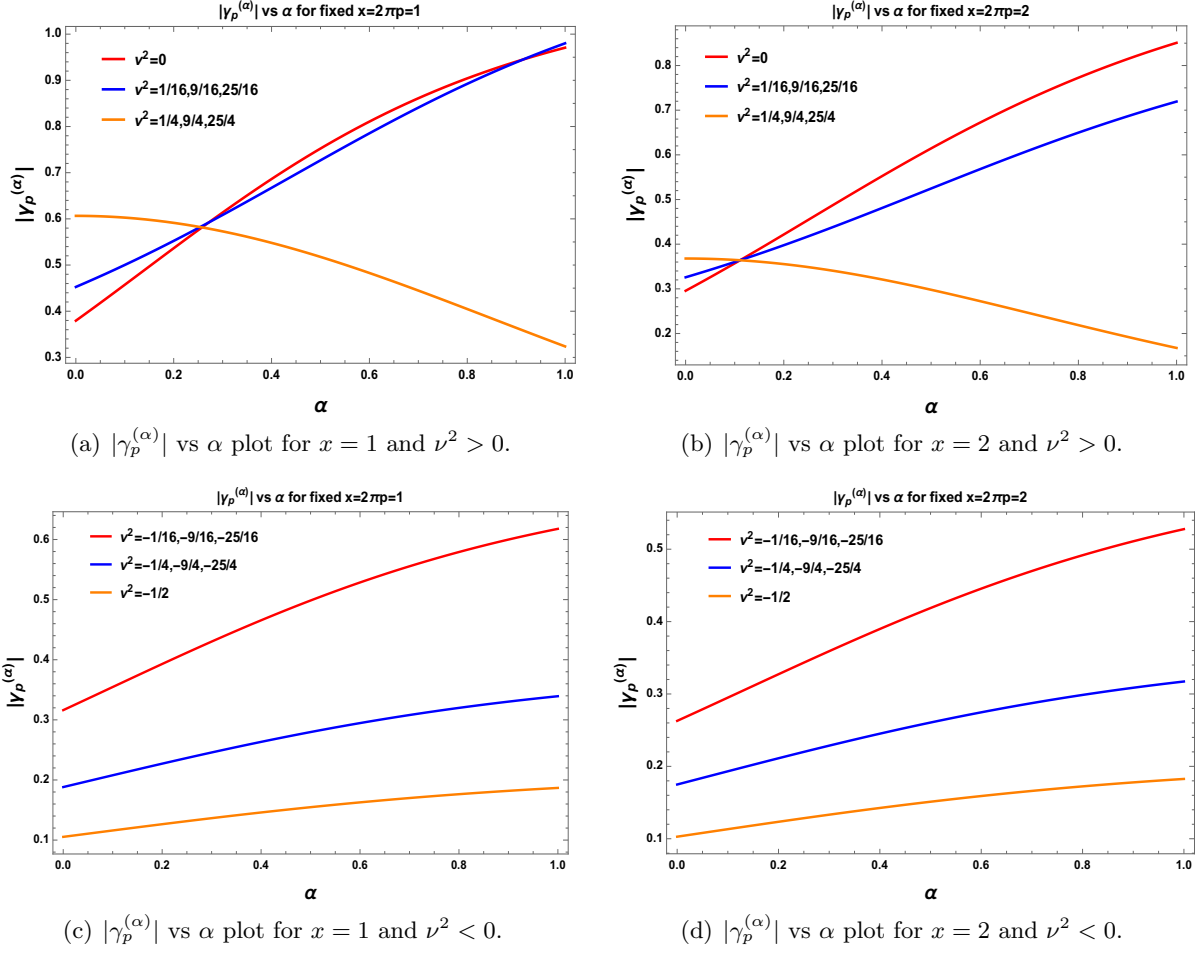


**Figure 5.** Behaviour of  $|\gamma_p^{(\alpha)}|$  in de Sitter space with respect to the parameter  $\alpha$  for ‘+’ branch of solution.

**Case I** and **Case II** as given by:

**Case I:**

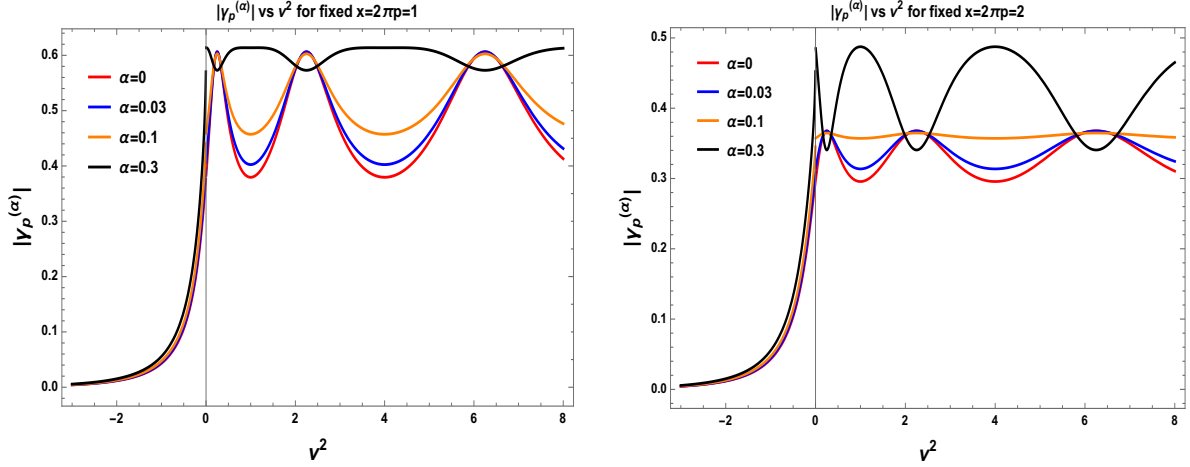
$$\gamma_p^{(\alpha)} \approx \pm i e^{\mp p\pi} \times \frac{1}{(\cosh^2 \alpha - \sinh^2 \alpha e^{-2\pi p})}, \quad (3.111)$$

$$\Gamma_{p,n}^{(\alpha)} \approx \pm i e^{\mp p_n\pi} \times \frac{1}{(\cosh^2 \alpha - \sinh^2 \alpha e^{-2\pi p_n})}. \quad (3.112)$$

**Case II:**

$$\gamma_p^{(\alpha)} \approx i \frac{\sqrt{2}}{\sqrt{\cosh 2\pi p + \cos 2\pi\nu \pm \sqrt{\cosh 2\pi p + \cos 2\pi\nu + 2}}} \times \frac{[\cosh^2 \alpha + \sinh^2 \alpha e^{2i\pi\nu} + \sinh 2\alpha \cos \pi\nu e^{i\pi\nu}]}{(\cosh^2 \alpha + \sinh^2 \alpha e^{-2\pi(p-i\nu)}), \quad (3.113)$$

$$\Gamma_{p,n}^{(\alpha)} \approx i \frac{\sqrt{2}}{\sqrt{\cosh 2\pi p_n + \cos 2\pi\nu \pm \sqrt{\cosh 2\pi p_n + \cos 2\pi\nu + 2}}} \times \frac{[\cosh^2 \alpha + \sinh^2 \alpha e^{2i\pi\nu} + \sinh 2\alpha \cos \pi\nu e^{i\pi\nu}]}{(\cosh^2 \alpha + \sinh^2 \alpha e^{-2\pi(p_n-i\nu)}}. \quad (3.114)$$



(a)  $|\gamma_p^{(\alpha)}|$  vs  $\nu^2$  plot for  $x = 1$  and  $\alpha = 0, 0.03, 0.1, 0.3$ . (b)  $|\gamma_p^{(\alpha)}|$  vs  $\nu^2$  plot for  $x = 2$  and  $\alpha = 0, 0.03, 0.1, 0.3$ .

**Figure 6.** Behaviour of  $|\gamma_p^{(\alpha)}|$  in de Sitter space with respect to mass parameter  $\nu^2$  for  $x = 1$ . for ‘+’ branch of solution.

In fig. (3) we have shown the behaviour of the magnitude of the solution  $|\gamma_p^{(\alpha)}|$  with the variation of the rescaled  $\mathbf{SO}(1, 3)$  quantum number  $x = 2\pi p$  for  $\alpha = 0$  (fig. (3(a))),  $\alpha = 0.03$  (fig. (3(b))),  $\alpha = 0.1$  (fig. (3(c))) and  $\alpha = 0.3$  (fig. (3(d))) along with the mass parameter  $\nu^2 \geq 0$  respectively. In fig. (3(a)), fig. (3(b)), fig. (3(c)) and fig. (3(d)) we use  $\nu^2 = 0$  (red),  $\nu^2 = 1/16, 9/16, 25/16$  (blue) and  $\nu^2 = 1/4, 9/4, 25/4$  (orange). For all  $\nu^2 \geq 0$  with  $\alpha = 0$  (fig. (3(a))) and  $\alpha = 0.03$  (fig. (3(b))) show almost similar behaviour. However, at  $x = 0$  the magnitude of the solution  $|\gamma_p^{(\alpha)}|$  for  $\nu^2 = 0, 1/16, 9/16, 25/16$  with  $\alpha = 0.03$  is slightly larger compared to the result obtained for  $\alpha = 0$  (Bunch Davies vacuum) case. But for  $\nu^2 = 1/4, 9/4, 25/4$  with  $\alpha = 0$  (fig. (3(a))) and  $\alpha = 0.03$  (fig. (3(b))) both the plots show exactly same behaviour. After comparing fig. (3(a)) and fig. (3(b)), we also observe that at  $x \approx 3.5$  for all values of  $\nu^2 \geq 0$  the magnitude of the solution  $|\gamma_p^{(\alpha)}|$  coincides at a single point and then further. On the other hand, for  $\alpha = 0.1$  (fig. (3(c))) and  $\alpha = 0.3$  (fig. (3(d))) both the plots show distinguishable features for  $\nu^2 = 0, 1/16, 9/16, 25/16$  and similar behaviour for  $\nu^2 = 1/4, 9/4, 25/4$ . Also in fig. (3(c)) and fig. (3(d)) a cross over take place at  $x \approx 2.2$  and  $x \approx 0.8$  respectively. However, for large values of  $x$  the magnitude of the solution  $|\gamma_p^{(\alpha)}|$  decrease to a very small non-vanishing value.

Further in fig. (4) we have shown the behaviour of the magnitude of the solution  $|\gamma_p^{(\alpha)}|$  with the variation of the rescaled  $\mathbf{SO}(1, 3)$  quantum number  $x = 2\pi p$  for  $\alpha = 0$  (fig. (4(a))),  $\alpha = 0.03$  (fig. (4(b))),  $\alpha = 0.1$  (fig. (4(c))) and  $\alpha = 0.3$  (fig. (4(d))) along with the mass parameter  $\nu^2 < 0$  respectively. In fig. (4(a)), fig. (4(b)), fig. (4(c)) and fig. (4(d)) we use  $\nu^2 = 0$  (red),  $\nu^2 = 1/16, 9/16, 25/16$  (blue) and  $\nu^2 = 1/4, 9/4, 25/4$  (orange). For all  $\nu^2 < 0$  it is observed that plots for  $\alpha = 0, \alpha = 0.03, \alpha = 0.1$  and  $\alpha = 0.3$  identical features. For all these plots for large values of  $x$  the magnitude of the solution  $|\gamma_p^{(\alpha)}|$  decrease to a very small value and at  $x = 0$  magnitudes are different for  $\alpha = 0, \alpha = 0.03, \alpha = 0.1$  and  $\alpha = 0.3$ .

Next in fig. (5) we have shown the behaviour of the magnitude of the solution  $|\gamma_p^{(\alpha)}|$  with the variation of the parameter  $\alpha$  for mass parameter  $\nu^2 \geq 0$  with  $x = 1$  (fig. (5(a))) and  $x = 2$  (fig. (5(b))),  $\nu^2 < 0$  with  $x = 1$  (fig. (5(c))) and  $x = 2$  (fig. (5(d))) respectively. In fig. (5(a)) magnitude of the solution  $|\gamma_p^{(\alpha)}|$  increase with the increase in the parameter  $\alpha$  and in fig. (5(b)) it decrease with respect to  $\alpha$ . Most importantly a crossover take place at  $\alpha \approx 0.25$  and  $\alpha \approx 0.9$



(fig. (5(a))) and  $\alpha \approx 0.1$  (fig. (5(b))) respectively. In fig. (5(c)) and fig. (5(d)) magnitude of the solution  $|\gamma_p^{(\alpha)}|$  increase with the increase in the parameter  $\alpha$ . Most importantly no crossover take place in fig. (5(c)) and fig. (5(d)).

Finally, in fig. (6) we have shown the behaviour of the magnitude of the solution  $|\gamma_p^{(\alpha)}|$  with the mass parameter  $\nu^2$  for fixed value of the rescaled  $\mathbf{SO}(1, \mathbf{3})$  quantum number  $x = 1$  (fig. (6(a))) and  $x = 2$  (fig. (6(b))). In fig. (6(a)) and fig. (6(b)) we also fix the parameter  $\alpha$  at,  $\alpha = 0$  (red),  $\alpha = 0.03$  (blue),  $\alpha = 0.1$  (orange) and  $\alpha = 0.3$  (black) respectively. For  $x = 1$  and  $x = 2$  both the plots show discontinuity at  $\nu^2 = 0$  for  $\alpha = 0.3$ . For  $x = 1$  comparing the behaviour obtained for different values of  $\alpha$  in  $\nu^2 > 0$  region, it is observed that the amplitude of the aperiodic oscillations are larger for  $\alpha = 0, \alpha = 0.03$  and  $\alpha = 0.1$  compared to the result obtained for  $\alpha = 0.3$ . On the other hand for  $x = 2$  in the region  $\nu^2 > 0$  the amplitude of the aperiodic oscillations are larger for  $\alpha = 0.3$  compared to the results obtained for  $\alpha = 0, \alpha = 0.03$  and  $\alpha = 0.1$ . However for  $\nu^2 < 0$  region both the plots show similar features for all values of the parameter  $\alpha$ . This implies that only for small mass parameter range ( $\nu^2 > 0$ ) one can able to distinguish between the features obtained for the " + " branch solution of  $|\gamma_p^{(\alpha)}|$  for all values of the parameter  $\alpha$ . Also in the large mass limiting range ( $\nu^2 < 0$ ) we get indistinguishable features for both plots obtained for  $x = 1$  and  $x = 2$ .

### 3.2 Construction of density matrix using $\alpha$ vacua

In this subsection our prime objective is construct the density matrix using the  $\alpha$  vacuum state which is expressed in terms of another sets of annihilation and creation operators in the Bogoliubov transformed frame. Here the Bunch Davies vacuum state can be expressed as a product of the quantum state for each oscillator in the new frame after Bogoliubov transformation. Each oscillators are labeled by the quantum numbers  $p, l$  and  $m$  in this calculation. After tracing over the right part of the Hilbert space we get the following expression for the density matrix for the left part of the Hilbert space for the **Case I** and **Case II** as:

$$(\rho_{\mathbf{L}}(\alpha))_{p,l,m} = \text{Tr}_{\mathbf{R}} |\alpha\rangle\langle\alpha|, \quad (3.115)$$

where the  $\alpha$  vacuum state can be written in terms of  $\tilde{c}$  type of oscillators as:

$$|\alpha\rangle \approx \left[ 1 - \left( |\gamma_p^{(\alpha)}|^2 + \sum_{n=0}^{\infty} |\Gamma_{p,n}^{(\alpha)}|^2 \right) \right]^{1/2} \exp \left[ \gamma_p^{(\alpha)} \tilde{c}_{\mathbf{R}}^\dagger \tilde{c}_{\mathbf{L}}^\dagger + \sum_{n=0}^{\infty} \Gamma_{p,n}^{(\alpha)} \tilde{C}_{\mathbf{R},n}^\dagger \tilde{C}_{\mathbf{L},n}^\dagger \right] \left( |\mathbf{R}'\rangle \otimes |\mathbf{L}'\rangle \right)^{(\alpha)}, \quad (3.116)$$

which is already derived in the earlier section. Further substituting Eq (3.116) in Eq (3.115), we get the following simplified expression for the density matrix for the left part of the Hilbert space for  $\alpha$  vacuum as:

$$\begin{aligned} (\rho_{\mathbf{L}}(\alpha))_{p,l,m} = & \underbrace{\left( 1 - |\gamma_p^{(\alpha)}|^2 \right) \sum_{k=0}^{\infty} |\gamma_p^{(\alpha)}|^{2k} |k; \widetilde{p, l, m}\rangle \langle k; \widetilde{p, l, m}|}_{\text{Complementary part}} \\ & + \underbrace{(f_p^{(\alpha)})^2 \sum_{n=0}^{\infty} \sum_{r=0}^{\infty} |\Gamma_{p,n}^{(\alpha)}|^{2r} |n, r; \widetilde{p, l, m}\rangle \langle n, r; \widetilde{p, l, m}|}_{\text{Particular part}}, \end{aligned} \quad (3.117)$$

where  $\gamma_p^{(\alpha)}$  and  $\Gamma_{p,n}^{(\alpha)}$  are derived in the earlier section. Also we define the  $\alpha$  parameter dependent source normalization factor  $f_p^{(\alpha)}$  as:

$$f_p^{(\alpha)} = \left( \sum_{n=0}^{\infty} \frac{1}{1 - |\Gamma_{p,n}^{(\alpha)}|^2} \right)^{-1}. \quad (3.118)$$

In this computation the states  $|k; \widetilde{p, l, m}\rangle$  and  $|n, r; \widetilde{p, l, m}\rangle$  are defined in terms of the quantum state  $|\mathbf{L}'\rangle$  as:

$$|k; \widetilde{p, l, m}\rangle = \frac{1}{\sqrt{k!}} (\tilde{C}_{\mathbf{L}}^\dagger)^k |\mathbf{L}'\rangle, \quad |n, r; \widetilde{p, l, m}\rangle = \frac{1}{\sqrt{r!}} (\tilde{C}_{\mathbf{L},n}^\dagger)^r |\mathbf{L}'\rangle. \quad (3.119)$$

Here we note that:

1. For  $\alpha$  vacuum density matrix is diagonal for a given set of the  $\mathbf{SO}(1, 3)$  quantum numbers  $p, l, m$  and additionally depends on the parameter  $\alpha$  explicitly. This leads to the total density matrix to take the following simplified form as:

$$\rho_{\mathbf{L}}(\alpha) = \left(1 - |\gamma_p^{(\alpha)}|^2\right) \mathbf{diag} \left(1, |\gamma_p^{(\alpha)}|^2, |\gamma_p^{(\alpha)}|^4, |\gamma_p^{(\alpha)}|^6 \dots\right) + (f_p^{(\alpha)})^2 \sum_{n=0}^{\infty} \mathbf{diag} \left(1, |\Gamma_{p,n}^{(\alpha)}|^2, |\Gamma_{p,n}^{(\alpha)}|^4, |\Gamma_{p,n}^{(\alpha)}|^6 \dots\right), \quad (3.120)$$

Here it is important to note that, for  $\alpha = 0$  we get back the result obtained for Bunch Davies vacuum which is mentioned in ref. [14].

2. To find out an acceptable normalization of the total density matrix in presence of  $\alpha$  vacuum state, we use the following limiting results:

$$\sum_{k=0}^{\infty} |\gamma_p^{(\alpha)}|^{2k} = \lim_{k \rightarrow \infty} \frac{1 - |\gamma_p^{(\alpha)}|^{2k}}{1 - |\gamma_p^{(\alpha)}|^2} \xrightarrow{|\gamma_p^{(\alpha)}| < 1 \forall \alpha} \frac{1}{1 - |\gamma_p^{(\alpha)}|^2}, \quad (3.121)$$

$$\sum_{n=0}^{\infty} \sum_{r=0}^{\infty} |\Gamma_{p,n}^{(\alpha)}|^{2r} = \sum_{n=0}^{\infty} \lim_{r \rightarrow \infty} \frac{1 - |\Gamma_{p,n}^{(\alpha)}|^{2r}}{1 - |\Gamma_{p,n}^{(\alpha)}|^2} \xrightarrow{|\Gamma_{p,n}^{(\alpha)}| < 1 \forall n, \alpha} \sum_{n=0}^{\infty} \frac{1}{1 - |\Gamma_{p,n}^{(\alpha)}|^2} = (f_p^{(\alpha)})^{-1}. \quad (3.122)$$

Consequently using these results for  $\alpha$  vacuum we get:

$$\mathbf{Tr} \left[ \left(1 - |\gamma_p^{(\alpha)}|^2\right) \mathbf{diag} \left(1, |\gamma_p^{(\alpha)}|^2, |\gamma_p^{(\alpha)}|^4, |\gamma_p^{(\alpha)}|^6 \dots\right) \right] = \left(1 - |\gamma_p^{(\alpha)}|^2\right) \sum_{k=0}^{\infty} |\gamma_p^{(\alpha)}|^{2k} = 1, \quad (3.123)$$

$$\mathbf{Tr} \left[ (f_p^{(\alpha)})^2 \sum_{n=0}^{\infty} \mathbf{diag} \left(1, |\Gamma_{p,n}^{(\alpha)}|^2, |\Gamma_{p,n}^{(\alpha)}|^4, |\Gamma_{p,n}^{(\alpha)}|^6 \dots\right) \right] = (f_p^{(\alpha)})^2 \sum_{n=0}^{\infty} \sum_{r=0}^{\infty} |\Gamma_{p,n}^{(\alpha)}|^{2r} = f_p^{(\alpha)}, \quad (3.124)$$

Consequently the normalization condition of this total density matrix in presence of  $\alpha$  vacuum state is given by:

$$\mathbf{Tr} \rho_{\mathbf{L}}(\alpha) = 1 + f_p^{(\alpha)}. \quad (3.125)$$

This result is consistent with the ref. [10] where  $f_p^{(\alpha)} = 0 \forall \alpha$  and also ref. [14] where  $\alpha = 0$  and  $f_p^{(0)} = f_p$ . But for simplicity it is better to maintain always  $\mathbf{Tr} \rho_{\mathbf{L}}(\alpha) = 1$  and to get this

result for  $\alpha$  vacuum the total density matrix can be redefined by changing the normalization constant as:

$$\begin{aligned}
(\rho_{\mathbf{L}}(\alpha))_{p,l,m} &= \frac{(1 - |\gamma_p^{(\alpha)}|^2)}{1 + f_p^{(\alpha)}} \sum_{k=0}^{\infty} |\gamma_p^{(\alpha)}|^{2k} |\widetilde{k; p, l, m}\rangle \langle \widetilde{k; p, l, m}| \\
&\quad + \frac{(f_p^{(\alpha)})^2}{1 + f_p^{(\alpha)}} \sum_{n=0}^{\infty} \sum_{r=0}^{\infty} |\Gamma_{p,n}^{(\alpha)}|^{2r} |\widetilde{n, r; p, l, m}\rangle \langle \widetilde{n, r; p, l, m}|, \quad (3.126)
\end{aligned}$$

In this context equivalent convention for normalization factors can also be chosen such that it always satisfies  $\text{Tr} \rho_{\mathbf{L}}(\alpha) = 1$  even the presence of source contribution <sup>8</sup>.

3. For each set of values of the  $\mathbf{SO}(1, 3)$  quantum numbers  $p, l, m$ , the density matrix yields  $(\rho_{\mathbf{L}})_{p,l,m}$  and so that the total density matrix can be expressed as a product of all such possible contributions:

$$\rho_{\mathbf{L}}(\alpha) = \prod_{p=0}^{\infty} \prod_{l=0}^{p-1} \prod_{m=-l}^{+l} (\rho_{\mathbf{L}}(\alpha))_{p,l,m}. \quad (3.129)$$

This also indicates that in such a situation entanglement is absent among all states which carries non identical  $\mathbf{SO}(1, 3)$  quantum numbers  $p, l, m$ .

4. Finally, the total density matrix can be written in terms of entanglement modular Hamiltonian of the axionic pair as,  $\rho_{\mathbf{L}}(\alpha) = e^{-\beta \mathcal{H}_{\text{ENT}}}$ , where at finite temperature  $T_{\text{dS}}$  of de Sitter space  $\beta = 2\pi/T_{\text{dS}}$ . If we further assume that the dynamical Hamiltonian in de Sitter space is represented by entangled Hamiltonian then for a given principal quantum number  $p$  the Hamiltonian for axion can be expressed as:

$$\mathcal{H}_p(\alpha) = \left[ E_p^{(\alpha)} \tilde{c}_p^\dagger \tilde{c}_p + \sum_{n=0}^{\infty} \mathcal{E}_{p,n}^{(\alpha)} \tilde{C}_{p,n}^\dagger \tilde{C}_{p,n} \right]. \quad (3.130)$$

Acting this Hamiltonian on the  $\alpha$  vacuum state we find:

$$\begin{aligned}
\mathcal{H}_p(\alpha)|\alpha\rangle &\approx \left[ 1 - \left( |\gamma_p^{(\alpha)}|^2 + \sum_{n=0}^{\infty} |\Gamma_{p,n}^{(\alpha)}|^2 \right) \right]^{1/2} \times \\
&\quad \left[ E_p^{(\alpha)} \tilde{c}_p^\dagger \tilde{c}_p + \sum_{n=0}^{\infty} \mathcal{E}_{p,n}^{(\alpha)} \tilde{C}_{p,n}^\dagger \tilde{C}_{p,n} \right] \exp \left[ \gamma_p^{(\alpha)} \tilde{c}_{\mathbf{R}}^\dagger \tilde{c}_{\mathbf{L}}^\dagger + \sum_{m=0}^{\infty} \Gamma_{p,m}^{(\alpha)} \tilde{C}_{\mathbf{R},m}^\dagger \tilde{C}_{\mathbf{L},m}^\dagger \right] \left( |\mathbf{R}'\rangle \otimes |\mathbf{L}'\rangle \right)^{(\alpha)} \\
&= E_{\mathbf{T},p}^{(\alpha)} |\alpha\rangle, \quad (3.131)
\end{aligned}$$

<sup>8</sup> Here one can choose the following equivalent ansatz for total density matrix in presence of  $\alpha$  vacuum as:

$$(\rho_{\mathbf{L}}(\alpha))_{p,l,m} = a_p^{(\alpha)} \left[ \underbrace{\sum_{k=0}^{\infty} |\gamma_p^{(\alpha)}|^{2k} |\widetilde{k; p, l, m}\rangle \langle \widetilde{k; p, l, m}|}_{\text{Complementary part}} + \underbrace{(f_p^{(\alpha)})^2 \sum_{n=0}^{\infty} \sum_{r=0}^{\infty} |\Gamma_{p,n}^{(\alpha)}|^{2r} |\widetilde{n, r; p, l, m}\rangle \langle \widetilde{n, r; p, l, m}|}_{\text{Particular part}} \right], \quad (3.127)$$

where the overall factor  $a_p^{(\alpha)}$  is defined as:

$$a_p^{(\alpha)} = \left[ \frac{1}{1 - |\gamma_p^{(\alpha)}|^2} + f_p^{(\alpha)} \right]^{-1}. \quad (3.128)$$

where the total energy spectrum of this system for  $\alpha$  vacuum can be written as:

$$\boxed{E_{\mathbf{T},p}^{(\alpha)} = E_p^{(\alpha)} + \sum_{n=0}^{\infty} \mathcal{E}_{p,n}^{(\alpha)} \quad \forall \alpha}, \quad (3.132)$$

where the energy spectrum corresponding to the complementary and particular part of the wave function corresponding to the  $\alpha$  vacuum state are given by:

$$E_p^{(\alpha)} = -\frac{1}{2\pi} \ln(|\gamma_p^{(\alpha)}|^2), \quad \mathcal{E}_{p,n}^{(\alpha)} = -\frac{1}{2\pi} \ln \left( B_{p,n}^{(\alpha)} \right). \quad (3.133)$$

One can also recast the total energy spectrum of for  $\alpha$  vacuum as:

$$\boxed{E_{\mathbf{T},p}^{(\alpha)} = -\frac{1}{2\pi} \ln \left( |\gamma_p^{(\alpha)}|^2 \prod_{n=0}^{\infty} B_{p,n}^{(\alpha)} \right)} \quad \text{with} \quad B_{p,n}^{(\alpha)} = \frac{1}{1 - |\Gamma_{p,n}^{(\alpha)}|^2}, \quad (3.134)$$

Now if we consider any arbitrary mass parameter  $\nu$  and any arbitrary value of the parameter  $\alpha$ , in that case the  $\mathbf{SO}(1, 3)$  principal quantum number  $p$  dependent spectrum can be expressed as:

$$E_p^{(\alpha)} = -\frac{1}{2\pi} \ln \left\{ \frac{1}{2|\tilde{m}_{\mathbf{RL}}|^2} \left[ (1 + |\tilde{m}_{\mathbf{RL}}|^4 + |\tilde{m}_{\mathbf{RR}}|^4 - 2|\tilde{m}_{\mathbf{RR}}|^2 - \tilde{m}_{\mathbf{RR}}^2(\tilde{m}_{\mathbf{RL}}^*)^2 - \tilde{m}_{\mathbf{RL}}^2(\tilde{m}_{\mathbf{RR}}^*)^2) \pm \left\{ (-1 - |\tilde{m}_{\mathbf{RL}}|^4 - |\tilde{m}_{\mathbf{RR}}|^4 + 2|\tilde{m}_{\mathbf{RR}}|^2 + \tilde{m}_{\mathbf{RR}}^2(\tilde{m}_{\mathbf{RL}}^*)^2 + \tilde{m}_{\mathbf{RL}}^2(\tilde{m}_{\mathbf{RR}}^*)^2)^2 - 4|\tilde{m}_{\mathbf{RL}}|^4 \right\}^{\frac{1}{2}} \right] \right\}, \quad (3.135)$$

$$\mathcal{E}_{p,n}^{(\alpha)} = \frac{1}{2\pi} \ln \left\{ 1 - \frac{1}{2|\tilde{m}_{\mathbf{RL},n}|^2} \left[ (1 + |\tilde{m}_{\mathbf{RL},n}|^4 + |\tilde{m}_{\mathbf{RR},n}|^4 - 2|\tilde{m}_{\mathbf{RR},n}|^2 - \tilde{m}_{\mathbf{RR},n}^2(\tilde{m}_{\mathbf{RL},n}^*)^2 - \tilde{m}_{\mathbf{RL},n}^2(\tilde{m}_{\mathbf{RR},n}^*)^2) \pm \left\{ (-1 - |\tilde{m}_{\mathbf{RL},n}|^4 - |\tilde{m}_{\mathbf{RR},n}|^4 + 2|\tilde{m}_{\mathbf{RR},n}|^2 + \tilde{m}_{\mathbf{RR},n}^2(\tilde{m}_{\mathbf{RL},n}^*)^2 + \tilde{m}_{\mathbf{RL},n}^2(\tilde{m}_{\mathbf{RR},n}^*)^2)^2 - 4|\tilde{m}_{\mathbf{RL},n}|^4 \right\}^{\frac{1}{2}} \right] \right\}. \quad (3.136)$$

In this case, the total energy spectrum for arbitrary parameter  $\alpha$  can be recast as:

$$E_{\mathbf{T},p}^{(\alpha)} = \frac{1}{2\pi} \ln 2 + \frac{1}{\pi} \ln |\tilde{m}_{\mathbf{RL}}| - \frac{1}{2\pi} \ln \left[ (1 + |\tilde{m}_{\mathbf{RL}}|^4 + |\tilde{m}_{\mathbf{RR}}|^4 - 2|\tilde{m}_{\mathbf{RR}}|^2 - \tilde{m}_{\mathbf{RR}}^2(\tilde{m}_{\mathbf{RL}}^*)^2 - \tilde{m}_{\mathbf{RL}}^2(\tilde{m}_{\mathbf{RR}}^*)^2) \pm \left\{ (-1 - |\tilde{m}_{\mathbf{RL}}|^4 - |\tilde{m}_{\mathbf{RR}}|^4 + 2|\tilde{m}_{\mathbf{RR}}|^2 + \tilde{m}_{\mathbf{RR}}^2(\tilde{m}_{\mathbf{RL}}^*)^2 + \tilde{m}_{\mathbf{RL}}^2(\tilde{m}_{\mathbf{RR}}^*)^2)^2 - 4|\tilde{m}_{\mathbf{RL}}|^4 \right\}^{\frac{1}{2}} \right] \right. \\ \left. + \frac{1}{2\pi} \ln \left\{ 1 - \frac{1}{2|\tilde{m}_{\mathbf{RL},n}|^2} \left[ (1 + |\tilde{m}_{\mathbf{RL},n}|^4 + |\tilde{m}_{\mathbf{RR},n}|^4 - 2|\tilde{m}_{\mathbf{RR},n}|^2 - \tilde{m}_{\mathbf{RR},n}^2(\tilde{m}_{\mathbf{RL},n}^*)^2 - \tilde{m}_{\mathbf{RL},n}^2(\tilde{m}_{\mathbf{RR},n}^*)^2) \pm \left\{ (-1 - |\tilde{m}_{\mathbf{RL},n}|^4 - |\tilde{m}_{\mathbf{RR},n}|^4 + 2|\tilde{m}_{\mathbf{RR},n}|^2 + \tilde{m}_{\mathbf{RR},n}^2(\tilde{m}_{\mathbf{RL},n}^*)^2 + \tilde{m}_{\mathbf{RL},n}^2(\tilde{m}_{\mathbf{RR},n}^*)^2)^2 - 4|\tilde{m}_{\mathbf{RL},n}|^4 \right\}^{\frac{1}{2}} \right] \right\} \right]. \quad (3.137)$$

Here the components  $\tilde{m}_{\mathbf{RR}} = \tilde{m}_{\mathbf{LL}}$ ,  $\tilde{m}_{\mathbf{RL}} = \tilde{m}_{\mathbf{LR}}$  and  $\tilde{m}_{\mathbf{RR},n} = \tilde{m}_{\mathbf{LL},n}$ ,  $\tilde{m}_{\mathbf{RL},n} = \tilde{m}_{\mathbf{LR},n}$  are defined for **Case I** and **Case II** in Eqn (3.61), Eqn (3.62), Eqn (3.63), Eqn (3.64) and Eqn (3.71), Eqn (3.72), Eqn (3.73), Eqn (3.74) respectively. Further using Eq (3.111),

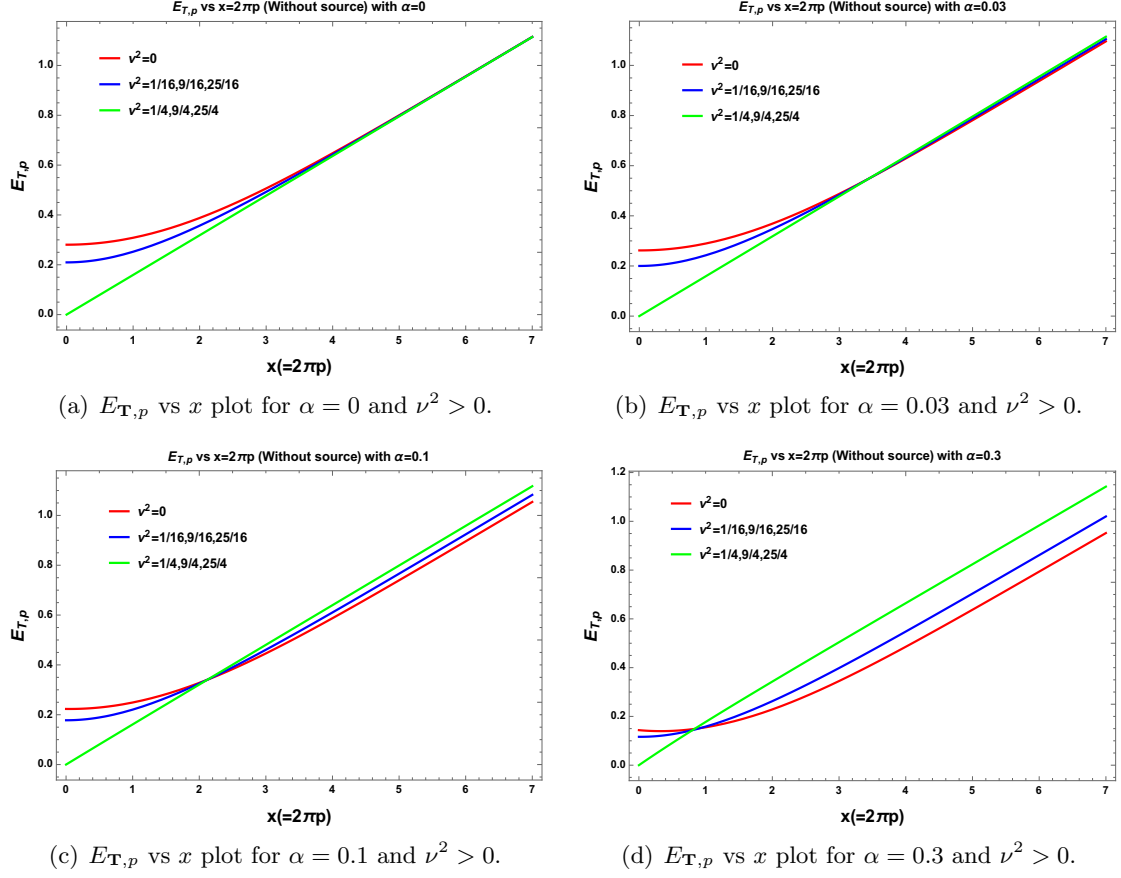


**Figure 7.** Behaviour of energy spectrum for axion in de Sitter space with respect to the rescaled  $\mathbf{SO}(3, 1)$  quantum number  $x$  for ‘+’ branch of solution of  $|\gamma_p^{(\alpha)}|$  and  $|\Gamma_{p,n}^{(\alpha)}|$ .

Eq (3.112), Eq (3.109) and Eq (3.110) in Eq (3.133) and Eq (3.133), we get the following simplified expressions:

**Case I :**

$$E_p^{(\alpha)} \approx \pm p - \frac{1}{\pi} \ln (\cosh^2 \alpha - \sinh^2 \alpha e^{-2\pi p}), \mathcal{E}_{p,n}^{(\alpha)} \approx \frac{1}{2\pi} \ln \left[ 1 - \frac{e^{\mp 2p_n \pi}}{(\cosh^2 \alpha - \sinh^2 \alpha e^{-2\pi p})^2} \right]. \quad (3.138)$$

**Case II :**

$$E_p^{(\alpha)} \approx -\frac{1}{2\pi} \ln \left[ \frac{2}{(\sqrt{\cosh 2\pi p} + \cos 2\pi\nu \pm \sqrt{\cosh 2\pi p} + \cos 2\pi\nu + 2})^2} \times \left| \frac{[\cosh^2 \alpha + \sinh^2 \alpha e^{2i\pi\nu} + \sinh 2\alpha \cos \pi\nu e^{i\pi\nu}]}{(\cosh^2 \alpha + \sinh^2 \alpha e^{-2\pi(p-i\nu)})} \right|^2 \right],$$

$$\mathcal{E}_{p,n}^{(\alpha)} \approx \frac{1}{2\pi} \ln \left[ 1 - \frac{2}{(\sqrt{\cosh 2\pi p_n} + \cos 2\pi\nu \pm \sqrt{\cosh 2\pi p_n} + \cos 2\pi\nu + 2})^2} \times \left| \frac{[\cosh^2 \alpha + \sinh^2 \alpha e^{2i\pi\nu} + \sinh 2\alpha \cos \pi\nu e^{i\pi\nu}]}{(\cosh^2 \alpha + \sinh^2 \alpha e^{-2\pi(p_n-i\nu)})} \right|^2 \right]. \quad (3.139)$$

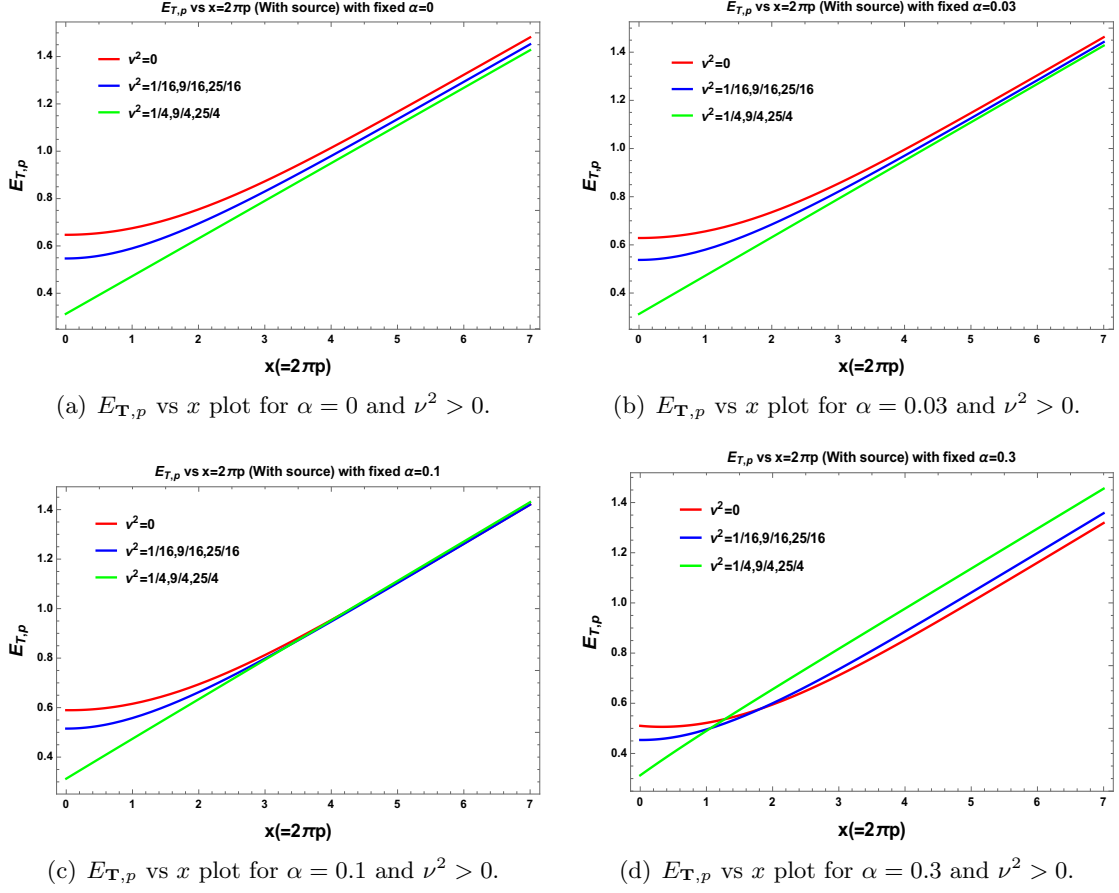


**Figure 8.** Behaviour of energy spectrum for axion in de Sitter space with respect to the rescaled  $\mathbf{SO}(3, 1)$  quantum number  $x$  for ‘+’ branch of solution of  $|\gamma_p^{(\alpha)}|$  and  $|\Gamma_{p,n}^{(\alpha)}|$ .

Also the total energy spectrum for arbitrary parameter  $\alpha$  can be simplified as:

**Case I :**

$$E_{\mathbf{T},p}^{(\alpha)} = \pm p - \frac{1}{\pi} \ln (\cosh^2 \alpha - \sinh^2 \alpha e^{-2\pi p}) - \frac{1}{2\pi} \ln \left( \prod_{n=0}^{\infty} \frac{1}{1 - \frac{e^{\mp 2pn\pi}}{(\cosh^2 \alpha - \sinh^2 \alpha e^{-2\pi p})^2}} \right), \quad (3.140)$$

**Case II :**

$$E_{\mathbf{T},p}^{(\alpha)} = -\frac{1}{2\pi} \ln 2 + \frac{1}{\pi} \ln \left[ \sqrt{\cosh 2\pi p + \cos 2\pi\nu} \pm \sqrt{\cosh 2\pi p + \cos 2\pi\nu + 2} \right] - \frac{1}{\pi} \ln \left| \frac{[\cosh^2 \alpha + \sinh^2 \alpha e^{2i\pi\nu} + \sinh 2\alpha \cos \pi\nu e^{i\pi\nu}]}{(\cosh^2 \alpha + \sinh^2 \alpha e^{-2\pi(p-i\nu)})} \right| - \frac{1}{2\pi} \ln \left( \prod_{n=0}^{\infty} \left[ 1 - \frac{2}{(\sqrt{\cosh 2\pi p_n + \cos 2\pi\nu} \pm \sqrt{\cosh 2\pi p_n + \cos 2\pi\nu + 2})^2} \times \left| \frac{[\cosh^2 \alpha + \sinh^2 \alpha e^{2i\pi\nu} + \sinh 2\alpha \cos \pi\nu e^{i\pi\nu}]}{(\cosh^2 \alpha + \sinh^2 \alpha e^{-2\pi(p_n-i\nu)})} \right|^2 \right]^{-1} \right), \quad (3.141)$$

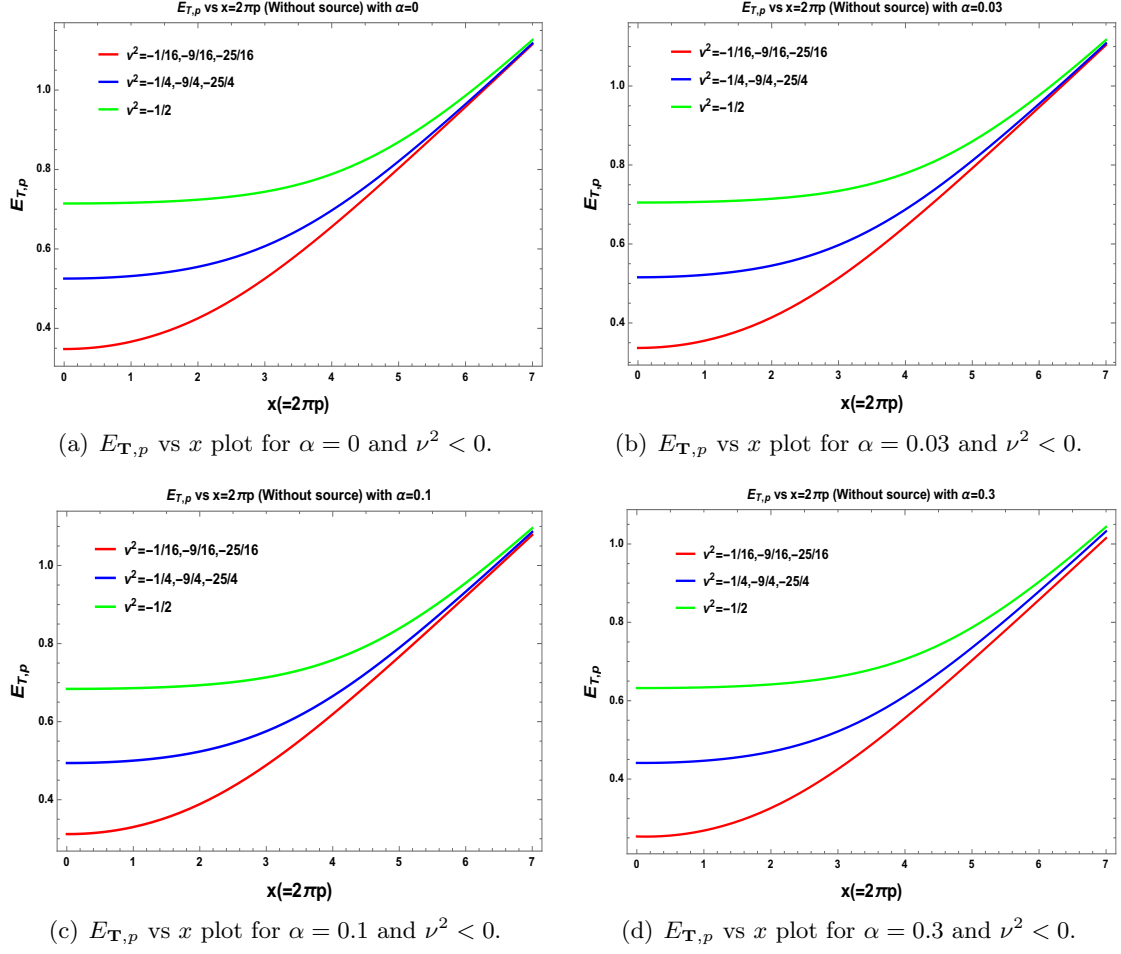


**Figure 9.** Behaviour of energy spectrum for axion in de Sitter space with respect to the rescaled  $\mathbf{SO}(3, 1)$  quantum number  $x$  for ‘+’ branch of solution of  $|\gamma_p^{(\alpha)}|$  and  $|\Gamma_{p,n}^{(\alpha)}|$ .

These results imply that for with arbitrary parameter  $\nu$  and  $\alpha$  the entangled Hamiltonian ( $\mathcal{H}_{\mathbf{ENT}}$ ) and the Hamiltonian for axion ( $\mathcal{H}_p$ ) $_{\mathbf{R} \times \mathbf{H}^3}$  are significantly differ compared to the result obtained in absence of linear source term and  $\alpha = 0$ . For conformally coupled axion ( $\nu = 1/2$ ) and for minimally coupled axion ( $\nu = 3/2$ ) with  $\alpha = 0$  the  $\mathbf{SO}(1, 3)$  principal quantum number  $p$  dependent total energy spectrum can be expressed as:

**Case I :**

$$E_{\mathbf{T},p}^{(\alpha)} \xrightarrow{\alpha=0 + \text{source}} E_{\mathbf{T},p}^{(0)} = \pm p - \frac{1}{2\pi} \ln \left( \prod_{n=0}^{\infty} \frac{1}{1 - e^{\mp 2pn\pi}} \right), \quad (3.142)$$

$$E_{\mathbf{T},p}^{(\alpha)} \xrightarrow{\alpha \neq 0 + \text{No source}} E_{\mathbf{T},p}^{(0)} = \pm p - \frac{1}{\pi} \ln (\cosh^2 \alpha - \sinh^2 \alpha e^{-2\pi p}), \quad (3.143)$$

$$E_{\mathbf{T},p}^{(\alpha)} \xrightarrow{\alpha=0 + \text{No source}} E_{\mathbf{T},p}^{(0)} = \pm p. \quad (3.144)$$

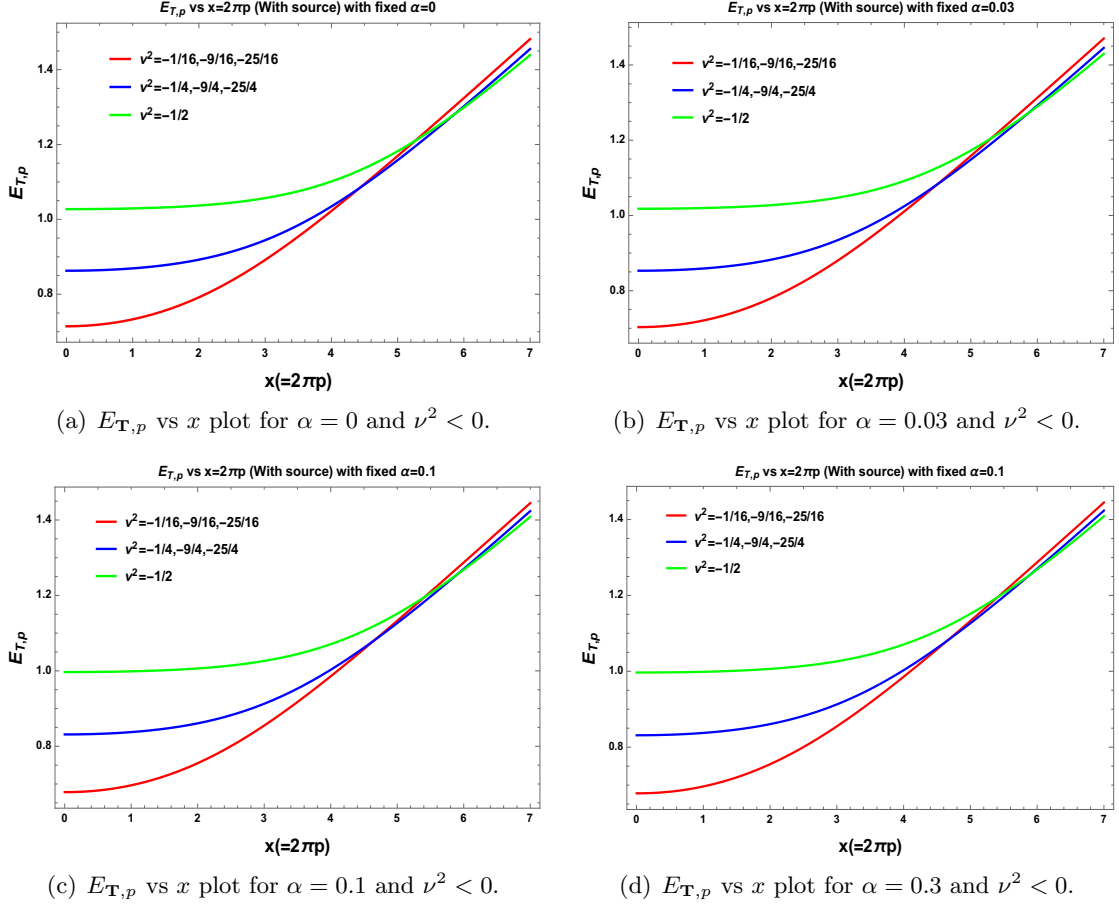


**Figure 10.** Behaviour of energy spectrum for axion in de Sitter space with respect to the rescaled  $\mathbf{SO}(3, 1)$  quantum number  $x$  for ‘+’ branch of solution of  $|\gamma_p^{(\alpha)}|$  and  $|\Gamma_{p,n}^{(\alpha)}|$ .

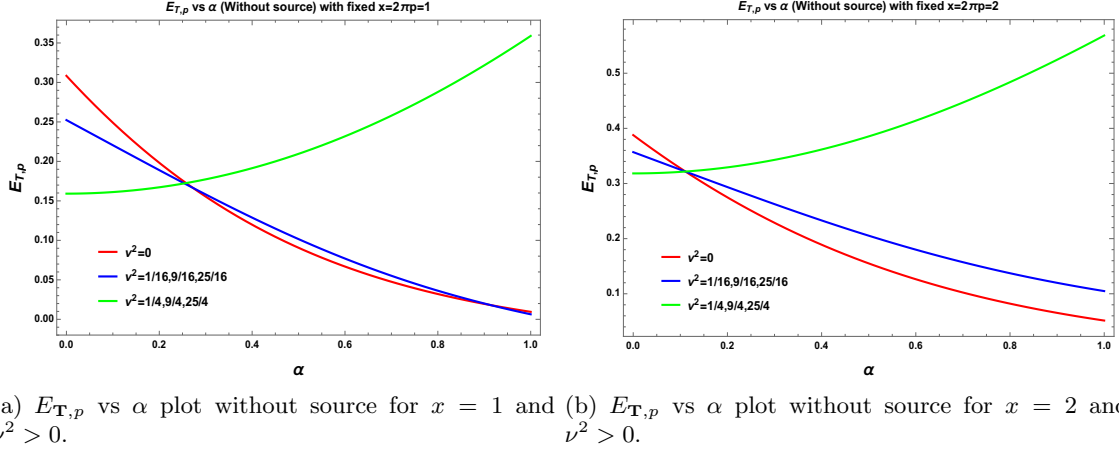
**Case II :**

$$E_{\mathbf{T},p}^{(\alpha)} \xrightarrow{\alpha=0 + \text{source}} E_{\mathbf{T},p}^{(0)} = -\frac{1}{2\pi} \ln 2 + \frac{1}{\pi} \ln \left[ \sqrt{\cosh 2\pi p + \cos 2\pi\nu} \pm \sqrt{\cosh 2\pi p + \cos 2\pi\nu + 2} \right] - \frac{1}{2\pi} \ln \left( \prod_{n=0}^{\infty} \frac{1}{1 - \frac{2}{\left[ \sqrt{\cosh 2\pi p_n + \cos 2\pi\nu} \pm \sqrt{\cosh 2\pi p_n + \cos 2\pi\nu + 2} \right]^2}} \right), \quad (3.145)$$

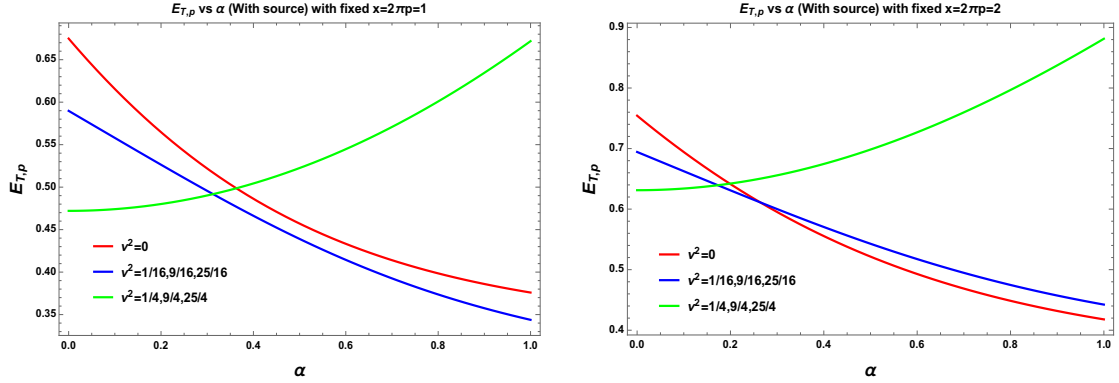
$$E_{\mathbf{T},p}^{(\alpha)} \xrightarrow{\alpha \neq 0 + \text{No source}} E_{\mathbf{T},p}^{(0)} = -\frac{1}{2\pi} \ln 2 + \frac{1}{\pi} \ln \left[ \sqrt{\cosh 2\pi p + \cos 2\pi\nu} \pm \sqrt{\cosh 2\pi p + \cos 2\pi\nu + 2} \right] - \frac{1}{\pi} \ln \left| \frac{[\cosh^2 \alpha + \sinh^2 \alpha e^{2i\pi\nu} + \sinh 2\alpha \cos \pi\nu e^{i\pi\nu}]}{(\cosh^2 \alpha + \sinh^2 \alpha e^{-2\pi(p-i\nu)})} \right|, \quad (3.146)$$

$$E_{\mathbf{T},p}^{(\alpha)} \xrightarrow{\alpha=0 + \text{No source}} E_{\mathbf{T},p}^{(0)} = -\frac{1}{2\pi} \ln 2 + \frac{1}{\pi} \ln \left[ \sqrt{\cosh 2\pi p + \cos 2\pi\nu} \pm \sqrt{\cosh 2\pi p + \cos 2\pi\nu + 2} \right]. \quad (3.147)$$





(a)  $E_{T,p}$  vs  $\alpha$  plot without source for  $x = 1$  and  $\nu^2 > 0$ . (b)  $E_{T,p}$  vs  $\alpha$  plot without source for  $x = 2$  and  $\nu^2 > 0$ .



(c)  $E_{T,p}$  vs  $\alpha$  plot with source for  $x = 1$  and  $\nu^2 > 0$ . (d)  $E_{T,p}$  vs  $\alpha$  plot with source for  $x = 2$  and  $\nu^2 > 0$ .

**Figure 11.** Behaviour of energy spectrum for axion in de Sitter space with respect to the parameter  $\alpha$  for ‘+’ branch of solution of  $|\gamma_p^{(\alpha)}|$  and  $|\Gamma_{p,n}^{(\alpha)}|$ .

This implies that for conformally coupled axion ( $\nu = 1/2$ ) and for minimally coupled axion ( $\nu = 3/2$ ) the entangled Hamiltonian ( $\mathcal{H}_{\text{ENT}}$ ) and the Hamiltonian for axion ( $\mathcal{H}_p$ ) $_{\mathbf{R} \times \mathbf{H}^3}$  are equivalent in absence of the linear source term in the effective action with the choice  $\alpha = 0$  of quantum vacuum state.

In fig. (7) and fig. (8) we have depicted the behaviour of the total energy spectrum for axion in absence and presence of linear source with respect to the rescaled  $\mathbf{SO}(1, 3)$  quantum number  $x = 2\pi p$  for a fixed value of the mass parameter  $\nu^2 > 0$  respectively. Here in both the plots we use set the parameter value  $\alpha = 0$  (fig. (7(a)) and fig. (8(a))),  $\alpha = 0.03$  (fig. (7(b)) and fig. (8(b))),  $\alpha = 0.1$  (fig. (7(c)) and fig. (8(c))) and  $\alpha = 0.3$  (fig. (7(d)) and fig. (8(d))) to demonstrate our result in presence of  $\alpha$  vacuum. From both the plots it is clearly observed that for minimally coupled axion ( $\nu = 3/2$ ), conformally coupled axion ( $\nu = 1/2$ ) and for  $\nu = 5/2$  the energy spectrum is linear and represented by **green** colour. Also it is important to note that in presence of linear source contribution the slope and intercept of **green** coloured line will change. Further if we decrease the value of the mass parameter to  $\nu = 1/4$ ,  $\nu = 3/4$  and  $\nu = 5/4$  then it show small deviation from linearity for very small values of  $x$  as shown by **blue** coloured line. Amount of deviation from the linearity will be larger if we set the mass parameter  $\nu = 0$  as depicted by **red** coloured line.

In fig. (9) and fig. (10) we have depicted the behaviour of the total energy spectrum for axion

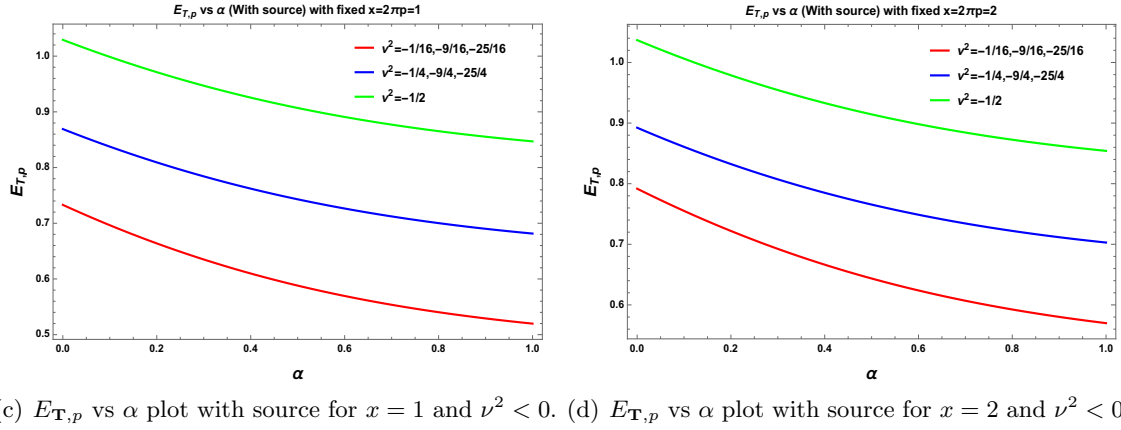
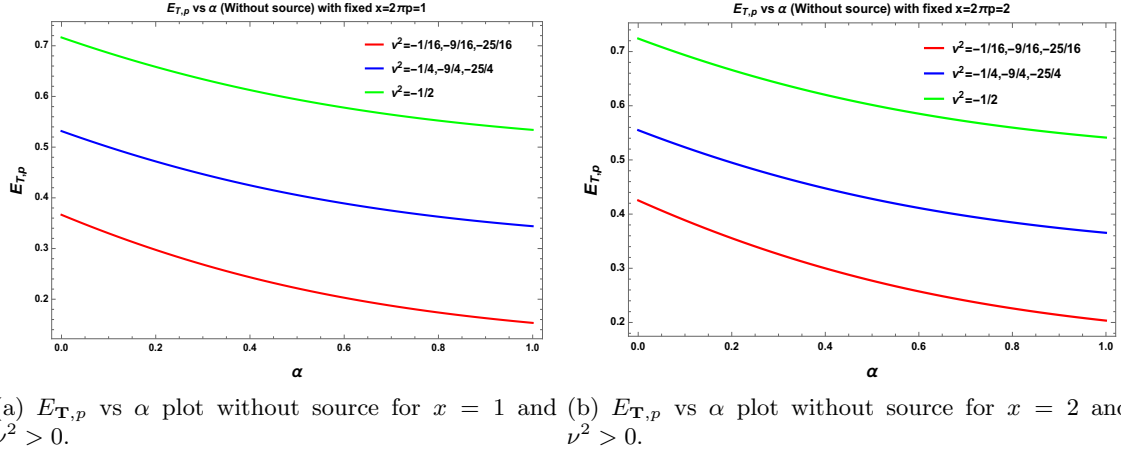


**Figure 12.** Behaviour of energy spectrum for axion in de Sitter space with respect to the parameter  $\alpha$  for ‘+’ branch of solution of  $|\gamma_p^{(\alpha)}|$  and  $|\Gamma_{p,n}^{(\alpha)}|$ .

in absence and presence of linear source with respect to the rescaled  $\mathbf{SO}(1,3)$  quantum number  $x = 2\pi p$  for a fixed value of the large axion mass with mass parameter  $\nu^2 < 0$  respectively. Here in both the plots we use set the parameter value  $\alpha = 0$  (fig. (9(a)) and fig. (10(a))),  $\alpha = 0.03$  (fig. (9(b)) and fig. (10(b))),  $\alpha = 0.1$  (fig. (9(c)) and fig. (10(c))) and  $\alpha = 0.3$  (fig. (9(d)) and fig. (10(d))) to demonstrate our result in presence of  $\alpha$  vacuum. From both the plots it is clearly observed that for  $\nu^2 = -1/2$  the energy spectrum is represented by **green** colour. Also it is important to note that in presence of linear source contribution the slope of **green** coloured curve will change. Further if we decrease the value of the mass parameter to  $\nu^2 = -1/4, -9/4, -25/4$  then it show significant deviation from the result obtained for  $\nu^2 = -1/2$  for very small values of  $x$  as shown by **blue** coloured curve. Amount of deviation is larger if we set the mass parameter  $\nu^2 = -1/16, -9/16, -25/16$  as depicted by **red** coloured curve.

Next in fig. (11) and fig. (12) we have depicted the behaviour of the total energy spectrum for axion in absence and presence of linear source with respect to the variation of the parameter  $\alpha$  for mass parameter  $\nu^2 \geq 0$  with  $x = 1$  (fig. (11(a)) and fig. (11(c))) and  $x = 2$  (fig. (11(b)) and fig. (11(d))),  $\nu^2 < 0$  with  $x = 1$  (fig. (12(a)) and fig. (12(c))) and  $x = 2$  (fig. (12(b)) and fig. (12(d))) respectively. In fig. (11) we have used  $\nu = 0$  (**red**),  $\nu = 1/4, 3/4, 5/4$  (**blue**) and  $\nu = 1/2, 3/2, 5/2$  (**green**) to show the behaviour of the spectrum in  $\nu^2 \geq 0$  region. Also

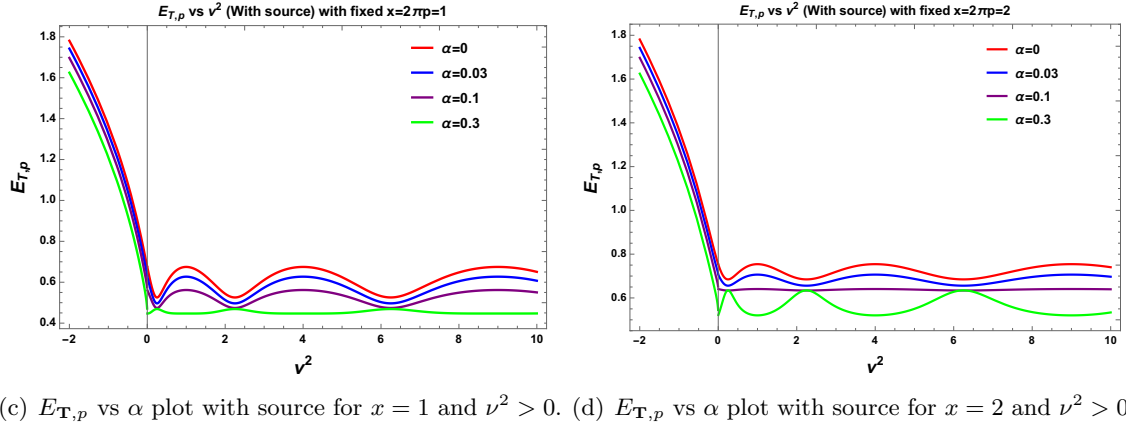
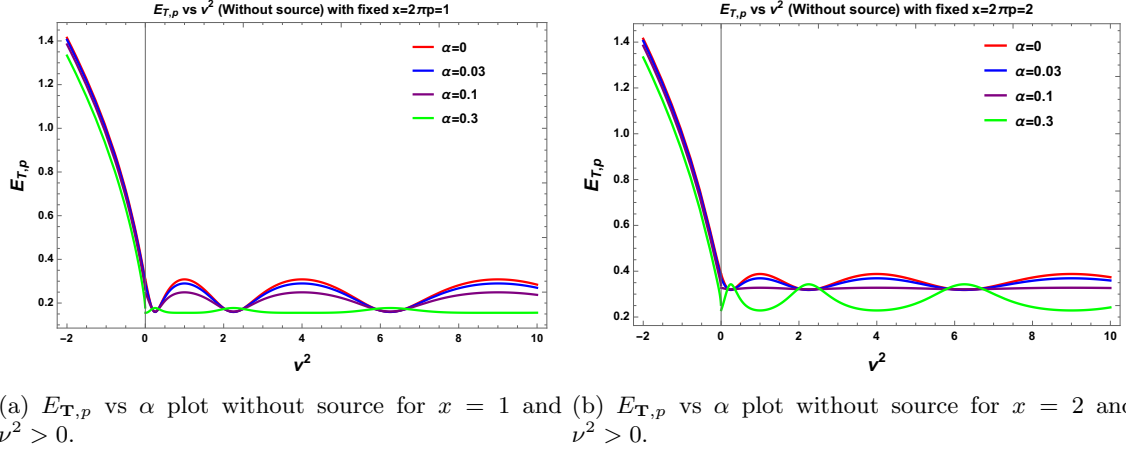


**Figure 13.** Behaviour of energy spectrum for axion in de Sitter space with respect to the parameter  $\alpha$  for ‘+’ branch of solution of  $|\gamma_p^{(\alpha)}|$  and  $|\Gamma_{p,n}^{(\alpha)}|$ .

it is important to note that for small values of the parameter  $\alpha$  cross over take place for  $x = 1$  and  $x = 2$ . Here it is clearly visible the difference between the total energy spectrum for axion in absence and presence of axionic linear source contribution from fig. (11(a)) and fig. (11(c)), fig. (11(b)) and fig. (11(d)). For all  $\nu = 0$  and  $\nu = 1/4, 3/4, 5/4$  as the value of the parameter  $\alpha$  decreases total energy of axion is also decreasing and for  $\nu = 12, 3/2, 5/2$  we get completely opposite feature. On the other hand in fig. (12) we have used  $\nu^2 = -1/2$  (green),  $\nu^2 = -1/16, -9/16, -25/16$  (red) and  $\nu^2 = -1/4, -9/4, -25/4$  (blue) to show the behaviour of the spectrum in the large mass  $\nu^2 < 0$  region. Additionally, it is important to mention that for the prescribed range of  $\nu^2 < 0$  in presence and absence of axionic linear source no cross over takes place as the green, red and blue curves are parallel to each other for  $x = 1$  and  $x = 2$ . Here also one can find out the small but crucial differences between fig. (12(a)) and fig. (12(c)), fig. (12(b)) and fig. (12(d)).

Finally, in fig. (13) we have demonstrated the behaviour of the magnitude of the solution total energy spectrum for axion with the mass parameter  $\nu^2$  for fixed value of the rescaled **SO(1, 3)** quantum number  $x = 1$  (fig. (13(a)) and fig. (13(c))) and  $x = 2$  (fig. (13(b)) and fig. (13(d))) in absence and presence of axionic source contribution. In fig. (13(a)), fig. (13(b)), fig. (13(c)) and fig. (13(d)) we also fix the parameter  $\alpha$  at,  $\alpha = 0$  (red),  $\alpha = 0.03$  (blue),  $\alpha = 0.1$  (violet) and  $\alpha = 0.3$  (green) respectively. For  $x = 1$  and  $x = 2$  both the

plots show distinctive features at all representative values of  $\alpha$ . For  $x = 1$  and  $x = 2$  with  $\nu^2 < 0$  it is observed that the total energy spectrum of the axion decrease if we move towards  $\nu^2 = 0$ . After that in  $\nu^2 > 0$  region, aperiodic oscillations are observed for  $\alpha = 0, \alpha = 0.03$  and  $\alpha = 0.1$  and  $\alpha = 0.3$ .

### 3.3 Computation of entanglement entropy using $\alpha$ vacua

In this subsection our prime objective is to derive the expression for entanglement entropy in de Sitter space in presence of  $\alpha$  vacuum state. In general the entanglement entropy with arbitrary  $\alpha$  can be expressed as:

$$S(p, \nu, \alpha) = -\mathbf{Tr} [\rho_{\mathbf{L}}(p, \alpha) \ln \rho_{\mathbf{L}}(p, \alpha)], \quad (3.148)$$

where the parameter  $\nu$  and the corresponding  $\alpha$  vacuum state are defined in the earlier section. In this context the expression for entanglement entropy for a given  $\mathbf{SO}(1, 3)$  principal quantum number  $p$  can be expressed as <sup>9</sup>:

$$S(p, \nu, \alpha) = - \left( 1 + \frac{f_p^{(\alpha)}}{1 + f_p^{(\alpha)}} \right) \left[ \ln \left( 1 - |\gamma_p^{(\alpha)}|^2 \right) + \frac{|\gamma_p^{(\alpha)}|^2}{\left( 1 - |\gamma_p^{(\alpha)}|^2 \right)} \ln \left( |\gamma_p^{(\alpha)}|^2 \right) \right] - \left( 1 - f_p^{(\alpha)} \right) \ln \left( 1 + f_p^{(\alpha)} \right). \quad (3.150)$$

Then the final expression for the entanglement entropy in de Sitter space can be expressed as a sum over all possible quantum states which carries  $\mathbf{SO}(1, 3)$  principal quantum number  $p$ . Consequently, the final expression for the entanglement entropy in de Sitter space is given by the following expression:

$$S(\nu, \alpha) = \sum_{\text{States}} \sum_{p=0}^{\infty} S(p, \nu, \alpha) \rightarrow V_{\mathbf{H}^3} \int_{p=0}^{\infty} dp \mathcal{D}_3(p) S(p, \nu, \alpha) = \mathbf{c}_6(\alpha, \nu) V_{\mathbf{H}^3} / V_{\mathbf{H}^3}^{\text{REG}}, \quad (3.151)$$

where  $\mathcal{D}_3(p) = p^2/2\pi^2$  characterize the density of stat for radial functions on the Hyperboloid  $\mathbf{H}^3$ . Additionally, it is important to note that the volume of the hyperboloid  $\mathbf{H}^3$  is denoted by the overall factor  $V_{\mathbf{H}^3}$ . Here the regularized volume of the hyperboloid  $\mathbf{H}^3$  for  $r \leq L_c$  can be written as:

$$V_{\mathbf{H}^3} = V_{\mathbf{S}^2} \int_{r=0}^{L_c} dr \sinh^2 r \xrightarrow{\text{large } L_c} \frac{\pi}{2} [e^{2L_c} - 4L_c] = \left[ \mathbf{A}_{\text{ENT}} - \pi \ln \mathbf{A}_{\text{ENT}} + \pi \ln \left( \frac{\pi}{2} \right) \right] = V_{\mathbf{H}^3}^{\text{REG}} \left[ \frac{1}{4\eta^2} + \ln \eta \right]. \quad (3.152)$$

where  $\mathbf{A}_{\text{ENT}}$  is the entangling area and we use  $V_{\mathbf{S}^2} = 4\pi$ . Here the cutoff  $L_c$  can be written as,  $L_c \sim -\ln \eta$ . In this context we define regularized volume of the hyperboloid  $\mathbf{H}^3$  as,  $V_{\mathbf{H}^3}^{\text{REG}} = V_{\mathbf{S}^3}/2 = 2\pi$ .

<sup>9</sup>If we follow the equivalent ansatz of density matrix as mentioned in Eq (3.127), the expression for entanglement entropy for a given  $\mathbf{SO}(1, 3)$  principal quantum number  $p$  can be expressed as:

$$S(p, \nu, \alpha) = -\ln a_p^{(\alpha)} - a_p^{(\alpha)} \frac{|\gamma_p^{(\alpha)}|^2}{\left( 1 - |\gamma_p^{(\alpha)}|^2 \right)^2} \ln \left( |\gamma_p^{(\alpha)}|^2 \right) \left( 1 + f_p^{(\alpha)} \left( 1 - |\gamma_p^{(\alpha)}|^2 \right) \right) - a_p^{(\alpha)} f_p^{(\alpha)} \ln \left( 1 + f_p^{(\alpha)} \left( 1 - |\gamma_p^{(\alpha)}|^2 \right) \right) - a_p^{(\alpha)} \left( f_p^{(\alpha)} \right)^2 \left( 1 - |\gamma_p^{(\alpha)}|^2 \right) \ln \left( 1 + f_p^{(\alpha)} \right). \quad (3.149)$$

For our computation we will not further use this ansatz.

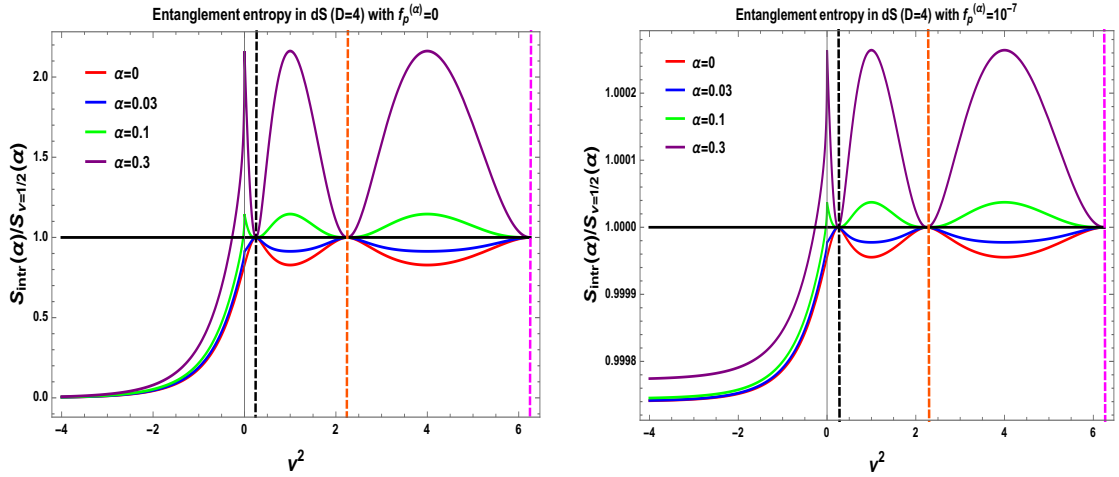
Here in 3 + 1 D in presence of  $\alpha$  vacuum long range quantum correlation is measured by  $\mathbf{c}_6(\alpha, \nu)$ , which is defined as:

$$\mathbf{c}_6(\alpha, \nu) \equiv S_{\text{intr}}(\alpha, \nu) = \left[ \left( 1 + \frac{f_p^{(\alpha)}}{1 + f_p^{(\alpha)}} \right) \mathcal{I}^{(\alpha)} + \left( 1 - f_p^{(\alpha)} \right) \ln \left( 1 + f_p^{(\alpha)} \right) \mathcal{V} \right], \quad (3.153)$$

where the integrals  $\mathcal{I}^{(\alpha)}$  and  $\mathcal{V}$  can be written in 3 + 1 dimensional space-time as:

$$\mathcal{I}^{(\alpha)} = -\frac{1}{\pi} \int_{p=0}^{\infty} dp p^2 \left[ \ln \left( 1 - |\gamma_p^{(\alpha)}|^2 \right) + \frac{|\gamma_p^{(\alpha)}|^2}{\left( 1 - |\gamma_p^{(\alpha)}|^2 \right)} \ln \left( |\gamma_p^{(\alpha)}|^2 \right) \right], \quad (3.154)$$

$$\mathcal{V} = -\frac{1}{\pi} \int_{p=0}^{\infty} dp p^2. \quad (3.155)$$



(a) Normalized entanglement entropy vs  $\nu^2$  in 3 + 1 D de Sitter space in presence of  $\alpha$  vacuum and in de Sitter space in presence of  $\alpha$  vacuum and absence axionic source ( $f_p^{(\alpha)} = 0$ ). (b) Normalized entanglement entropy vs  $\nu^2$  in 3+1 D de Sitter space in presence of  $\alpha$  vacuum and axionic source ( $f_p^{(\alpha)} = 10^{-7}$ ).

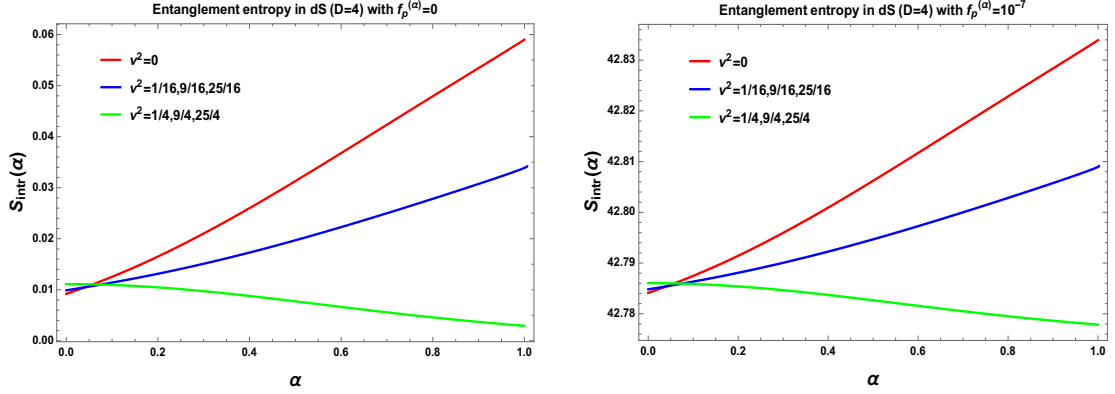
**Figure 14.** Normalized entanglement entropy  $S_{\text{intr}}/S_{\nu=1/2}$  vs mass parameter  $\nu^2$  in 3 + 1 D de Sitter space in absence of axionic source ( $f_p^{(\alpha)} = 0$ ) and in presence of axionic source ( $f_p^{(\alpha)} = 10^{-7}$ ) for ‘+’ branch of solution of  $\alpha$  vacuum i.e  $|\gamma_p^{(\alpha)}|$  and  $|\Gamma_{p,n}^{(\alpha)}|$ . In both the situations we have normalized with conformal  $\nu = 1/2$  result in presence of  $\alpha$  vacuum.

Here it is important to mention that:

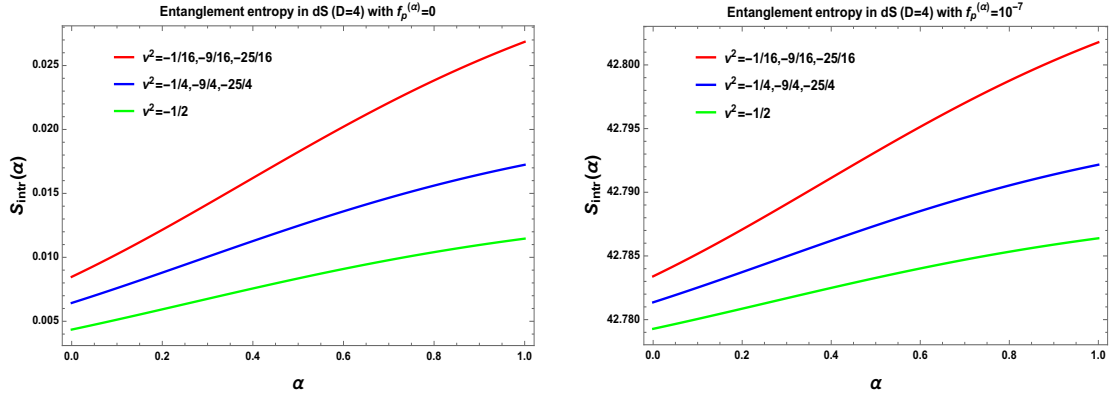
- Here the integral  $\mathcal{V}$  diverges. To make it finite we need to regularize this by introducing a change in variable by using  $x = 2\pi p$  and introducing a cut-off  $\Lambda_{\mathbf{C}}$  we get:

$$\mathcal{V} = -\frac{1}{8\pi^4} \int_{x=0}^{\Lambda_{\mathbf{C}}} dx x^2 = -\frac{\Lambda_{\mathbf{C}}^3}{24\pi^4}. \quad (3.156)$$

- On the other hand, for **Case I** we get one solution for  $|\gamma_p^{(\alpha)}|$  as given by,  $|\gamma_p^{(\alpha)}| = e^{-\pi p} (\cosh^2 \alpha - \sinh^2 \alpha e^{-2\pi p})^{-1}$ . Using this solution we compute the integral  $\mathcal{I}^{(\alpha)}$  for **Case I**



(a) Entanglement entropy vs  $\alpha$  in 3 + 1 D de Sitter space without axionic source ( $f_p^{(\alpha)} = 0$ ). (b) Entanglement entropy vs  $\alpha$  in 3 + 1 D de Sitter space with axionic source ( $f_p^{(\alpha)} = 10^{-7}$ ).



(c) Entanglement entropy vs  $\alpha$  in 3 + 1 D de Sitter space with axionic source ( $f_p^{(\alpha)} = 10^{-7}$ ). (d) Entanglement entropy vs  $\alpha$  in 3 + 1 D de Sitter space with axionic source ( $f_p^{(\alpha)} = 10^{-7}$ ).

**Figure 15.** Entanglement entropy  $S_{intr}(\alpha)$  vs parameter  $\alpha$  in 3 + 1 D de Sitter space in absence of axionic source ( $f_p^{(\alpha)} = 0$ ) and in presence of axionic source ( $f_p^{(\alpha)} = 10^{-7}$ ) for ‘+’ branch of solution of  $|\gamma_p^{(\alpha)}|$  and  $|\Gamma_{p,n}^{(\alpha)}|$ . Here we fix the value of the parameter  $\nu^2$  at different positive and negative values including zero.

for any arbitrary value of the parameter  $\alpha$ . Further we use the rescaled  $\mathbf{SO}(1, 3)$  quantum number  $x = 2\pi p$  with cut-off  $\Lambda_C$  to compute this integral. Consequently we get:

$$\mathcal{I}(\alpha) = -\frac{1}{8\pi^4} \int_{x=0}^{\Lambda_C} dx x^2 \left[ \ln \left( 1 - \frac{e^{-x}}{(\cosh^2 \alpha - \sinh^2 \alpha e^{-x})^2} \right) - \frac{e^{-x}}{((\cosh^2 \alpha - \sinh^2 \alpha e^{-x})^2 - e^{-x})} \{x + 2 \ln (\cosh^2 \alpha - \sinh^2 \alpha e^{-x})\} \right]. \quad (3.157)$$

Next if we take the Bunch Davies limit  $\alpha = 0$  and  $f_p^{(\alpha)} \rightarrow 0$ ,  $\Lambda_C \rightarrow \infty$  then we get:

$$\boxed{\mathbf{c}_6 \left( 0, \frac{1}{2} \right) = \mathbf{c}_6 \left( 0, \frac{3}{2} \right) = \frac{1}{90}}. \quad (3.158)$$

Similarly, for **Case I** we get another solution,  $|\gamma_p^{(\alpha)}| = e^{\pi p} (\cosh^2 \alpha - \sinh^2 \alpha e^{-2\pi p})^{-1}$ . Using this solution we compute the integral  $\mathcal{I}^{(\alpha)}$  for **Case I** for any arbitrary value of the parameter  $\alpha$ . Consequently we get:

$$\mathcal{I}^{(\alpha)} = -\frac{1}{8\pi^4} \int_{x=0}^{\Lambda_{\mathbf{C}}} dx x^2 \left[ \ln \left( 1 - \frac{e^x}{(\cosh^2 \alpha - \sinh^2 \alpha e^{-x})^2} \right) + \frac{e^x}{\left( (\cosh^2 \alpha - \sinh^2 \alpha e^{-x})^2 - e^x \right)} \left\{ x - 2 \ln (\cosh^2 \alpha - \sinh^2 \alpha e^{-x}) \right\} \right]. \quad (3.159)$$

Next if we take the Bunch Davies limit  $\alpha = 0$  and  $f_p^{(\alpha)} \rightarrow 0$ ,  $\Lambda_{\mathbf{C}} \rightarrow \infty$  then we get:

$$\boxed{\mathbf{c}_6 \left( 0, \frac{1}{2} \right) = \mathbf{c}_6 \left( 0, \frac{3}{2} \right) \rightarrow \infty}. \quad (3.160)$$

- Further we analyze the integral  $\mathcal{I}^{(\alpha)}$  using both of the solutions obtained for arbitrary  $\nu$  and  $\nu = 3/2$ . Following the previous logical argument here we also put a cut-off  $\Lambda_{\mathbf{C}}$  to perform the integral on the rescaled **SO(1, 3)** quantum number  $x = 2\pi p$  and after performing the integral we will check the behaviour of both of the results. First of all we start with the following integral with “ $\pm$ ” signature, as given by:

$$\mathcal{I}^{(\alpha)} = -\frac{1}{8\pi^4} \int_{x=0}^{\Lambda_{\mathbf{C}}} dx x^2 \left[ \ln (1 - 2G_{\pm}(x, \nu, \alpha)) + \frac{2G_{\pm}(x, \nu, \alpha)}{(1 - 2G_{\pm}(x, \nu, \alpha))} \ln (2G_{\pm}(x, \nu, \alpha)) \right], \quad (3.161)$$

where  $G_{\pm}(x, \nu, \alpha)$  for any arbitrary value of the parameter  $\alpha$  is defined as:

$$G_{\pm}(x, \nu, \alpha) = \frac{1}{4|\tilde{m}_{\mathbf{RL}}|^2} \left[ (1 + |\tilde{m}_{\mathbf{RL}}|^4 + |\tilde{m}_{\mathbf{RR}}|^4 - 2|\tilde{m}_{\mathbf{RR}}|^2 - \tilde{m}_{\mathbf{RR}}^2 (\tilde{m}_{\mathbf{RL}}^*)^2 - \tilde{m}_{\mathbf{RL}}^2 (\tilde{m}_{\mathbf{RR}}^*)^2) \pm \left\{ (-1 - |\tilde{m}_{\mathbf{RL}}|^4 - |\tilde{m}_{\mathbf{RR}}|^4 + 2|\tilde{m}_{\mathbf{RR}}|^2 + \tilde{m}_{\mathbf{RR}}^2 (\tilde{m}_{\mathbf{RL}}^*)^2 + \tilde{m}_{\mathbf{RL}}^2 (\tilde{m}_{\mathbf{RR}}^*)^2) - 4|\tilde{m}_{\mathbf{RL}}|^4 \right\}^{\frac{1}{2}} \right], \quad (3.162)$$

where the components  $\tilde{m}_{\mathbf{RR}} = \tilde{m}_{\mathbf{LL}}$  and  $\tilde{m}_{\mathbf{RL}} = \tilde{m}_{\mathbf{LR}}$  are redefined in terms of the new variable  $x = 2\pi p$ .

Here small axion mass ( $\nu^2 > 0$ ) limiting situations are considered in  $\nu = 1/2$  conformal mass as well in  $\nu = 3/2$  case which is appearing in **Case I** in presence of an additional arbitrary parameter  $\alpha$ . Additionally, we consider large axion mass ( $\nu^2 < 0$  where  $\nu \rightarrow -i|\nu|$ ) limiting situation which is important to study the physics from **Case II**. In this large axion mass limiting situation we consider the window of **SO(1, 3)** principal quantum number is  $0 < p < |\nu|$ . Consequently, the entries of the coefficient matrix  $\tilde{m}$  can be approximated as:

$$\tilde{m}_{\mathbf{RR}} = -\sqrt{\frac{\cosh(|\nu| - p)}{\cosh(|\nu| + p)} \frac{2}{(e^{2\pi p} + e^{2\pi|\nu|}) \cosh^2 \alpha + (e^{2\pi p} + e^{2\pi|\nu|}) \sinh^2 \alpha}} \left[ \cosh 2\alpha \cosh^2 \pi|\nu| - \sinh 2\alpha \sinh^2 \pi p + \frac{1}{2} \sinh 2\pi|\nu| \right], \quad (3.163)$$

$$\tilde{m}_{\mathbf{RL}} = -\sqrt{\frac{\cosh(|\nu| - p)}{\cosh(|\nu| + p)} \frac{2i}{(e^{2\pi p} + e^{2\pi|\nu|}) \cosh^2 \alpha + (e^{2\pi p} + e^{2\pi|\nu|}) \sinh^2 \alpha}} \left[ (\cosh 2\alpha + \sinh 2\alpha) \cosh \pi|\nu| + \sinh \pi|\nu| \right]. \quad (3.164)$$

This implies that for  $\alpha$  vacuum if we consider the large axion mass ( $\nu^2 < 0$  where  $\nu \rightarrow -i|\nu|$ ) limiting situation we get always real value for  $\tilde{m}_{\mathbf{RR}}$  and imaginary value for  $\tilde{m}_{\mathbf{RL}}$ . Consequently one can easily reduce the four sets of Eqn. (3.101), Eqn. (3.102), Eqn. (3.103) and Eqn. (3.104) into two sets of equations as exactly we have done in ref. [14] for Bunch Davies vacuum. In this large axion mass ( $\nu^2 < 0$  where  $\nu \rightarrow -i|\nu|$ ) limiting situation the two solutions for the  $\gamma_p^{(\alpha)}$  for  $\alpha$  vacuum are given by:

$$\gamma_p^{(\alpha)} \approx \frac{1}{2|\tilde{m}_{\mathbf{RL}}|} \left[ (1 + |\tilde{m}_{\mathbf{RL}}|^2 - \tilde{m}_{\mathbf{RR}}^2) \pm \sqrt{(1 + |\tilde{m}_{\mathbf{RL}}|^2 - \tilde{m}_{\mathbf{RR}}^2)^2 - 4|\tilde{m}_{\mathbf{RL}}|^2} \right]. \quad (3.165)$$

Small mass limiting situations are explicitly appearing in  $\nu = 1/2$  and  $\nu = 3/2$  case which we have discussed for **Case I**. For our study here we consider large mass limiting situation which is important to study the physical outcomes from **Case II**. In this situation we divide the total window of  $p$  into two regions, as given by  $0 < p < |\nu|$  and  $|\nu| < p < \Lambda_{\mathbf{C}}$ . Here in these region of interests the two solutions for  $\gamma_p^{(\alpha)}$  in presence of  $\alpha$  vacuum can be approximately written as:

$$|\gamma_p^{(\alpha)}| \approx \begin{cases} e^{-\pi|\nu|} (1 + \tan \alpha) & \text{for } 0 < p < |\nu| \\ \frac{e^{-\pi p} (1 + \tan \alpha) (1 + \tan \alpha e^{2\pi|\nu|})}{(1 + \tan^2 \alpha e^{-2\pi p})} & \text{for } |\nu| < p < \Lambda_{\mathbf{C}}/2\pi. \end{cases} \quad (3.166)$$

and

$$|\gamma_p| = \begin{cases} e^{\pi|\nu|} (1 + \tan \alpha) & \text{for } 0 < p < |\nu| \\ \frac{e^{\pi p} (1 + \tan \alpha) (1 + \tan \alpha e^{2\pi|\nu|})}{(1 + \tan^2 \alpha e^{-2\pi p})} & \text{for } |\nu| < p < \Lambda_{\mathbf{C}}/2\pi. \end{cases} \quad (3.167)$$

As a result, for large mass limiting range the  $\alpha$  parameter dependent regularized integral  $\mathcal{I}_1^{(\alpha)}$  for the first solution for  $|\gamma_p^{(\alpha)}|$  can be written as:

$$\mathcal{I}_1^{(\alpha)} = \begin{cases} \left[ -\frac{\mathcal{A}(\nu)}{8\pi^4} \left[ \ln \left( 1 - e^{-2\pi\nu} (1 + \tan \alpha)^2 \right) \right. \right. \\ \quad \left. \left. + \frac{(2 \ln (1 + \tan \alpha) - 2\pi\nu) e^{-2\pi\nu} (1 + \tan \alpha)^2}{(1 - e^{-2\pi\nu} (1 + \tan \alpha)^2)} \right] \right] & \text{for } 0 < x < 2\pi|\nu| \\ -\frac{\mathcal{B}(\nu, \alpha, \Lambda_{\mathbf{C}})}{8\pi^4} & \text{for } 2\pi|\nu| < x < \Lambda_{\mathbf{C}}. \end{cases} \quad (3.168)$$

and for the second solution for  $|\gamma_p^{(\alpha)}|$  we get:

$$\mathcal{I}_1^{(\alpha)} = \begin{cases} \left[ -\frac{\mathcal{A}(\nu)}{8\pi^4} \left[ \ln \left( 1 - e^{2\pi\nu} (1 + \tan \alpha)^2 \right) \right. \right. \\ \quad \left. \left. + \frac{(2 \ln (1 + \tan \alpha) + 2\pi\nu) e^{2\pi\nu} (1 + \tan \alpha)^2}{(1 - e^{2\pi\nu} (1 + \tan \alpha)^2)} \right] \right] & \text{for } 0 < x < 2\pi|\nu| \\ -\frac{\mathcal{C}(\nu, \alpha, \Lambda_{\mathbf{C}})}{8\pi^4} & \text{for } 2\pi|\nu| < x < \Lambda_{\mathbf{C}}. \end{cases} \quad (3.169)$$



In Eq. (3.168) and Eq (3.169) coefficients  $\mathcal{A}(\nu)$ ,  $\mathcal{B}(\nu, \alpha, \Lambda_{\mathbf{C}})$  and  $\mathcal{C}(\nu, \alpha, \Lambda_{\mathbf{C}})$  are defined by the following expressions:

$$\mathcal{A}(\nu) = \int_{x=0}^{2\pi\nu} dx x^2 = \frac{8\pi^3}{3} \nu^3, \quad (3.170)$$

$$\begin{aligned} \mathcal{B}(\nu, \alpha, \Lambda_{\mathbf{C}}) \approx & \int_{x=2\pi\nu}^{\Lambda_{\mathbf{C}}} dx x^2 \left[ \ln \left( 1 - \frac{e^{-x} (1 + \tan \alpha)^2 (1 + \tan \alpha e^{2\pi|\nu|})^2}{(1 - \tan^2 \alpha e^{-x})^2} \right) \right. \\ & + \frac{\frac{e^{-x} (1 + \tan \alpha)^2 (1 + \tan \alpha e^{2\pi|\nu|})^2}{(1 - \tan^2 \alpha e^{-x})^2}}{\left( 1 - \frac{e^{-x} (1 + \tan \alpha)^2 (1 + \tan \alpha e^{2\pi|\nu|})^2}{(1 - \tan^2 \alpha e^{-x})^2} \right)} \left\{ 2 \ln((1 + \tan \alpha) (1 + \tan \alpha e^{2\pi|\nu|})) \right. \\ & \left. \left. - 2 \ln(1 - \tan^2 \alpha e^{-x}) - x \right\} \right], \quad (3.171) \end{aligned}$$

$$\begin{aligned} \mathcal{C}(\nu, \alpha, \Lambda_{\mathbf{C}}) = & \int_{x=2\pi\nu}^{\Lambda_{\mathbf{C}}} dx x^2 \left[ \ln \left( 1 - \frac{e^x (1 + \tan \alpha)^2 (1 + \tan \alpha e^{2\pi|\nu|})^2}{(1 - \tan^2 \alpha e^{-x})^2} \right) \right. \\ & + \frac{\frac{e^x (1 + \tan \alpha)^2 (1 + \tan \alpha e^{2\pi|\nu|})^2}{(1 - \tan^2 \alpha e^{-x})^2}}{\left( 1 - \frac{e^x (1 + \tan \alpha)^2 (1 + \tan \alpha e^{2\pi|\nu|})^2}{(1 - \tan^2 \alpha e^{-x})^2} \right)} \left\{ 2 \ln((1 + \tan \alpha) (1 + \tan \alpha e^{2\pi|\nu|})) \right. \\ & \left. \left. - 2 \ln(1 - \tan^2 \alpha e^{-x}) + x \right\} \right]. \quad (3.172) \end{aligned}$$

Further within the window  $0 < x < 2\pi|\nu|$  we take the large mass limit  $|\nu| \gg 1$  in the first solution for  $|\gamma_p^{(\alpha)}|$  in presence of  $\alpha$  vacuum:

$$\lim_{|\nu| \gg 1} \mathcal{I}_1^{(\alpha)} \approx \frac{2\nu^4}{3} e^{-2\pi\nu} (1 + \tan \alpha)^2 \left\{ 1 - \frac{1}{\pi\nu} \ln(1 + \tan \alpha) \right\} \left[ 1 + (1 + \tan \alpha)^2 \mathcal{O}(\nu^{-1}) \right]. \quad (3.173)$$

This result is perfectly consistent with the result obtained for Bunch Davies vacuum ( $\alpha = 0$ ) in ref. [14], where we get:

$$\boxed{\lim_{|\nu| \gg 1} \mathcal{I}_1^{(0)} \approx \frac{2\nu^4}{3} e^{-2\pi\nu} [1 + \mathcal{O}(\nu^{-1})]}. \quad (3.174)$$

Similarly the integral  $\mathcal{V}$  can be written as:

$$\mathcal{V} = \begin{cases} -\frac{1}{8\pi^4} \int_{x=0}^{2\pi|\nu|} dx x^2 = -\frac{|\nu|^3}{3\pi} & \text{for } 0 < x < 2\pi|\nu| \\ -\frac{1}{8\pi^4} \int_{x=2\pi|\nu|}^{\Lambda_{\mathbf{C}}} dx x^2 = -\frac{1}{24\pi^4} (\Lambda_{\mathbf{C}}^3 - 8\pi^3|\nu|^3). & \text{for } 2\pi|\nu| < x < \Lambda_{\mathbf{C}}. \end{cases} \quad (3.175)$$

Consequently in the large mass limiting situation ( $0 < x < 2\pi|\nu|$ ) we get the following expression for the entanglement entropy:

$$\begin{aligned} \lim_{|\nu| \gg 1} \mathbf{c}_6(\alpha, \nu) \approx & \left( 1 + \frac{f_p^{(\alpha)}}{1 + f_p^{(\alpha)}} \right) \frac{2\nu^4}{3} e^{-2\pi\nu} (1 + \tan \alpha)^2 \\ & \times \left\{ 1 - \frac{1}{\pi\nu} \ln(1 + \tan \alpha) \right\} \left[ 1 + (1 + \tan \alpha)^2 \mathcal{O}(\nu^{-1}) \right] \\ & - \left( 1 - f_p^{(\alpha)} \right) \ln \left( 1 + f_p^{(\alpha)} \right) \frac{\nu^3}{3\pi}, \quad (3.176) \end{aligned}$$

Further in absence of the source contribution in the large mass limit the long range quantum correlation can be expressed as:

$$\lim_{|\nu| \gg 1, f_p \rightarrow 0} \mathbf{c}_6(\alpha, \nu) \approx \frac{2\nu^4}{3} e^{-2\pi\nu} (1 + \tan \alpha)^2 \left\{ 1 - \frac{1}{\pi\nu} \ln(1 + \tan \alpha) \right\} \times \left[ 1 + (1 + \tan \alpha)^2 \mathcal{O}(\nu^{-1}) \right], \quad (3.177)$$

which is also consistent with the Bunch Davies ( $\alpha = 0$ ) result [14]:

$$\boxed{\lim_{|\nu| \gg 1, f_p \rightarrow 0} \mathbf{c}_6(0, \nu) \approx \frac{2\nu^4}{3} e^{-2\pi\nu} [1 + \mathcal{O}(\nu^{-1})]} \quad (3.178)$$

For the second solution of  $|\gamma_p^{(\alpha)}|$  in presence of  $\alpha$  vacuum, we get:

$$\lim_{|\nu| \gg 1} \mathcal{I}_1^{(\alpha)} = -\frac{\nu^3}{3\pi} \left[ \ln \left( 1 - e^{2\pi\nu} (1 + \tan \alpha)^2 \right) + \frac{(2 \ln(1 + \tan \alpha) + 2\pi\nu) e^{2\pi\nu} (1 + \tan \alpha)^2}{(1 - e^{2\pi\nu} (1 + \tan \alpha)^2)} \right]. \quad (3.179)$$

This result is perfectly consistent with the result obtained for Bunch Davies vacuum ( $\alpha = 0$ ) in ref. [14], where we get:

$$\boxed{\lim_{|\nu| \gg 1} \mathcal{I}_1^{(0)} = -\frac{\nu^3}{3\pi} \left[ \ln(1 - e^{2\pi\nu}) + \frac{2\pi\nu e^{2\pi\nu}}{(1 - e^{2\pi\nu})} \right]} \quad (3.180)$$

Consequently in the large mass limiting situation ( $0 < x < 2\pi|\nu|$ ) we get the following expression for the entanglement entropy:

$$\lim_{|\nu| \gg 1} \mathbf{c}_6(\alpha, \nu) \approx - \left( 1 + \frac{f_p^{(\alpha)}}{1 + f_p^{(\alpha)}} \right) \frac{\nu^3}{3\pi} \left[ \ln \left( 1 - e^{2\pi\nu} (1 + \tan \alpha)^2 \right) + \frac{(2 \ln(1 + \tan \alpha) + 2\pi\nu) e^{2\pi\nu} (1 + \tan \alpha)^2}{(1 - e^{2\pi\nu} (1 + \tan \alpha)^2)} \right] - \left( 1 - f_p^{(\alpha)} \right) \ln \left( 1 + f_p^{(\alpha)} \right) \frac{\nu^3}{3\pi}, \quad (3.181)$$

Further in absence of the source contribution in the large mass limit the long range quantum correlation can be expressed as:

$$\lim_{|\nu| \gg 1, f_p \rightarrow 0} \mathbf{c}_6(\alpha, \nu) \approx -\frac{\nu^3}{3\pi} \left[ \ln \left( 1 - e^{2\pi\nu} (1 + \tan \alpha)^2 \right) + \frac{(2 \ln(1 + \tan \alpha) + 2\pi\nu) e^{2\pi\nu} (1 + \tan \alpha)^2}{(1 - e^{2\pi\nu} (1 + \tan \alpha)^2)} \right], \quad (3.182)$$

which is consistent with the Bunch Davies result ( $\alpha = 0$ ), as given by [14]:

$$\boxed{\lim_{|\nu| \gg 1, f_p \rightarrow 0} \mathbf{c}_6(0, \nu) = -\frac{\nu^3}{3\pi} \left[ \ln(1 - e^{2\pi\nu}) + \frac{2\pi\nu e^{2\pi\nu}}{(1 - e^{2\pi\nu})} \right]} \quad (3.183)$$

Small mass parameter $\nu$ ( $\nu^2 \geq 0$ )	Axion mass $m_{axion}/H$	Normalized entanglement entropy $\frac{c_6(0,\nu)}{c_6(0,\frac{1}{2})}$ from BD vacuum (without source)	Parameter $\alpha$	Normalized entanglement entropy $\frac{c_6(\alpha,\nu)}{c_6(\alpha,\frac{1}{2})}$ from $\alpha$ vacuum (without source)
0, 1, 2, 3	$\frac{3}{2}, \frac{\sqrt{5}}{2}, \frac{\sqrt{7}}{2}i, \frac{\sqrt{27}}{2}i$	0.8	$\Leftarrow \alpha = 0$ $\alpha = 0.03 \Rightarrow$ $\alpha = 0.1 \Rightarrow$ $\alpha = 0.3 \Rightarrow$	 0.9 1.15 2.15
$\frac{1}{2}, \frac{3}{2}, \frac{5}{2}, \frac{7}{2}$	$\sqrt{2}, 0, 2i, \sqrt{10}i$	1	$\Leftarrow \alpha = 0$ $\alpha = 0.03 \Rightarrow$ $\alpha = 0.1 \Rightarrow$ $\alpha = 0.3 \Rightarrow$	 1 1 1
$\sqrt{2}, \sqrt{3}, \sqrt{5}$	$\frac{1}{2}, \frac{\sqrt{3}}{2}i, \frac{\sqrt{11}}{2}i$	0.95	$\Leftarrow \alpha = 0$ $\alpha = 0.03 \Rightarrow$ $\alpha = 0.1 \Rightarrow$ $\alpha = 0.3 \Rightarrow$	 0.96 1.03 1.1

**Table 2.** Comparison between the normalized entanglement entropy obtained from BD vacuum and  $\alpha$  vacuum in absence of axion source ( $f_p^{(\alpha)} = 0$ ) for  $\nu^2 \geq 0$ .

In fig. (14(a)) and fig. (14(b)), we have demonstrated the behaviour of entanglement entropy in  $D = 4$  de Sitter space in absence ( $f_p^{(\alpha)} = 0$ ) and in presence ( $f_p^{(\alpha)} = 10^{-7}$ ) of axionic source with respect to the mass parameter  $\nu^2$ . In both the cases we have normalized the entanglement entropy with the result obtained from conformal mass parameter  $\nu = 1/2$  in presence of  $\alpha$  vacuum. In fig. (14(a)), it is clearly observed that in absence of axionic source in the large mass regime (where  $\nu^2 < 0$ ) the normalized entanglement entropy  $S_{intr}(\alpha)/S_{\nu=1/2}(\alpha)$  asymptotically approaches towards zero. In the large mass regime the measure of long range correlation (or more precisely the entanglement entropy) in presence of  $\alpha$  vacuum for axion

Small mass parameter $\nu$ ( $\nu^2 \geq 0$ )	Axion mass $m_{axion}/H$	Normalized entanglement entropy $\frac{c_6(0,\nu)}{c_6(0,\frac{1}{2})}$ from BD vacuum (with source)	Parameter $\alpha$	Normalized entanglement entropy $\frac{c_6(\alpha,\nu)}{c_6(\alpha,\frac{1}{2})}$ from $\alpha$ vacuum (with source)
0, 1, 2, 3	$\frac{3}{2}, \frac{\sqrt{5}}{2}, \frac{\sqrt{7}}{2}i, \frac{\sqrt{27}}{2}i$	0.99999	$\Leftarrow \alpha = 0$ $\alpha = 0.03 \Rightarrow$ $\alpha = 0.1 \Rightarrow$ $\alpha = 0.3 \Rightarrow$	 0.99998 1.00004 1.00026
$\frac{1}{2}, \frac{3}{2}, \frac{5}{2}, \frac{7}{2}$	$\sqrt{2}, 0, 2i, \sqrt{10}i$	1	$\Leftarrow \alpha = 0$ $\alpha = 0.03 \Rightarrow$ $\alpha = 0.1 \Rightarrow$ $\alpha = 0.3 \Rightarrow$	 1 1 1
$\sqrt{2}, \sqrt{3}, \sqrt{5}$	$\frac{1}{2}, \frac{\sqrt{3}}{2}i, \frac{\sqrt{11}}{2}i$	0.99998	$\Leftarrow \alpha = 0$ $\alpha = 0.03 \Rightarrow$ $\alpha = 0.1 \Rightarrow$ $\alpha = 0.3 \Rightarrow$	 0.99999 1.00001 1.00003

**Table 3.** Comparison between the normalized entanglement entropy obtained from BD vacuum and  $\alpha$  vacuum in presence of axion source ( $f_p^{(\alpha)} = 10^{-7}$ ) for  $\nu^2 \geq 0$ .

can be expressed for  $\gamma_p^{(\alpha)} = e^{-\pi|m_{axion}/H|} (1 + \tan \alpha)$  as:

$$\begin{aligned}
c_6 \left( \alpha, |\nu| \approx \frac{m_{axion}}{H} \right) &= S_{\text{intr}} \left( \alpha, |\nu| \approx \frac{m_{axion}}{H} \right) \\
&\approx \frac{2}{3} \left( \frac{m_{axion}}{H} \right)^4 e^{-\frac{2\pi m_{axion}}{H}} (1 + \tan \alpha)^2 \\
&\quad \times \left\{ 1 - \frac{H}{\pi m_{axion}} \ln(1 + \tan \alpha) \right\} \left[ 1 + (1 + \tan \alpha)^2 \mathcal{O} \left( \frac{H}{m_{axion}} \right) \right],
\end{aligned} \tag{3.184}$$

in which by fixing  $\alpha = 0$  we get the result for Bunch Davies vacuum as given by [14]:

$$c_6 \left( 0, |\nu| \approx \frac{m_{axion}}{H} \right) = S_{\text{intr}} \left( 0, |\nu| \approx \frac{m_{axion}}{H} \right) \approx \frac{2}{3} \left( \frac{m_{axion}}{H} \right)^4 e^{-\frac{2\pi m_{axion}}{H}}. \tag{3.185}$$

If we further compare Eq (3.184) and Eq (3.185) then it is clearly observed that in presence of  $\alpha$  vacuum one can able to get considerably large entanglement compared to the

Large mass parameter $\nu$ ( $\nu^2 < 0$ )	Axion mass $m_{axion}/H$	Normalized entanglement entropy $\frac{c_6(0,\nu)}{c_6(0,\frac{1}{2})}$ from BD vacuum (without source)	Parameter $\alpha$	Normalized entanglement entropy $\frac{c_6(\alpha,\nu)}{c_6(\alpha,\frac{1}{2})}$ from $\alpha$ vacuum (without source)
$\frac{i}{2}$	$\sqrt{\frac{5}{2}}$	0.55	$\leftarrow \alpha = 0$ $\alpha = 0.03 \Rightarrow$ $\alpha = 0.1 \Rightarrow$ $\alpha = 0.3 \Rightarrow$	0.63 0.7 1.12
$i$	$\frac{\sqrt{13}}{2}$	0.12	$\leftarrow \alpha = 0$ $\alpha = 0.03 \Rightarrow$ $\alpha = 0.1 \Rightarrow$ $\alpha = 0.3 \Rightarrow$	0.15 0.2 0.35
$\sqrt{2}i$	$\frac{\sqrt{17}}{2}$	0.02	$\leftarrow \alpha = 0$ $\alpha = 0.03 \Rightarrow$ $\alpha = 0.1 \Rightarrow$ $\alpha = 0.3 \Rightarrow$	0.04 0.06 0.1

**Table 4.** Comparison between the normalized entanglement entropy obtained from BD vacuum and  $\alpha$  vacuum in absence of axion source ( $f_p^{(\alpha)} = 0$ ) for  $\nu^2 < 0$ .

result obtained for Bunch Davies vacuum ( $\alpha = 0$ ) for large mass regime ( $\nu^2 < 0$ ). To demonstrate this clearly we have depicted the numerical values of the entanglement entropy for  $\alpha = 0$  (red),  $\alpha = 0.03$  (blue),  $\alpha = 0.1$  (green) and  $\alpha = 0.3$  (violet). Now from the fig. (14(a)) it is observed that in  $\nu^2 > 0$  region  $S_{intr}(\alpha)/S_{\nu=1/2}(\alpha)$  reach its maximum value at  $\alpha = 0.1$  (green) and  $\alpha = 0.3$  (violet) with  $\nu = 0$  (or  $m_{axion} = 3H/2$ ), as given by,  $(S_{intr}(0.1)/S_{\nu=1/2}(0.1))_{\max,\nu=0} \sim 1.2$  and  $(S_{intr}(0.3)/S_{\nu=1/2}(0.3))_{\max,\nu=0} \sim 2.1$ . On the other hand, at  $\alpha = 0.03$  (blue) and  $\alpha = 0$  and  $\alpha = 0.3$  (red) with  $\nu = 1/2$  (or  $m_{axion} = \sqrt{2}H$ ) the maximum value of  $S_{intr}(\alpha)/S_{\nu=1/2}(\alpha)$  is given by,  $(S_{intr}(0.03)/S_{\nu=1/2}(0.03))_{\max,\nu=1/2} \sim (S_{intr}(0)/S_{\nu=1/2}(0))_{\max,\nu=1/2} \sim 1$ . Further if we consider the interval  $3/2 < \nu < 5/2$  then  $S_{intr}(\alpha)/S_{\nu=1/2}(\alpha)$  show one oscillation with different amplitude for all values of the parameter  $\alpha$ . After that it reach its maximum value for  $\alpha = 0$  and  $\alpha = 0.03$ , as given by,  $(S_{intr}(0.03)/S_{\nu=1/2}(0.03))_{\max,3/2 < \nu < 5/2} \sim (S_{intr}(0)/S_{\nu=1/2}(0))_{\max,3/2 < \nu < 5/2} \sim 1$ . On the other hand,  $S_{intr}(\alpha)/S_{\nu=1/2}(\alpha)$  reach its minimum value for  $\alpha = 0.1$  and  $\alpha = 0.3$ , as given

Large mass parameter $\nu$ ( $\nu^2 < 0$ )	Axion mass $m_{axion}/H$	Normalized entanglement entropy $\frac{c_6(0,\nu)}{c_6(0,\frac{1}{2})}$ from BD vacuum (with source)	Parameter $\alpha$	Normalized entanglement entropy $\frac{c_6(\alpha,\nu)}{c_6(\alpha,\frac{1}{2})}$ from $\alpha$ vacuum (with source)
$\frac{i}{2}$	$\sqrt{\frac{5}{2}}$	0.99987	$\Leftarrow \alpha = 0$ $\alpha = 0.03 \Rightarrow$ $\alpha = 0.1 \Rightarrow$ $\alpha = 0.3 \Rightarrow$	0.99988 0.99992 1.00002
$i$	$\frac{\sqrt{13}}{2}$	0.99976	$\Leftarrow \alpha = 0$ $\alpha = 0.03 \Rightarrow$ $\alpha = 0.1 \Rightarrow$ $\alpha = 0.3 \Rightarrow$	0.99978 0.99981 0.99986
$\sqrt{2}i$	$\frac{\sqrt{17}}{2}$	0.99973	$\Leftarrow \alpha = 0$ $\alpha = 0.03 \Rightarrow$ $\alpha = 0.1 \Rightarrow$ $\alpha = 0.3 \Rightarrow$	0.99974 0.99975 0.99976

**Table 5.** Comparison between the normalized entanglement entropy obtained from BD vacuum and  $\alpha$  vacuum in presence of axion source ( $f_p^{(\alpha)} = 10^{-7}$ ) for  $\nu^2 < 0$ .

by,  $(S_{intr}(0.1)/S_{\nu=1/2}(0.1))_{\min,3/2 < \nu < 5/2} \sim 1$  and  $(S_{intr}(0.3)/S_{\nu=1/2}(0.3))_{\min,3/2 < \nu < 5/2} \sim 1$ . Similarly in the interval  $5/2 < \nu < 7/2$  we can observe the same feature for the same values of  $\alpha$  with larger period of oscillation. In fig. (14(b)), the significant role of axionic source term is explicitly shown. In both  $\nu^2 < 0$  and  $\nu^2 > 0$  regime the behaviour of  $S_{intr}(\alpha)/S_{\nu=1/2}(\alpha)$  is exactly same as depicted in fig. (14(a)). But in presence of axionic source term the amount of  $S_{intr}(\alpha)/S_{\nu=1/2}(\alpha)$  increase for  $\alpha = 0$ ,  $\alpha = 0.03$  and decrease for  $\alpha = 0.1$ ,  $\alpha = 0.3$  compared to fig. (14(a)). Also it is important to note that, the amplitude of the maximum and minimum of the oscillations change in presence of axionic source term.

On the other hand, for  $\gamma_p = e^{\pi|m_{axion}/H|} (1 + \tan \alpha)$  the entanglement entropy for axion in

the large mass limiting range is given by the following expression:

$$\begin{aligned} \mathbf{c}_6 \left( \alpha, |\nu| \approx \frac{m_{axion}}{H} \right) &= S_{\text{intr}} \left( \alpha, |\nu| \approx \frac{m_{axion}}{H} \right) \\ &\approx -\frac{1}{3\pi} \left( \frac{m_{axion}}{H} \right)^3 \left[ \ln \left( 1 - e^{\frac{2\pi m_{axion}}{H}} (1 + \tan \alpha)^2 \right) \right. \\ &\quad \left. + \frac{(2 \ln(1 + \tan \alpha) + \frac{2\pi m_{axion}}{H}) e^{\frac{2\pi m_{axion}}{H}} (1 + \tan \alpha)^2}{\left( 1 - e^{\frac{2\pi m_{axion}}{H}} (1 + \tan \alpha)^2 \right)} \right], \end{aligned} \quad (3.186)$$

in which by fixing  $\alpha = 0$  we get the result for Bunch Davies vacuum as given by:

$$\begin{aligned} \mathbf{c}_6 \left( 0, |\nu| \approx \frac{m_{axion}}{H} \right) &= S_{\text{intr}} \left( 0, |\nu| \approx \frac{m_{axion}}{H} \right) \\ &\approx -\frac{1}{3\pi} \left( \frac{m_{axion}}{H} \right)^3 \left[ \ln \left( 1 - e^{\frac{2\pi m_{axion}}{H}} \right) \right. \\ &\quad \left. + \frac{2\pi m_{axion}}{H} \frac{e^{\frac{2\pi m_{axion}}{H}}}{\left( 1 - e^{\frac{2\pi m_{axion}}{H}} \right)} \right], \end{aligned} \quad (3.187)$$

However, as mentioned in ref. [14] that due to the complicated sturcture of this solution we have not use this solution for our further discussion.

Next, in fig. (15), we have depicted the behaviour of entanglement entropy  $S_{\text{intr}}(\alpha)$  with respect to the parameter  $\alpha$  in absence ( $f_p^{(\alpha)} = 0$ ) and presence ( $f_p^{(\alpha)} = 10^{-7}$ ) of axionic source for the mass parameter  $\nu^2 < 0$  and  $\nu^2 > 0$  respectively. In fig. (15(a)) and fig. (15(b)) it is observed that a crossover takes place for  $\nu^2 = 1/4, 9/4, 25/4$  (green),  $\nu^2 = 1/16, 9/16, 25/16$  (blue) and  $\nu^2 = 0$  (red) with small values of the parameter  $\alpha$ . We also observe that for  $\nu^2 = 1/4, 9/4, 25/4$  (green) entanglement entropy decreases with increasing value of the parameter  $\alpha$ . On the other hand, for  $\nu^2 = 1/16, 9/16, 25/16$  (blue) and  $\nu^2 = 0$  (red) entanglement entropy increases with increasing value of the parameter  $\alpha$ . Additionally, we observe that, in presence of axionic source the entanglement entropy is significantly larger compared to the result obtained in absence of source contribution. In fig. (15(c)) and fig. (15(d)) it is observed that no crossover takes place for  $\nu^2 = -1/2$  (green),  $\nu^2 = -1/4, -9/4, -25/4$  (blue) and  $\nu^2 = -1/16, -9/16, -25/16$  (red) with all values of the parameter  $\alpha$ . Also it is important to note that, for all values of  $\nu^2 < 0$  entanglement entropy increases with increasing value of the parameter  $\alpha$ .

In table (2) and table (3), we have mentioned the numerical estimate of the normalized entanglement entropy in absence ( $f_p^{(\alpha)} = 0$ ) and presence ( $f_p^{(\alpha)} = 10^{-7}$ ) of axionic source contribution for Bunch Davies vacuum and  $\alpha$  vacuum with small mass parameter ( $\nu^2 \geq 0$ ). On the other hand, in table (4) and table (5), we have mentioned the numerical estimate of the normalized entanglement entropy in absence ( $f_p^{(\alpha)} = 0$ ) and presence ( $f_p^{(\alpha)} = 10^{-7}$ ) of axionic source contribution for Bunch Davies vacuum and  $\alpha$  vacuum with large mass parameter ( $\nu^2 < 0$ ). Here numerical results from both  $\nu^2 \geq 0$  and  $\nu^2 < 0$  region suggests that the quantum entanglement is significantly larger in presence of axionic source, compared to the result obtained in absence of axionic source. It is also important to note that, in presence of axionic source contribution in small  $\alpha$  region (lying within the window  $0 < \alpha < 0.3$ ), **A.** entanglement entropy is insensitive to the change in the parameter  $\alpha$ . **B.** entanglement entropy increases with the increase in the value of the mass parameter  $|\nu| \approx m_{axion}/H$ . But in absence of axionic source both the observations from the numerical results are completely opposite.

### 3.4 Computation of Rényi entropy using $\alpha$ vacua

In this context one can further use the density matrix to compute the Rényi entropy for  $\alpha$  vacuum, which is defined as:

$$S_q(p, \nu, \alpha) = \frac{1}{1-q} \ln \text{Tr} [\rho_{\mathbf{L}}(p, \alpha)]^q. \quad \text{with } q > 0. \quad (3.188)$$

For the **Case I** and **Case II** the of the obtained solution for  $\alpha$  vacuum with a given  $\mathbf{SO}(1, 3)$  principal quantum number  $p$  can be written as:

$$S_q(p, \nu, \alpha) = \left[ \frac{q}{1-q} \ln \left( 1 - |\gamma_p^{(\alpha)}|^2 \right) - \frac{1}{1-q} \ln \left( 1 - |\gamma_p^{(\alpha)}|^{2q} \right) \right] - \frac{q}{1-q} \ln \left( 1 + f_p^{(\alpha)} \right) + \frac{1}{1-q} \ln \left[ 1 + \sum_{k=1}^q {}^q C_k (f_p^{(\alpha)})^k \frac{\left( 1 - |\gamma_p^{(\alpha)}|^2 \right)^{-k}}{\left( 1 - |\gamma_p^{(\alpha)}|^{-2k} \right)} \right], \quad (3.189)$$

using which the interesting part of the Rényi entropy in de Sitter space for  $\alpha$  vacuum can be written as:

$$S_{q, \text{intr}}(\alpha, \nu) = \frac{1}{\pi} \int_{p=0}^{\infty} dp p^2 S_q(p, \nu, \alpha). \quad (3.190)$$

Now to study the properties of the derived result we check the following physical limiting situations as given by:

- If we take the limit  $q \rightarrow 1$  limit then from the Rényi entropy in  $\alpha$  vacuum we get,  $\lim_{q \rightarrow 1} S_q(p, \nu, \alpha) \neq S(p, \nu, \alpha)$ . which shows that in presence of axionic source, the entanglement entropy and Rényi entropy are not same in the limit  $q \rightarrow 1$ . Now if we take further  $f_p \rightarrow 0$  then entanglement entropy and Rényi entropy both are same.
- Further if we take the limit  $q \rightarrow \infty$  limit then from the Rényi entropy in  $\alpha$  vacuum we get:

$$\lim_{q \rightarrow \infty} S_q(p, \nu, \alpha) = -\ln[\rho_{\mathbf{L}}]_{\text{max}} \approx \ln \left( \frac{1 + f_p^{(\alpha)}}{1 - |\gamma_p^{(\alpha)}|^2} \right). \quad (3.191)$$

which directly implies the largest eigenvalue of density matrix. Now if we take further  $f_p \rightarrow 0$  in Eqn (3.191) then entanglement entropy and Rényi entropy both are same.

Further substituting the expression for entanglement entropy  $S(p, \nu, \alpha)$  computed in presence of axion for  $\alpha$  vacuum and integrating over all possible  $\mathbf{SO}(1, 3)$  principal quantum number, lying within the window  $0 < p < \infty$ , we get:

$$S_{q, \text{intr}}(\alpha, \nu) = \left[ \mathcal{M}_{1,q} + \ln \left( 1 + f_p^{(\alpha)} \right) \mathcal{M}_{2,q}^{(\alpha)} + \mathcal{M}_{3,q}^{(\alpha)} \right], \quad (3.192)$$

where the integrals  $\mathcal{M}_{1,q}$ ,  $\mathcal{M}_{2,q}^{(\alpha)}$  and  $\mathcal{M}_{3,q}^{(\alpha)}$  can be written as:

$$\mathcal{M}_{1,q} = \frac{1}{\pi} \int_{p=0}^{\infty} dp p^2 \left[ \frac{q}{1-q} \ln \left( 1 - |\gamma_p^{(\alpha)}|^2 \right) - \frac{1}{1-q} \ln \left( 1 - |\gamma_p^{(\alpha)}|^{2q} \right) \right], \quad (3.193)$$

$$\mathcal{M}_{2,q}^{(\alpha)} = -\frac{1}{\pi} \frac{q}{1-q} \int_{p=0}^{\infty} dp p^2, \quad (3.194)$$

$$\mathcal{M}_{3,q}^{(\alpha)} = \frac{1}{\pi} \frac{1}{1-q} \int_{p=0}^{\infty} dp p^2 \ln \left[ 1 + \sum_{k=1}^q {}^q C_k (f_p^{(\alpha)})^k \frac{\left( 1 - |\gamma_p^{(\alpha)}|^2 \right)^{-k}}{\left( 1 - |\gamma_p^{(\alpha)}|^{-2k} \right)} \right]. \quad (3.195)$$

Here it is important to note that:



- Here the integral  $\mathcal{M}_{2,q}^{(\alpha)}$  diverges. Further introducing a change in variable to  $x = 2\pi p$  along with a cut-off  $\Lambda_{\mathbf{C}}$  the regularized version of this integral can be written as:

$$\mathcal{M}_{2,q}^{(\alpha)} = -\frac{1}{8\pi^4} \frac{q}{1-q} \int_{x=0}^{\Lambda_{\mathbf{C}}} dx x^2 = -\frac{\Lambda_{\mathbf{C}}^3}{24\pi^4} \frac{q}{1-q}. \quad (3.196)$$

- Here for **Case I** we get one solution for  $|\gamma_p^{(\alpha)}|$  as given by,

$$|\gamma_p^{(\alpha)}| = e^{-\pi p} (\cosh^2 \alpha - \sinh^2 \alpha e^{-2\pi p})^{-1}. \quad (3.197)$$

Using this solution we compute the integrals  $\mathcal{M}_{1,q}^{(\alpha)}$  and  $\mathcal{M}_{3,q}^{(\alpha)}$  for **Case I** with any arbitrary value of the parameter  $\alpha$ . Further we use the rescaled **SO(1, 3)** quantum number  $x = 2\pi p$  with cut-off  $\Lambda_{\mathbf{C}}$  to compute this integral. Consequently we get:

$$\mathcal{M}_{1,q}^{(\alpha)} = \frac{1}{8\pi^4} \int_{x=0}^{\Lambda_{\mathbf{C}}} dx x^2 \left[ \frac{q}{1-q} \ln \left( 1 - \frac{e^{-x}}{(\cosh^2 \alpha - \sinh^2 \alpha e^{-x})^2} \right) - \frac{1}{1-q} \ln \left( 1 - \frac{e^{-xq}}{(\cosh^2 \alpha - \sinh^2 \alpha e^{-x})^{2q}} \right) \right], \quad (3.198)$$

$$\mathcal{M}_{3,q}^{(\alpha)} = \frac{1}{8\pi^4} \frac{1}{1-q} \int_{x=0}^{\infty} dx x^2 \ln \left[ 1 + \sum_{k=1}^q q \mathbf{C}_k (f_p^{(\alpha)})^k \frac{\left( 1 - \frac{e^{-x}}{(\cosh^2 \alpha - \sinh^2 \alpha e^{-x})^2} \right)^{-k}}{\left( 1 - \frac{e^{xk}}{(\cosh^2 \alpha - \sinh^2 \alpha e^{-x})^{-2k}} \right)} \right]. \quad (3.199)$$

Here the exact expression for  $\mathcal{M}_{3,q}^{(\alpha)}$  is not computable in the small  $\alpha$  (i.e.  $\alpha \ll 1$ ) limiting range. To check the consistency of our derived result with the Bunch Davies case we further take  $\alpha = 0$  and  $\Lambda_{\mathbf{C}} \rightarrow \infty$  limit, which gives:

$$\lim_{\Lambda_{\mathbf{C}} \rightarrow \infty} \mathcal{M}_{1,q}^{(0)} = \frac{(q+1)(q^2+1)}{360q^3}. \quad (3.200)$$

Further taking  $q \rightarrow 1$  and  $f_p^{(0)} \rightarrow 0$  on Eq (3.200) we finally get:

$$\begin{aligned} \mathbf{c}_6 \left( 0, \frac{1}{2} \right) &= \mathbf{c}_6 \left( 0, \frac{3}{2} \right) = \lim_{f_p^{(0)} \rightarrow 0} \lim_{q \rightarrow 1} \lim_{\Lambda_{\mathbf{C}} \rightarrow \infty} \mathcal{M}_{1,q}^{(0)} \\ &= \lim_{f_p^{(0)} \rightarrow 0} \lim_{q \rightarrow 1} \frac{(q+1)(q^2+1)}{360q^3} = \frac{1}{90}, \end{aligned} \quad (3.201)$$

$$\lim_{f_p^{(0)} \rightarrow 0} \lim_{q \rightarrow 1} \lim_{\Lambda_{\mathbf{C}} \rightarrow \infty} \mathcal{M}_{3,q}^{(0)} = 0, \quad (3.202)$$

which are perfectly consistent with the result obtained in refs. [14] for  $\nu = 1/2$  and  $\nu = 3/2$ .

Similarly, for **Case I** we get another solution,

$$|\gamma_p^{(\alpha)}| = e^{\pi p} (\cosh^2 \alpha - \sinh^2 \alpha e^{-2\pi p})^{-1}. \quad (3.203)$$

Using this solution we compute the integral  $\mathcal{I}^{(\alpha)}$  for **Case I** for any arbitrary value of the parameter  $\alpha$ . Consequently we get:

$$\mathcal{M}_{1,q}^{(\alpha)} = \frac{1}{8\pi^4} \int_{x=0}^{\Lambda_{\mathbf{C}}} dx x^2 \left[ \frac{q}{1-q} \ln \left( 1 - \frac{e^x}{(\cosh^2 \alpha - \sinh^2 \alpha e^{-x})^2} \right) - \frac{1}{1-q} \ln \left( 1 - \frac{e^{xq}}{(\cosh^2 \alpha - \sinh^2 \alpha e^{-x})^{2q}} \right) \right]. \quad (3.204)$$

Further To check the consistency of our derived result with the Bunch Davies case we take  $\alpha = 0$ ,  $q \rightarrow 1$  and  $f_p^{(0)} \rightarrow 0$  with large  $\Lambda_{\mathbf{C}}$ , which gives:

$$\begin{aligned} \mathbf{c}_6 \left( 0, \frac{1}{2} \right) &= \mathbf{c}_6 \left( 0, \frac{3}{2} \right) = \lim_{f_p^{(0)} \rightarrow 0} \lim_{q \rightarrow 1} \lim_{\Lambda_{\mathbf{C}} \rightarrow \text{Large}} \mathcal{M}_{1,q}^{(0)} \\ &= \frac{1}{8\pi^4} \left[ \Lambda_{\mathbf{C}}^3 \ln(1 - e^{\Lambda_{\mathbf{C}}}) + 4\Lambda_{\mathbf{C}}^2 \text{Li}_2(e^{\Lambda_{\mathbf{C}}}) \right. \\ &\quad \left. - 8\Lambda_{\mathbf{C}} \text{Li}_3(e^{\Lambda_{\mathbf{C}}}) + 8\text{Li}_4(e^{\Lambda_{\mathbf{C}}}) - \frac{4\pi^4}{45} \right]. \end{aligned} \quad (3.205)$$

$$\lim_{f_p^{(0)} \rightarrow 0} \lim_{q \rightarrow 1} \lim_{\Lambda_{\mathbf{C}} \rightarrow \text{Large}} \mathcal{M}_{3,q}^{(0)} = 0, \quad (3.206)$$

which are perfectly consistent with the result obtained in refs. [14] for  $\nu = 1/2$  and  $\nu = 3/2$ .

- On the other hand for arbitrary  $\nu$  and  $\alpha$  (**Case II**) we get:

$$\mathcal{M}_{1,q}^{(\alpha)} = \frac{1}{8\pi^4} \int_{x=0}^{\Lambda_{\mathbf{C}}} dx x^2 \left[ \frac{q}{1-q} \ln(1 - 2G_{\pm}(x, \nu, \alpha)) - \frac{1}{1-q} \ln(1 - (2G_{\pm}(x, \nu, \alpha))^q) \right], \quad (3.207)$$

$$\mathcal{M}_{3,q}^{(\alpha)} = \frac{1}{8\pi^4} \frac{1}{1-q} \int_{x=0}^{\Lambda_{\mathbf{C}}} dx x^2 \ln \left[ 1 + \sum_{k=1}^q q \mathbf{C}_k (f_p^{(\alpha)})^k \frac{(1 - 2G_{\pm}(x, \nu, \alpha))^{-k}}{(1 - (2G_{\pm}(x, \nu, \alpha))^{-k})} \right], \quad (3.208)$$

where  $G_{\pm}(x, \nu, \alpha)$  is defined in Eqn (3.162). we consider large axion mass ( $\nu^2 < 0$  where  $\nu \rightarrow -i|\nu|$ ) limiting situation which is important to study the physics from **Case II**. In this large axion mass limiting situation we consider the window of **SO(1, 3)** principal quantum number is  $0 < p < |\nu|$ .

As a result, the regularized integral  $\mathcal{M}_{1,q}^{(\alpha)}$  and  $\mathcal{M}_{3,q}^{(\alpha)}$  for the first solution for  $|\gamma_p^{(\alpha)}|$  in presence of  $\alpha$  vacuum can be expressed as:

$$\mathcal{M}_{1,q}^{(\alpha)} = \begin{cases} \frac{\mathcal{A}(\nu)}{8\pi^4} \left[ \frac{q}{1-q} \ln \left( 1 - e^{-2\pi\nu} (1 + \tan \alpha)^2 \right) - \frac{1}{1-q} \ln \left( 1 - e^{-2\pi\nu q} (1 + \tan \alpha)^{2q} \right) \right] & \text{for } 0 < x < 2\pi|\nu| \\ \frac{\mathcal{D}(\nu, \alpha, \Lambda_{\mathbf{C}}, q)}{8\pi^4} & \text{for } 2\pi|\nu| < x < \Lambda_{\mathbf{C}}. \end{cases} \quad (3.209)$$

$$\mathcal{M}_{3,q}^{(\alpha)} = \begin{cases} \frac{\mathcal{A}(\nu)}{8\pi^4} \frac{1}{1-q} \ln \left[ 1 + \sum_{k=1}^q {}^q\mathbf{C}_k (f_p^{(\alpha)})^k \frac{\left(1 - e^{-2\pi\nu} (1 + \tan \alpha)^2\right)^{-k}}{\left(1 - e^{2\pi\nu k} (1 + \tan \alpha)^{-2k}\right)} \right] & \text{for } 0 < x < 2\pi|\nu| \\ \frac{1}{8\pi^4} \frac{1}{1-q} \int_{x=2\pi\nu}^{\Lambda_{\mathbf{C}}} dx x^2 & \\ \ln \left[ 1 + \sum_{k=1}^q {}^q\mathbf{C}_k (f_p^{(\alpha)})^k \frac{\left(1 - \frac{e^{-x}(1+\tan \alpha)^2(1+\tan \alpha e^{2\pi\nu})^2}{(1+\tan^2 \alpha e^{-x})^2}\right)^{-k}}{\left(1 - \frac{e^{xk}(1+\tan \alpha)^{-2k}(1+\tan \alpha e^{2\pi\nu})^{-2k}}{(1+\tan^2 \alpha e^{-x})^{-2k}}\right)} \right] & \text{for } 2\pi|\nu| < x < \Lambda_{\mathbf{C}}. \end{cases} \quad (3.210)$$

and for the second solution for  $|\gamma_p^{(\alpha)}|$  in presence of  $\alpha$  vacuum we get:

$$\mathcal{M}_{1,q}^{(\alpha)} = \begin{cases} \frac{\mathcal{A}(\nu)}{8\pi^4} \left[ \frac{q}{1-q} \ln \left(1 - e^{2\pi\nu} (1 + \tan \alpha)^2\right) \right. \\ \quad \left. - \frac{1}{1-q} \ln \left(1 - e^{2\pi\nu q} (1 + \tan \alpha)^{2q}\right) \right] & \text{for } 0 < x < 2\pi|\nu| \\ \frac{\mathcal{W}(\nu, \alpha, \Lambda_{\mathbf{C}}, q)}{8\pi^4} & \text{for } 2\pi|\nu| < x < \Lambda_{\mathbf{C}}. \end{cases} \quad (3.211)$$

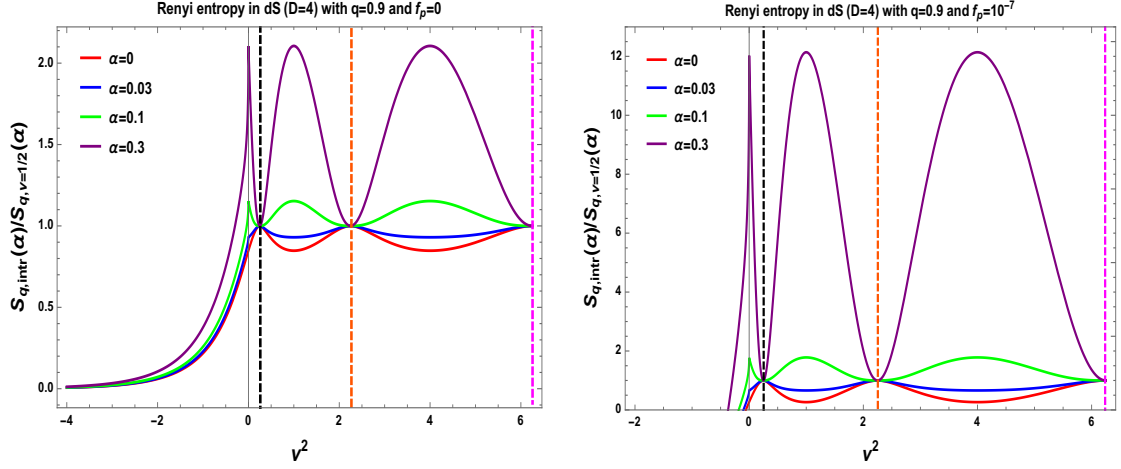
$$\mathcal{M}_{3,q}^{(\alpha)} = \begin{cases} \frac{\mathcal{A}(\nu)}{8\pi^4} \frac{1}{1-q} \ln \left[ 1 + \sum_{k=1}^q {}^q\mathbf{C}_k (f_p^{(\alpha)})^k \frac{\left(1 - e^{2\pi\nu} (1 + \tan \alpha)^2\right)^{-k}}{\left(1 - e^{-2\pi\nu k} (1 + \tan \alpha)^{-2k}\right)} \right] & \text{for } 0 < x < 2\pi|\nu| \\ \frac{1}{8\pi^4} \frac{1}{1-q} \int_{x=2\pi\nu}^{\Lambda_{\mathbf{C}}} dx x^2 & \\ \ln \left[ 1 + \sum_{k=1}^q {}^q\mathbf{C}_k (f_p^{(\alpha)})^k \frac{\left(1 - \frac{e^x(1+\tan \alpha)^2(1+\tan \alpha e^{2\pi\nu})^2}{(1+\tan^2 \alpha e^{-x})^2}\right)^{-k}}{\left(1 - \frac{e^{-xk}(1+\tan \alpha)^{-2k}(1+\tan \alpha e^{2\pi\nu})^{-2k}}{(1+\tan^2 \alpha e^{-x})^{-2k}}\right)} \right] & \text{for } 2\pi|\nu| < x < \Lambda_{\mathbf{C}}. \end{cases} \quad (3.212)$$

Here the coefficient function  $\mathcal{A}(\nu)$  is defined in Eq (3.171) and other  $\alpha$  parameter dependent functions  $\mathcal{D}(\nu, \alpha, \Lambda_{\mathbf{C}})$  and  $\mathcal{W}(\nu, \alpha, \Lambda_{\mathbf{C}})$  are defined as:

$$\mathcal{D}(\nu, \alpha, \Lambda_{\mathbf{C}}, q) = \int_{x=2\pi\nu}^{\Lambda_{\mathbf{C}}} dx x^2 \left[ \frac{q}{1-q} \ln \left(1 - \frac{e^{-x} (1 + \tan \alpha)^2 (1 + \tan \alpha e^{2\pi\nu})^2}{(1 + \tan^2 \alpha e^{-x})^2}\right) \right. \\ \left. - \frac{1}{1-q} \ln \left(1 - \frac{e^{-xq} (1 + \tan \alpha)^{2q} (1 + \tan \alpha e^{2\pi\nu})^{2q}}{(1 + \tan^2 \alpha e^{-x})^{2q}}\right) \right], \quad (3.213)$$

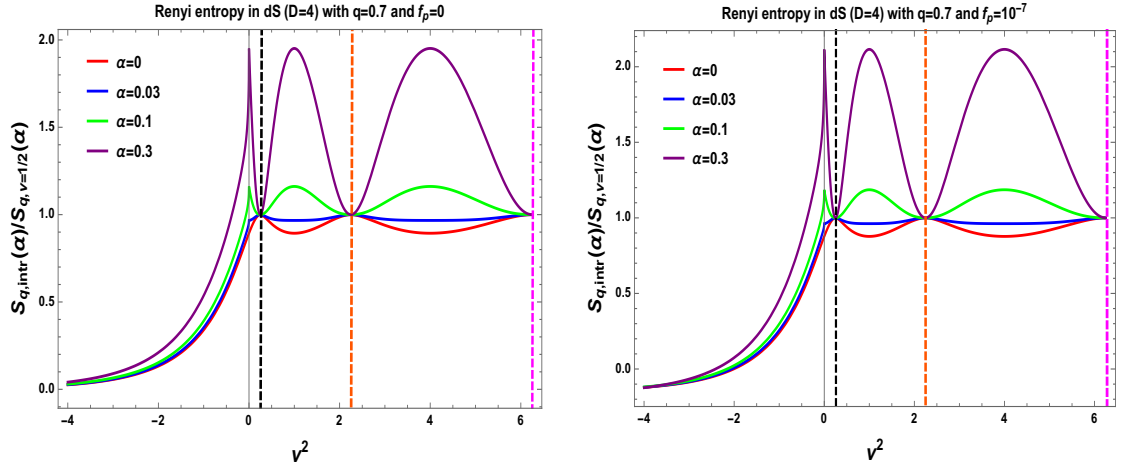
$$\mathcal{W}(\nu, \alpha, \Lambda_{\mathbf{C}}, q) = \int_{x=2\pi\nu}^{\Lambda_{\mathbf{C}}} dx x^2 \left[ \frac{q}{1-q} \ln \left(1 - \frac{e^x (1 + \tan \alpha)^2 (1 + \tan \alpha e^{2\pi\nu})^2}{(1 + \tan^2 \alpha e^{-x})^2}\right) \right. \\ \left. - \frac{1}{1-q} \ln \left(1 - \frac{e^{xq} (1 + \tan \alpha)^{2q} (1 + \tan \alpha e^{2\pi\nu})^{2q}}{(1 + \tan^2 \alpha e^{-x})^{2q}}\right) \right]. \quad (3.214)$$

Further, using the results obtained from the first solution for  $|\gamma_p^{(\alpha)}|$ , within the range  $0 < x < 2\pi|\nu|$  with  $\nu^2 < 0$ , we take  $q \rightarrow 1$  limit. This gives the following simplified expression



(a) Normalized Rényi entropy vs  $\nu^2$  in 3 + 1 D de Sitter space without axionic source ( $f_p^{(\alpha)} = 0$ ). (b) Normalized Rényi entropy vs  $\nu^2$  in 3 + 1 D de Sitter space without axionic source ( $f_p^{(\alpha)} = 10^{-7}$ ).

**Figure 16.** Normalized Rényi entropy  $S_{q,intr}(\alpha)/S_{q,\nu=1/2}(\alpha)$  vs mass parameter  $\nu^2$  in 3 + 1 D de Sitter space in absence of axionic source ( $f_p^{(\alpha)} = 0$ ) and in presence of axionic source ( $f_p^{(\alpha)} = 10^{-7}$ ) for  $q = 0.9$  and  $\alpha = 0$  (red),  $\alpha = 0.03$  (blue),  $\alpha = 0.1$  (green),  $\alpha = 0.3$  (violet) with ‘+’ branch of solution of  $|\gamma_p^{(\alpha)}|$  and  $|\Gamma_{p,n}^{(\alpha)}|$ . Here we set the cut-off  $\Lambda_C = 300$  for numerical computation.

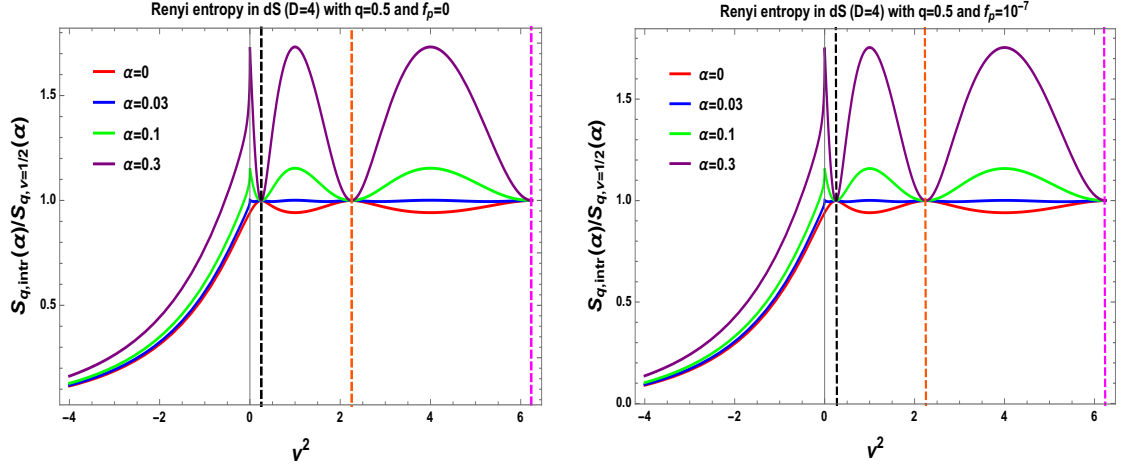


(a) Normalized Rényi entropy vs  $\nu^2$  in 3 + 1 D de Sitter space without axionic source ( $f_p^{(\alpha)} = 0$ ). (b) Normalized Rényi entropy vs  $\nu^2$  in 3 + 1 D de Sitter space without axionic source ( $f_p^{(\alpha)} = 10^{-7}$ ).

**Figure 17.** Normalized Rényi entropy  $S_{q,intr}(\alpha)/S_{q,\nu=1/2}(\alpha)$  vs mass parameter  $\nu^2$  in 3 + 1 D de Sitter space in absence of axionic source ( $f_p^{(\alpha)} = 0$ ) and in presence of axionic source ( $f_p^{(\alpha)} = 10^{-7}$ ) for  $q = 0.7$  and  $\alpha = 0$  (red),  $\alpha = 0.03$  (blue),  $\alpha = 0.1$  (green),  $\alpha = 0.3$  (violet) with ‘+’ branch of solution of  $|\gamma_p^{(\alpha)}|$  and  $|\Gamma_{p,n}^{(\alpha)}|$ . Here we set the cut-off  $\Lambda_C = 300$  for numerical computation.

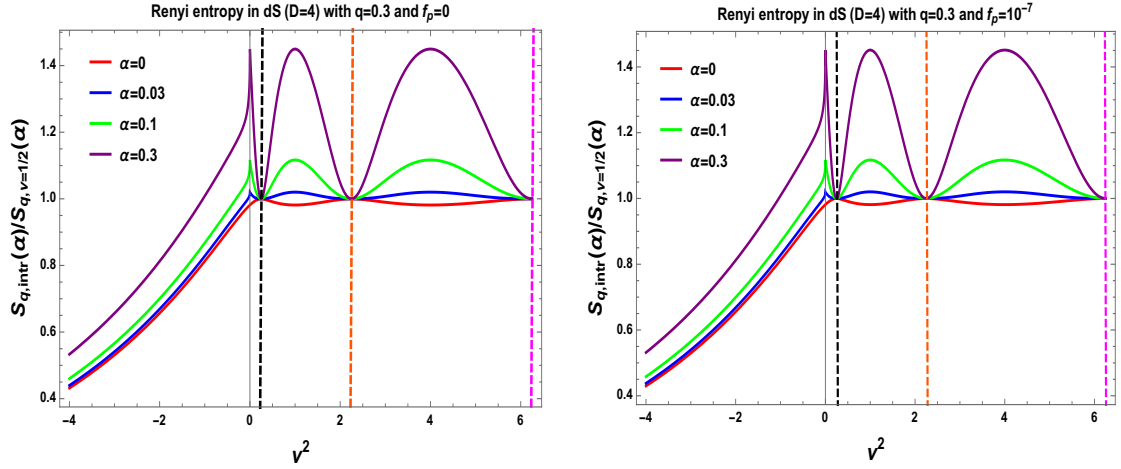
for the integral  $\mathcal{M}_{1,q}^{(\alpha)}$ :

$$\lim_{q \rightarrow 1} \mathcal{M}_{1,q}^{(\alpha)} = \frac{\nu^3}{3} \left[ \frac{2(1 + \tan \alpha)^2 \left\{ \nu - \frac{1}{\pi} \ln(1 + \tan \alpha) \right\}}{(e^{2\pi\nu} - (1 + \tan \alpha)^2)} - \frac{\ln \left( 1 - e^{-2\pi\nu} (1 + \tan \alpha)^2 \right)}{\pi} \right], \quad (3.215)$$



(a) Normalized Rényi entropy vs  $\nu^2$  in 3 + 1 D de Sitter space without axionic source ( $f_p^{(\alpha)} = 0$ ). (b) Normalized Rényi entropy vs  $\nu^2$  in 3 + 1 D de Sitter space without axionic source ( $f_p^{(\alpha)} = 10^{-7}$ ).

**Figure 18.** Normalized Rényi entropy  $S_{q,intr}(\alpha)/S_{q,\nu=1/2}(\alpha)$  vs mass parameter  $\nu^2$  in 3 + 1 D de Sitter space in absence of axionic source ( $f_p^{(\alpha)} = 0$ ) and in presence of axionic source ( $f_p^{(\alpha)} = 10^{-7}$ ) for  $q = 0.5$  and  $\alpha = 0$  (red),  $\alpha = 0.03$  (blue),  $\alpha = 0.1$  (green),  $\alpha = 0.3$  (violet) with ‘+’ branch of solution of  $|\gamma_p^{(\alpha)}|$  and  $|\Gamma_{p,n}^{(\alpha)}|$ . Here we set the cut-off  $\Lambda_C = 300$  for numerical computation.

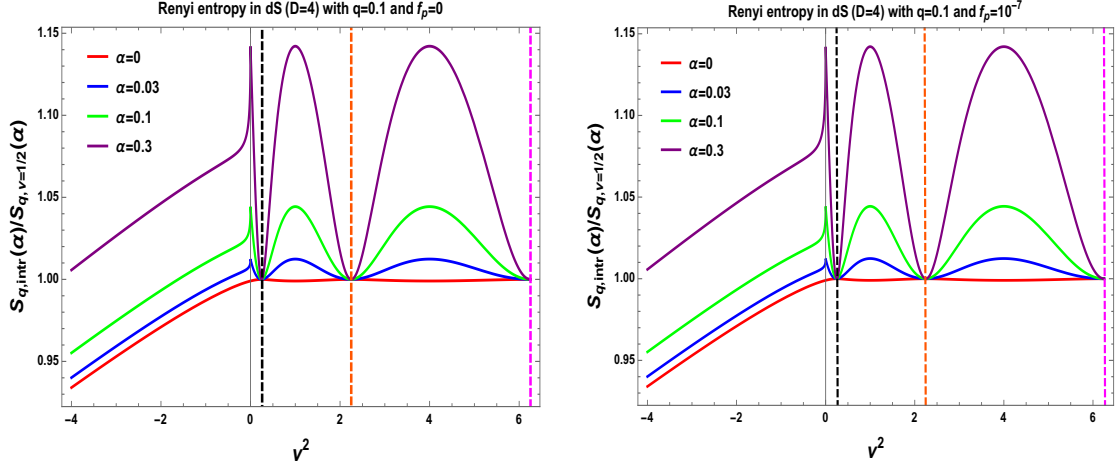


(a) Normalized Rényi entropy vs  $\nu^2$  in 3 + 1 D de Sitter space without axionic source ( $f_p^{(\alpha)} = 0$ ). (b) Normalized Rényi entropy vs  $\nu^2$  in 3 + 1 D de Sitter space without axionic source ( $f_p^{(\alpha)} = 10^{-7}$ ).

**Figure 19.** Normalized Rényi entropy  $S_{q,intr}(\alpha)/S_{q,\nu=1/2}(\alpha)$  vs mass parameter  $\nu^2$  in 3 + 1 D de Sitter space in absence of axionic source ( $f_p^{(\alpha)} = 0$ ) and in presence of axionic source ( $f_p^{(\alpha)} = 10^{-7}$ ) for  $q = 0.3$  and  $\alpha = 0$  (red),  $\alpha = 0.03$  (blue),  $\alpha = 0.1$  (green),  $\alpha = 0.3$  (violet) with ‘+’ branch of solution of  $|\gamma_p^{(\alpha)}|$  and  $|\Gamma_{p,n}^{(\alpha)}|$ . Here we set the cut-off  $\Lambda_C = 300$  for numerical computation.

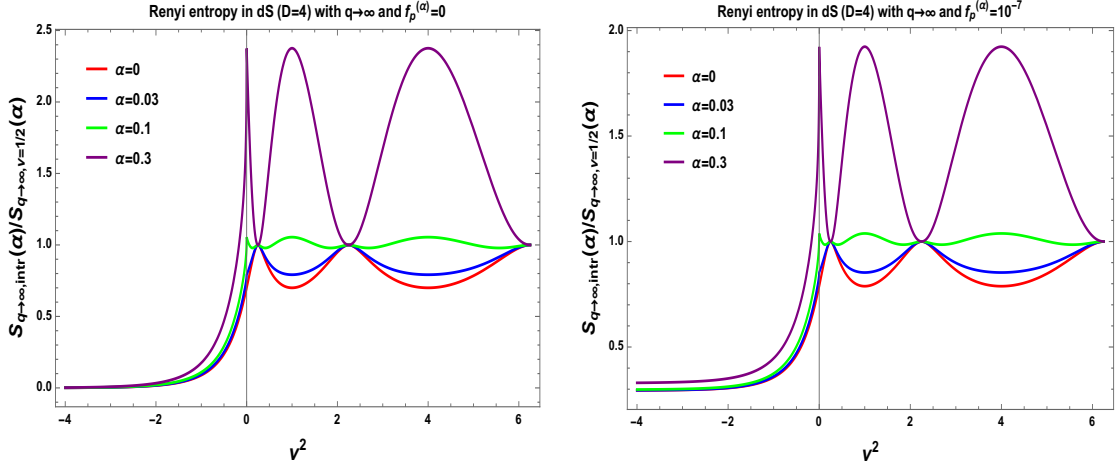
using which for Bunch davies vacuum ( $\alpha = 0$ ) we get [14]:

$$\lim_{q \rightarrow 1} \mathcal{M}_{1,q}^{(0)} = \frac{\nu^3}{3} \left( \frac{2\nu}{e^{2\pi\nu} - 1} - \frac{\ln(1 - e^{-2\pi\nu})}{\pi} \right). \quad (3.216)$$



(a) Normalized Rényi entropy vs  $\nu^2$  in 3 + 1 D de Sitter space without axionic source ( $f_p^{(\alpha)} = 0$ ). (b) Normalized Rényi entropy vs  $\nu^2$  in 3 + 1 D de Sitter space without axionic source ( $f_p^{(\alpha)} = 10^{-7}$ ).

**Figure 20.** Normalized Rényi entropy  $S_{q,intr}(\alpha)/S_{q,\nu=1/2}(\alpha)$  vs mass parameter  $\nu^2$  in 3 + 1 D de Sitter space in absence of axionic source ( $f_p^{(\alpha)} = 0$ ) and in presence of axionic source ( $f_p^{(\alpha)} = 10^{-7}$ ) for  $q = 0.1$  and  $\alpha = 0$  (red),  $\alpha = 0.03$  (blue),  $\alpha = 0.1$  (green),  $\alpha = 0.3$  (violet) with ‘+’ branch of solution of  $|\gamma_p^{(\alpha)}|$  and  $|\Gamma_{p,n}^{(\alpha)}|$ . Here we set the cut-off  $\Lambda_C = 300$  for numerical computation.

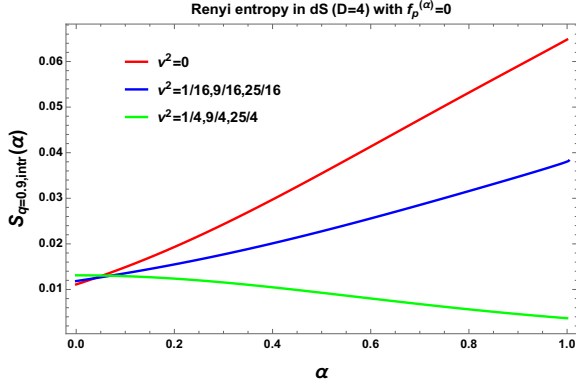


(a) Normalized Rényi entropy vs  $\nu^2$  in 3 + 1 D de Sitter space without axionic source ( $f_p = 0$ ). (b) Normalized Rényi entropy vs  $\nu^2$  in de Sitter space with axionic source ( $f_p = 10^{-7}$ ).

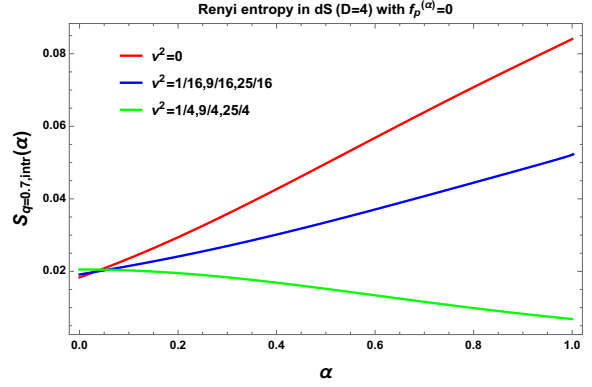
**Figure 21.** Normalized Rényi entropy  $S_{q \rightarrow \infty,intr}(\alpha)/S_{q \rightarrow \infty,\nu=1/2}(\alpha)$  vs mass parameter  $\nu^2$  in 3 + 1 D de Sitter space in absence of axionic source ( $f_p^{(\alpha)} = 0$ ) and in presence of axionic source ( $f_p^{(\alpha)} = 10^{-7}$ ) for  $q \rightarrow \infty$  and  $\alpha = 0$  (red),  $\alpha = 0.03$  (blue),  $\alpha = 0.1$  (green),  $\alpha = 0.3$  (violet) with ‘+’ branch of solution of  $|\gamma_p^{(\alpha)}|$  and  $|\Gamma_{p,n}^{(\alpha)}|$ , which quantifies largest eigenvalue of density matrix. Here we set the cut-off  $\Lambda_C = 300$  for numerical computation.

Now further using  $|\nu| \gg 1$  approximation in Eq (3.215) we get:

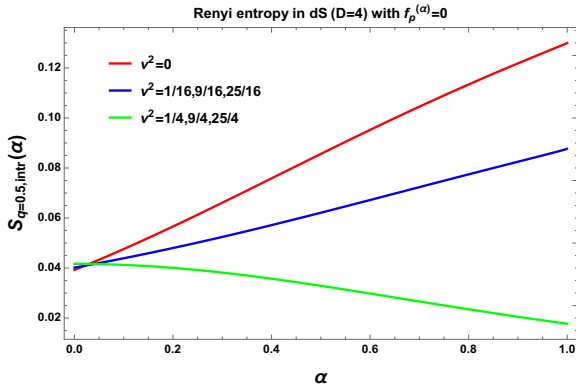
$$\lim_{|\nu| \gg 1, q \rightarrow 1} \mathcal{M}_{1,q}^{(\alpha)} = \frac{2\nu^4}{3} e^{-2\pi\nu} (1 + \tan \alpha)^2 \left\{ 1 - \frac{1}{\pi\nu} \ln(1 + \tan \alpha) \right\} \left[ 1 + (1 + \tan \alpha)^2 \mathcal{O}(\nu^{-1}) \right], \quad (3.217)$$



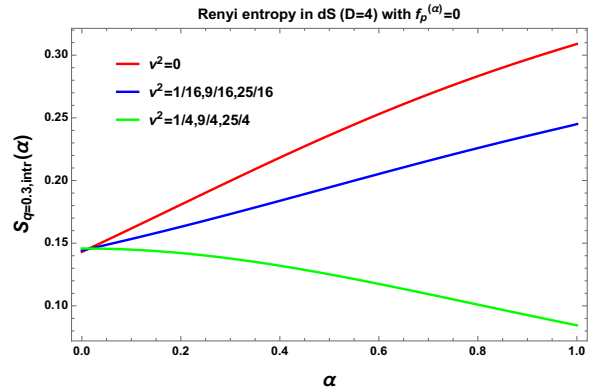
(a) For  $q = 0.9$  and  $\nu^2 > 0$ .



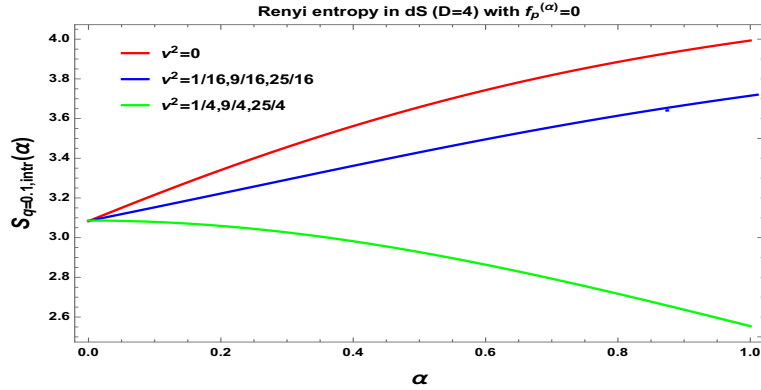
(b) For  $q = 0.7$  and  $\nu^2 > 0$ .



(c) For  $q = 0.5$  and  $\nu^2 > 0$ .



(d) For  $q = 0.3$  and  $\nu^2 > 0$ .



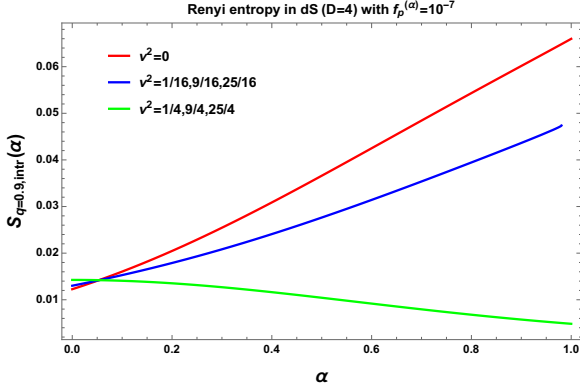
(e) For  $q = 0.1$  and  $\nu^2 > 0$ .

**Figure 22.** Rényi entropy  $S_{q, intr}(\alpha)$  vs parameter  $\alpha$  plot in 3 + 1 D de Sitter space in absence of axionic source ( $f_p^{(\alpha)} = 0$ ) for  $q = 0.1, q = 0.3, q = 0.5, q = 0.7, q = 0.9$  with ‘+’ branch of solution of  $|\gamma_p^{(\alpha)}|$  and  $|\Gamma_{p, n}^{(\alpha)}|$ .

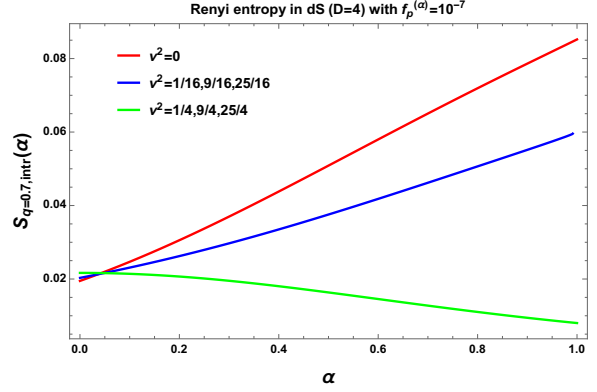
which is consistent with the Bunch Davies limiting result [14]:

$$\lim_{|\nu| \gg 1, q \rightarrow 1} \mathcal{M}_{1, q}^{(0)} \approx \frac{2\nu^4}{3} e^{-2\pi\nu} [1 + \mathcal{O}(\nu^{-1})]. \quad (3.218)$$

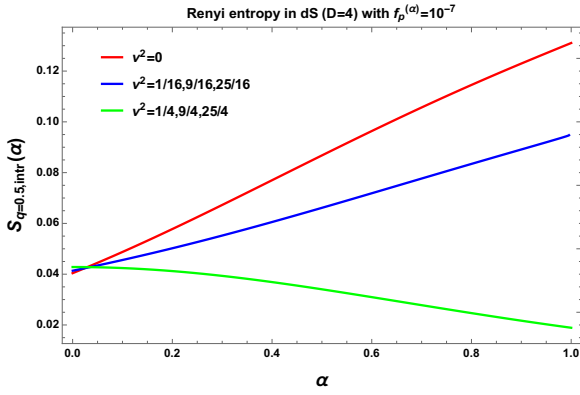
In this context further if we take the sourceless limit  $f_p^{(\alpha)} \rightarrow 0$  then the integral  $\mathcal{M}_{3, q}^{(\alpha)}$



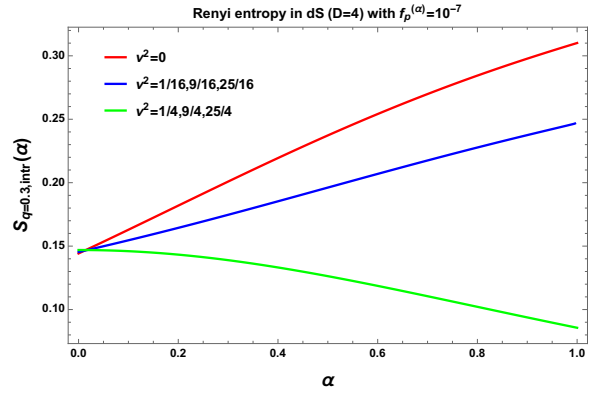
(a) For  $q = 0.9$  and  $\nu^2 > 0$ .



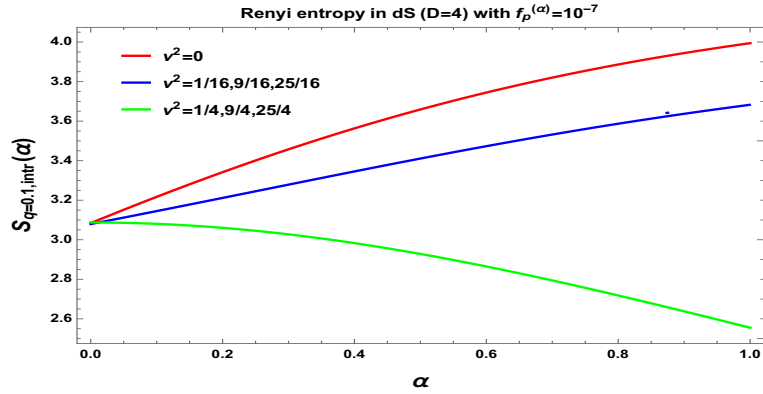
(b) For  $q = 0.7$  and  $\nu^2 > 0$ .



(c) For  $q = 0.5$  and  $\nu^2 > 0$ .



(d) For  $q = 0.3$  and  $\nu^2 > 0$ .



(e) For  $q = 0.1$  and  $\nu^2 > 0$ .

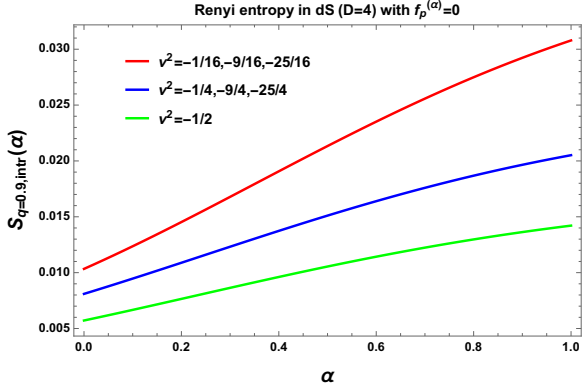
**Figure 23.** Rényi entropy  $S_{q, intr}(\alpha)$  vs parameter  $\alpha$  plot in 3 + 1 D de Sitter space in presence of axionic source ( $f_p^{(\alpha)} = 10^{-7}$ ) for  $q = 0.1, q = 0.3, q = 0.5, q = 0.7, q = 0.9$  with ‘+’ branch of solution of  $|\gamma_p^{(\alpha)}|$  and  $|\Gamma_{p, n}^{(\alpha)}|$ .

vanishes:

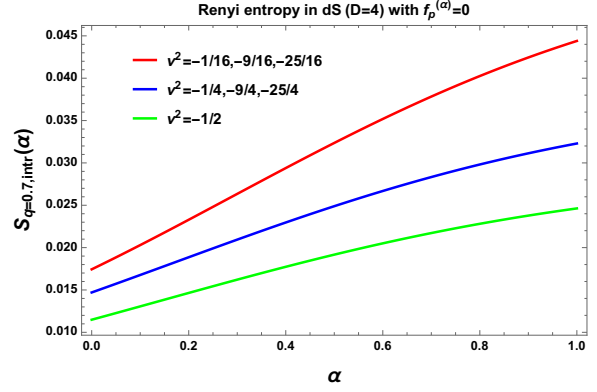
$$\lim_{q \rightarrow 1, |\nu| \gg 1, f_p \rightarrow 0} \mathcal{M}_{3, q}^{(\alpha)} = 0. \quad (3.219)$$

As a result in the large mass limiting situation with  $q \rightarrow 1$  the long range correlation can be

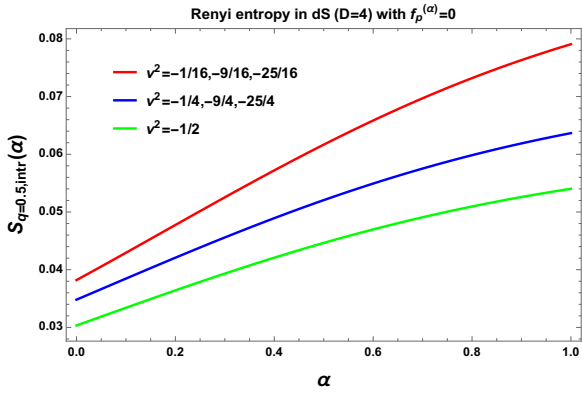




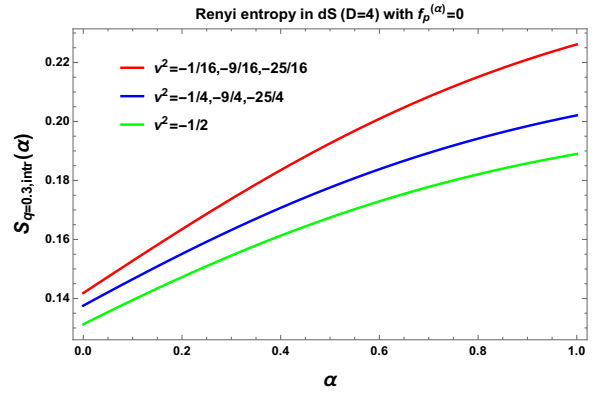
(a) For  $q = 0.9$  and  $\nu^2 < 0$ .



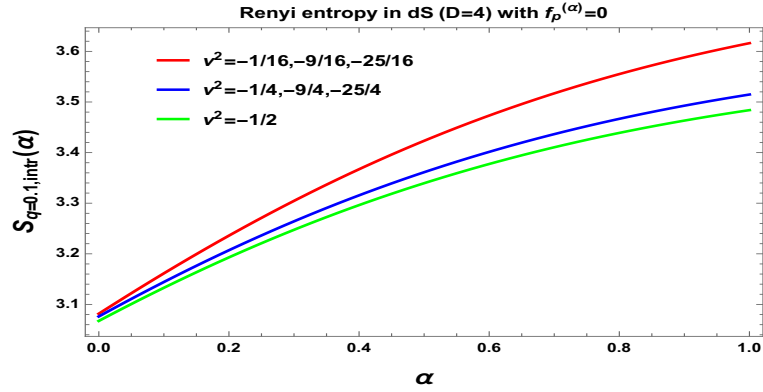
(b) For  $q = 0.7$  and  $\nu^2 < 0$ .



(c) For  $q = 0.5$  and  $\nu^2 < 0$ .



(d) For  $q = 0.3$  and  $\nu^2 < 0$ .

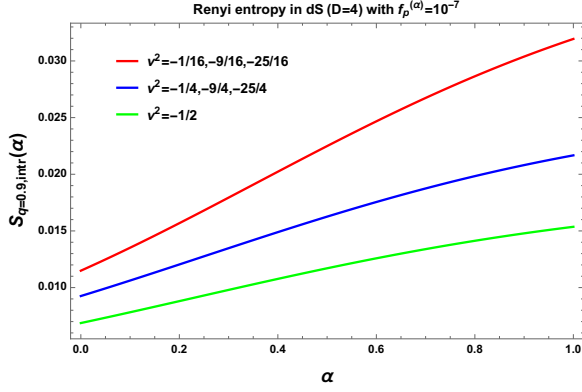


(e) For  $q = 0.1$  and  $\nu^2 < 0$ .

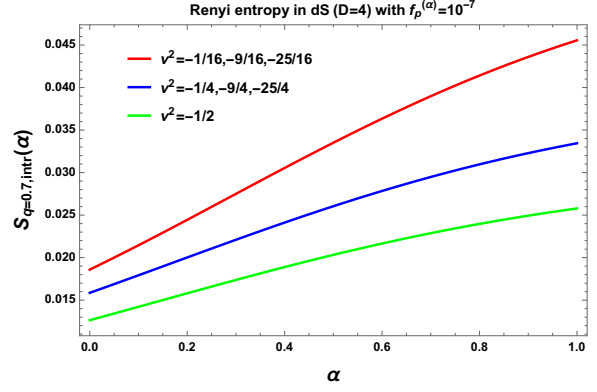
**Figure 24.** Rényi entropy  $S_{q, intr}(\alpha)$  vs parameter  $\alpha$  plot in 3 + 1 D de Sitter space in absence of axionic source ( $f_p^{(\alpha)} = 0$ ) for  $q = 0.1, q = 0.3, q = 0.5, q = 0.7, q = 0.9$  with ‘+’ branch of solution of  $|\gamma_p^{(\alpha)}|$  and  $|\Gamma_{p, n}^{(\alpha)}|$ .

expressed in terms of Rényi entropy as:

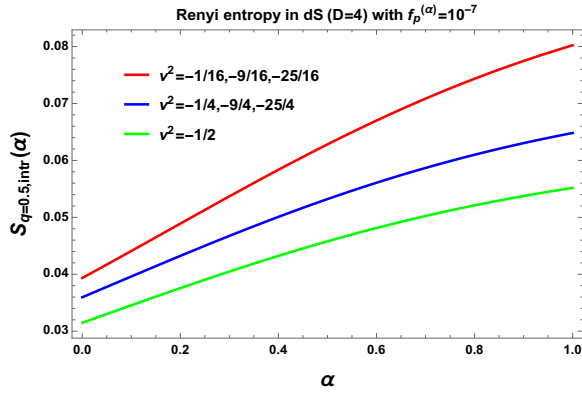
$$\begin{aligned}
\lim_{q \rightarrow 1, |\nu| \gg 1, f_p^{(\alpha)} \rightarrow 0} S_{q, intr}(\alpha) &\approx \frac{2\nu^4}{3} e^{-2\pi\nu} (1 + \tan \alpha)^2 \left\{ 1 - \frac{1}{\pi\nu} \ln(1 + \tan \alpha) \right\} \\
&\quad \times \left[ 1 + (1 + \tan \alpha)^2 \mathcal{O}(\nu^{-1}) \right] \\
&= S_{intr}(\alpha) = \lim_{|\nu| \gg 1, f_p^{(\alpha)} \rightarrow 0} \mathbf{c}_6(\alpha, \nu). \tag{3.220}
\end{aligned}$$



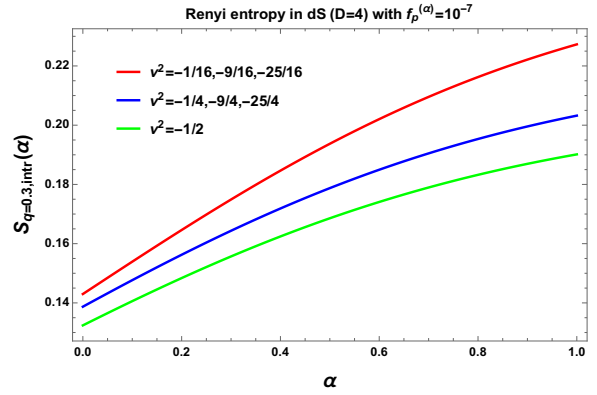
(a) For  $q = 0.9$  and  $\nu^2 < 0$ .



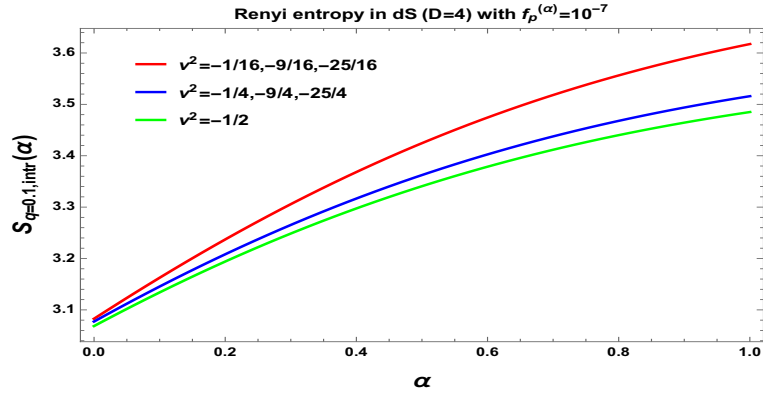
(b) For  $q = 0.7$  and  $\nu^2 < 0$ .



(c) For  $q = 0.5$  and  $\nu^2 < 0$ .



(d) For  $q = 0.3$  and  $\nu^2 < 0$ .



(e) For  $q = 0.1$  and  $\nu^2 < 0$ .

**Figure 25.** Rényi entropy  $S_{q, intr}(\alpha)$  vs parameter  $\alpha$  plot in 3 + 1 D de Sitter space in presence of axionic source ( $f_p^{(\alpha)} = 10^{-7}$ ) for  $q = 0.1, q = 0.3, q = 0.5, q = 0.7, q = 0.9$  with ‘+’ branch of solution of  $|\gamma_p^{(\alpha)}|$  and  $|\Gamma_{p, n}^{(\alpha)}|$ .

Further taking Bunch Davies vacuum ( $\alpha = 0$ ) we get [14]:

$$\lim_{q \rightarrow 1, |\nu| \gg 1, f_p \rightarrow 0} S_{q, intr}(0) \approx \frac{2\nu^4}{3} e^{-2\pi\nu} [1 + \mathcal{O}(\nu^{-1})] = S_{intr} \lim_{|\nu| \gg 1, f_p^{(\alpha)} \rightarrow 0} \mathbf{c}_6(0, \nu). \quad (3.221)$$

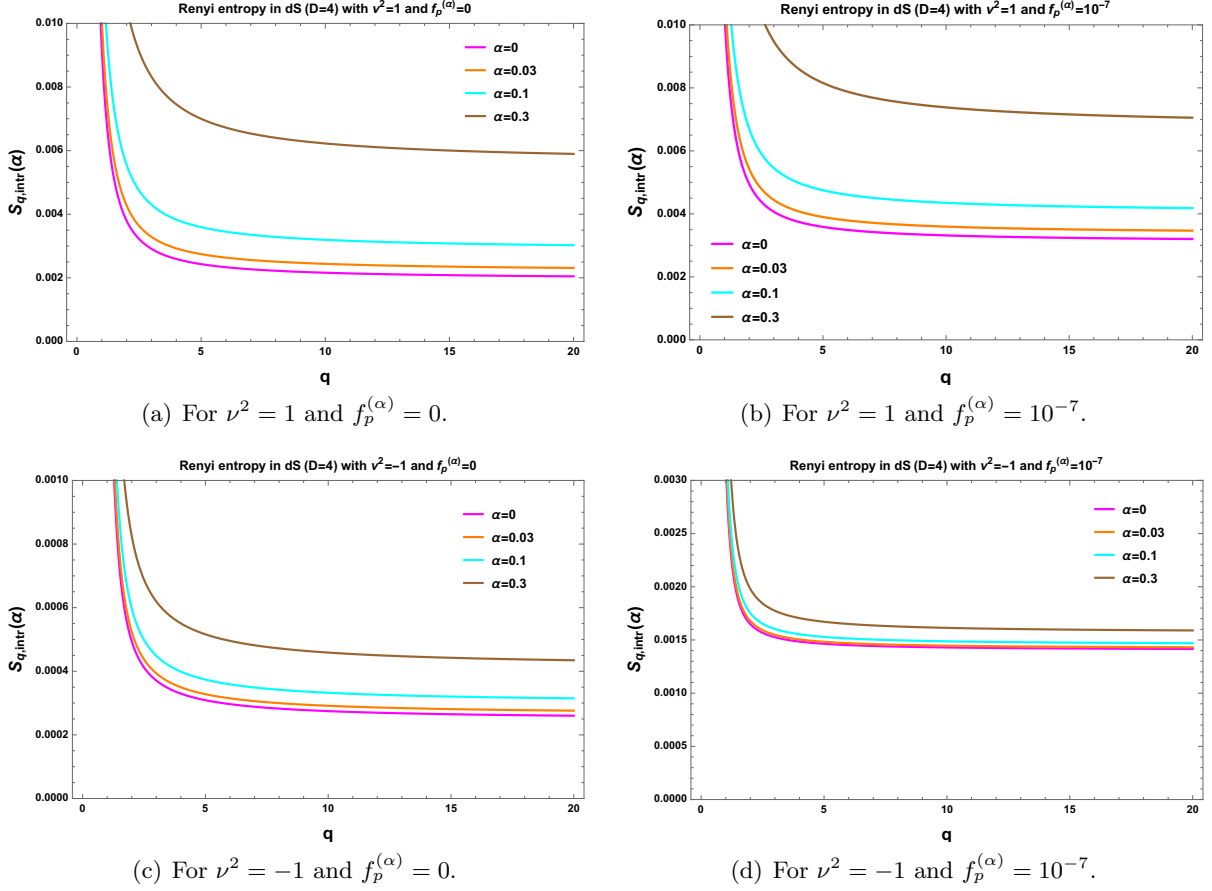


**Figure 26.** Rényi entropy  $S_{q,intr}(\alpha)$  vs  $q$  plot in 3 + 1 D de Sitter space in absence and presence of axionic source for  $\alpha = 0, \alpha = 0.03, \alpha = 0.1$  and  $\alpha = 0.3$  with ‘+’ branch of solution of  $|\gamma_p^{(\alpha)}|$  and  $|\Gamma_{p,n}^{(\alpha)}|$ .

Similarly using the results obtained from the second solution for  $|\gamma_p^{(\alpha)}|$ , within the range  $0 < x < 2\pi|\nu|$  with  $\nu^2 < 0$ , we take  $q \rightarrow 1$  limit. This gives the following simplified expression for the integral  $\mathcal{M}_{1,q}^{(\alpha)}$ :

$$\lim_{q \rightarrow 1} \mathcal{M}_{1,q}^{(\alpha)} = \frac{\nu^3}{3} \left[ \frac{2e^{2\pi\nu} (1 + \tan \alpha)^2 \{\nu + \ln(1 + \tan \alpha)\}}{e^{2\pi\nu} \tan^2 \alpha + 2e^{2\pi\nu} \tan \alpha + e^{2\pi\nu} - 1} - \frac{\ln(1 - e^{2\pi\nu} (1 + \tan \alpha)^2)}{\pi} \right], \quad (3.222)$$

$$\lim_{q \rightarrow 1, |\nu| \gg 1, f_p \rightarrow 0} \mathcal{M}_{3,q}^{(\alpha)} = 0. \quad (3.223)$$

using which for Bunch davies vacuum ( $\alpha = 0$ ) we get [14]:

$$\lim_{q \rightarrow 1} \mathcal{M}_{1,q}^{(0)} = \frac{\nu^3}{3} \left( \frac{2\nu e^{2\pi\nu}}{e^{2\pi\nu} - 1} - \frac{\ln(1 - e^{2\pi\nu})}{\pi} \right), \quad \lim_{q \rightarrow 1, |\nu| \gg 1, f_p \rightarrow 0} \mathcal{M}_{3,q}^{(0)} = 0. \quad (3.224)$$

As a result in the large mass limiting situation with  $q \rightarrow 1$  the long range correlation can be

Small mass parameter $\nu$ ( $\nu^2 \geq 0$ )	Axion mass $m_{axion}/H$	Parameter $q$	Normalized Rényi entropy $\frac{S_{q,\text{intr}}(0,\nu)}{S_{q,\text{intr}}(0,\frac{1}{2})}$ from BD vacuum (without source)	Parameter $\alpha$	Normalized Rényi entropy $\frac{S_{q,\text{intr}}(\alpha,\nu)}{S_{q,\text{intr}}(\alpha,\frac{1}{2})}$ from $\alpha$ vacuum (without source)
0, 1, 2, 3	$\frac{3}{2}, \frac{\sqrt{5}}{2}, \frac{\sqrt{7}}{2}i, \frac{\sqrt{27}}{2}i$	0.9, 0.1, $\infty$	0.85, 1, 0.8	$\Leftarrow \alpha = 0$ $\alpha = 0.03 \Rightarrow$ $\alpha = 0.1 \Rightarrow$ $\alpha = 0.3 \Rightarrow$	 0.95, 1.02, 0.85 1.25, 1.04, 1.05 2.1, 1.14, 2.4
$\frac{1}{2}, \frac{3}{2}, \frac{5}{2}, \frac{7}{2}$	$\sqrt{2}, 0, 2i, \sqrt{10}i$	0.9, 0.1, $\infty$	1, 1, 1	$\Leftarrow \alpha = 0$ $\alpha = 0.03 \Rightarrow$ $\alpha = 0.1 \Rightarrow$ $\alpha = 0.3 \Rightarrow$	 1, 1, 1 1, 1, 1 1, 1, 1
$\sqrt{2}$	$\frac{1}{2}$	0.9, 0.1, $\infty$	0.95, 1, 0.9	$\Leftarrow \alpha = 0$ $\alpha = 0.03 \Rightarrow$ $\alpha = 0.1 \Rightarrow$ $\alpha = 0.3 \Rightarrow$	 1.1, 1.01, 0.96 1.01, 1, 1.05 1.1, 1.01, 1.2

**Table 6.** Comparison between the normalized Rényi entropy obtained from BD vacuum and  $\alpha$  vacuum in absence of axion source ( $f_p^{(\alpha)} = 0$ ) for  $\nu^2 \geq 0$  and  $q = 0.9$ ,  $q = 0.1$  and  $q \rightarrow \infty$ .

expressed in terms of Rényi entropy as:

$$\begin{aligned}
\lim_{q \rightarrow 1, |\nu| \gg 1, f_p^{(\alpha)} \rightarrow 0} S_{q,\text{intr}}(\alpha) &\approx \frac{\nu^3}{3} \left[ \frac{2e^{2\pi\nu} (1 + \tan \alpha)^2 \{\nu + \ln(1 + \tan \alpha)\}}{e^{2\pi\nu} \tan^2 \alpha + 2e^{2\pi\nu} \tan \alpha + e^{2\pi\nu} - 1} - \frac{\ln(1 - e^{2\pi\nu} (1 + \tan \alpha)^2)}{\pi} \right] \\
&= S_{\text{intr}}(\alpha) = \lim_{|\nu| \gg 1, f_p^{(\alpha)} \rightarrow 0} \mathbf{c}_6(\alpha, \nu). \tag{3.225}
\end{aligned}$$

Further taking Bunch Davies vacuum ( $\alpha = 0$ ) we get [14]:

$$\lim_{q \rightarrow 1, |\nu| \gg 1, f_p^{(0)} \rightarrow 0} S_{q,\text{intr}}(0) \approx \frac{\nu^3}{3} \left( \frac{2\nu e^{2\pi\nu}}{e^{2\pi\nu} - 1} - \frac{\ln(1 - e^{2\pi\nu})}{\pi} \right) = S_{\text{intr}} = \lim_{|\nu| \gg 1, f_p^{(0)} \rightarrow 0} \mathbf{c}_6(0, \nu). \tag{3.226}$$

In fig. (16(a)), fig. (17(a)), fig. (18(a)), fig. (19(a)), fig. (20(a)), we have demonstrated the behaviour of Rényi entropy for  $q = 0.9$ ,  $q = 0.7$ ,  $q = 0.5$ ,  $q = 0.3$  and  $q = 0.1$  with respect to

Small mass parameter $\nu$ ( $\nu^2 \geq 0$ )	Axion mass $m_{axion}/H$	Parameter $q$	Normalized Rényi entropy $\frac{S_{q,\text{intr}}(0,\nu)}{S_{q,\text{intr}}(0,\frac{1}{2})}$ from BD vacuum (with source)	Parameter $\alpha$	Normalized Rényi entropy $\frac{S_{q,\text{intr}}(\alpha,\nu)}{S_{q,\text{intr}}(\alpha,\frac{1}{2})}$ from $\alpha$ vacuum (with source)
0, 1, 2, 3	$\frac{3}{2}, \frac{\sqrt{5}}{2}, \frac{\sqrt{7}}{2}i, \frac{\sqrt{27}}{2}i$	0.9, 0.1, $\infty$	0.2, 0.99, 0.8	$\leftarrow \alpha = 0$ $\alpha = 0.03 \Rightarrow$ $\alpha = 0.1 \Rightarrow$ $\alpha = 0.3 \Rightarrow$	0.4, 1.01, 0.9 0.78, 1.04, 1.05 12, 1.14, 1.9
$\frac{1}{2}, \frac{3}{2}, \frac{5}{2}, \frac{7}{2}$	$\sqrt{2}, 0, 2i, \sqrt{10}i$	0.9, 0.1, $\infty$	1, 1, 1	$\leftarrow \alpha = 0$ $\alpha = 0.03 \Rightarrow$ $\alpha = 0.1 \Rightarrow$ $\alpha = 0.3 \Rightarrow$	1, 1, 1 1, 1, 1 1, 1, 1
$\sqrt{2}$	$\frac{1}{2}$	0.9, 0.1, $\infty$	1.1, 1, 0.95	$\leftarrow \alpha = 0$ $\alpha = 0.03 \Rightarrow$ $\alpha = 0.1 \Rightarrow$ $\alpha = 0.3 \Rightarrow$	1, 1.005, 0.95 1, 1, 1.1 2, 1.02, 1.1

**Table 7.** Comparison between the normalized entanglement entropy obtained from BD vacuum and  $\alpha$  vacuum in presence of axion source ( $f_p^{(\alpha)} = 10^{-7}$ ) for  $\nu^2 \geq 0$  and  $q = 0.9$ ,  $q = 0.1$  and  $q \rightarrow \infty$ .

the mass parameter  $\nu^2$ . Here we did the computation in  $D = 4$  de Sitter space in absence ( $f_p^{(\alpha)} = 0$ ) of axionic source. Similarly in fig. (16(b)), fig. (17(b)), fig. (18(b)), fig. (19(b)), fig. (20(b)), we have demonstrated the behaviour of Rényi entropy for  $q = 0.9$ ,  $q = 0.7$ ,  $q = 0.5$ ,  $q = 0.3$  and  $q = 0.1$  with respect to the mass parameter  $\nu^2$ . Additionally, the largest eigenvalue of the density matrix ( $q \rightarrow \infty$ ) in absence and presence of axionic source are plotted in fig. (21(a)) and fig. (21(b)). Here we did the computation in  $D = 4$  de Sitter space in presence ( $f_p^{(\alpha)} = 10^{-7}$ ) of axionic source. In this both the cases we also have normalized the Rényi entropy with the result obtained from conformal mass parameter  $\nu = 1/2$  in presence of  $\alpha$  vacuum. For a given value of the parameter  $q$  we have shown the plots for  $\alpha = 0$  (red),  $\alpha = 0.03$  (blue),  $\alpha = 0.1$  (green) and  $\alpha = 0.3$  (violet) in both the cases. Here we observe the following features:

- For  $q = 0.9$  case in absence of the axionic source (see fig. (16(a))) in the large mass parameter range ( $\nu^2 < 0$ ) normalized Rényi entropy asymptotically approaches towards

Large mass parameter $\nu$ ( $\nu^2 < 0$ )	Axion mass $m_{axion}/H$	Parameter $q$	Normalized Rényi entropy $\frac{S_{q,\text{intr}}(0,\nu)}{S_{q,\text{intr}}(0,\frac{1}{2})}$ from BD vacuum (without source)	Parameter $\alpha$	Normalized Rényi entropy $\frac{S_{q,\text{intr}}(\alpha,\nu)}{S_{q,\text{intr}}(\alpha,\frac{1}{2})}$ from $\alpha$ vacuum (without source)
$\frac{i}{2}$	$\sqrt{\frac{5}{2}}$	0.9, 0.1, $\infty$	0.64, 0.95, 0.30	$\Leftarrow \alpha = 0$ $\alpha = 0.03 \Rightarrow$ $\alpha = 0.1 \Rightarrow$ $\alpha = 0.3 \Rightarrow$	0.65, 1.004, 0.31 0.85, 1.02, 0.35 1.15, 1.08, 0.85
$i$	$\frac{\sqrt{13}}{2}$	0.9, 0.1, $\infty$	0.25, 0.98, 0.05	$\Leftarrow \alpha = 0$ $\alpha = 0.03 \Rightarrow$ $\alpha = 0.1 \Rightarrow$ $\alpha = 0.3 \Rightarrow$	0.35, 0.99, 0.10 0.25, 1.005, 0.10 0.45, 1.065, 0.20
$\sqrt{2}i$	$\frac{\sqrt{17}}{2}$	0.9, 0.1, $\infty$	0.05, 0.97, 0.04	$\Leftarrow \alpha = 0$ $\alpha = 0.03 \Rightarrow$ $\alpha = 0.1 \Rightarrow$ $\alpha = 0.3 \Rightarrow$	0.10, 0.975, 0.02 0.02, 0.99, 0.05 0.15, 0.965, 0.04

**Table 8.** Comparison between the normalized Rényi entropy obtained from BD vacuum and  $\alpha$  vacuum in absence of axion source ( $f_p^{(\alpha)} = 0$ ) for  $\nu^2 < 0$ .

zero value. On the other hand in the small mass parameter range ( $\nu^2 > 0$ ) it show oscillations in aperiodic fashion. Here the amplitude of the oscillation is larger for  $\alpha = 0.3$  compared to the other values of  $\alpha$ . Also it is important to note that, at  $\nu = 1/2$ ,  $\nu = 3/2$  and  $\nu = 5/2$  we get extremas for the oscillation. Further in presence of the axionic source (see fig. (16(b))) in the large mass parameter range ( $\nu^2 < 0$ ) normalized Rényi entropy rapidly approaches to zero value for all values of the parameter  $\alpha$  considered in this paper. Also in the small mass parameter range ( $\nu^2 > 0$ ) the amplitude of the oscillation is significantly large for  $\alpha = 0.3$ . Also it is observed that for  $\nu^2 > 0$  the long range correlation is larger in presence of the axionic source. But for  $\nu^2 < 0$  the long range correlation is rapidly decaying with  $f_p^{(\alpha)} = 10^{-7}$  and asymptotically decaying with  $f_p^{(\alpha)} = 0$  for all values of  $\alpha$ .

- For other values of the parameter  $q$  i.e.  $q = 0.7$ ,  $q = 0.5$ ,  $q = 0.3$  and  $q = 0.1$  cases in absence of the axionic source (see fig. (17(a)), fig. (18(a)), fig. (19(a)) and fig. (20(a)))

Large mass parameter $\nu$ ( $\nu^2 < 0$ )	Axion mass $m_{axion}/H$	Parameter $q$	Normalized Rényi entropy $\frac{S_{q,intr}(0,\nu)}{S_{q,intr}(0,\frac{1}{2})}$ from BD vacuum (with source)	Parameter $\alpha$	Normalized Rényi entropy $\frac{S_{q,intr}(\alpha,\nu)}{S_{q,intr}(\alpha,\frac{1}{2})}$ from $\alpha$ vacuum (with source)
$\frac{i}{2}$	$\sqrt{\frac{5}{2}}$	0.9, 0.1, $\infty$	$\times, 0.96, 0.55$	$\Leftarrow \alpha = 0$ $\alpha = 0.03 \Rightarrow$ $\alpha = 0.1 \Rightarrow$ $\alpha = 0.3 \Rightarrow$	$\times, 1.004, 0.45$ $\times, 1.02, 0.65$ $2.00, 1.08, 0.87$
$i$	$\frac{\sqrt{13}}{2}$	0.9, 0.1, $\infty$	$\times, 0.98, 0.32$	$\Leftarrow \alpha = 0$ $\alpha = 0.03 \Rightarrow$ $\alpha = 0.1 \Rightarrow$ $\alpha = 0.3 \Rightarrow$	$\times, 0.99, 0.34$ $\times, 1.005, 0.35$ $\times, 1.065, 0.45$
$\sqrt{2}i$	$\frac{\sqrt{17}}{2}$	0.9, 0.1, $\infty$	$\times, 0.97, 0.31$	$\Leftarrow \alpha = 0$ $\alpha = 0.03 \Rightarrow$ $\alpha = 0.1 \Rightarrow$ $\alpha = 0.3 \Rightarrow$	$\times, 0.975, 0.32$ $\times, 0.99, 0.305$ $\times, 0.965, 0.30$

**Table 9.** Comparison between the normalized Rényi entropy obtained from BD vacuum and  $\alpha$  vacuum in presence of axion source ( $f_p^{(\alpha)} = 10^{-7}$ ) for  $\nu^2 < 0$ .

in the large mass parameter range ( $\nu^2 < 0$ ) normalized Rényi entropy asymptotically approaches towards zero value. On the other hand in the small mass parameter range ( $\nu^2 > 0$ ) it show oscillations in aperiodic fashion. Here the amplitude of the oscillation is larger for  $\alpha = 0.3$  compared to the other values of  $\alpha$ . Also it is important to note that, at  $\nu = 1/2$ ,  $\nu = 3/2$  and  $\nu = 5/2$  we get extremas for the oscillation. Further in presence of the axionic source (see fig. (17(b)), fig. (18(b)), fig. (19(b)) and fig. (20(b))) one can observe the exact behaviour as observed without any source contribution. It also implies that for all  $q < 0.9$  the normalized Rényi entropy is insensitive to the source contribution.

- For  $q \rightarrow \infty$  case in absence (see fig. (21(a))) and presence of the axionic source (see fig. (21(b))) variation of normalized Rényi entropy with  $\nu^2$  for all values of the parameter  $\alpha$  is similar. It is important to note that the amplitudes of the oscillations in  $\nu^2 > 0$  region and the saturation value in  $\nu^2 < 0$  region is larger in presence of axionic source.

Next, in fig. (22(a)), fig. (22(b)), fig. (22(c)), fig. (22(d)), fig. (22(e)) and fig. (26(b)), fig. (23(b)), fig. (23(c)), fig. (23(d)), fig. (23(e)), we have depicted the behaviour of Rényi entropy with respect to the parameter  $\alpha$  in absence ( $f_p^{(\alpha)} = 0$ ) and presence ( $f_p^{(\alpha)} = 10^{-7}$ ) of axionic source for the mass parameter  $\nu^2 > 0$ . In all figures it is observed that a crossover takes place for  $\nu^2 = 1/4, 9/4, 25/4$  (green),  $\nu^2 = 1/16, 9/16, 25/16$  (blue) and  $\nu^2 = 0$  (red) with small values of the parameter  $\alpha$ . We also observe that for  $\nu^2 = 1/4, 9/4, 25/4$  (green) Rényi entropy decreases with increasing value of the parameter  $\alpha$ . On the other hand, for  $\nu^2 = 1/16, 9/16, 25/16$  (blue) and  $\nu^2 = 0$  (red) Rényi entropy increases with increasing value of the parameter  $\alpha$ . Additionally, in presence of axionic source the Rényi entropy is slightly larger compared to the result obtained in absence of source contribution. In fig. (22(a)), fig. (22(b)), fig. (22(c)), fig. (22(d)), fig. (22(e)) and fig. (26(b)), fig. (23(b)), fig. (23(c)), fig. (23(d)), fig. (23(e)), it is observed that no crossover takes place for  $\nu^2 = -1/2$  (green),  $\nu^2 = -1/4, -9/4, -25/4$  (blue) and  $\nu^2 = -1/16, -9/16, -25/16$  (red) with all values of the parameter  $\alpha$ . Also it is important to note that, for all values of  $\nu^2 < 0$  Rényi entropy increases with increasing value of the parameter  $\alpha$ . Further in fig. (26(a)), fig. (26(b)), fig. (26(c)), fig. (26(d)), we have shown the variation of Rényi entropy with respect to the parameter  $q$  in absence and presence of axionic source for  $\alpha = 0$  (purple),  $\alpha = 0.03$  (orange),  $\alpha = 0.1$  (cyan) and  $\alpha = 0.3$  (brown) respectively. It is observed that for small values of the parameter  $q$  the value of the Rényi entropy for a given value of  $\alpha$  always increase. On the other hand for small values of the parameter  $q$  Rényi entropy saturates to a finite small value.

In table (6) and table (7), we have mentioned the numerical estimate of the normalized Rényi entropy in absence ( $f_p^{(\alpha)} = 0$ ) and presence ( $f_p^{(\alpha)} = 10^{-7}$ ) of axionic source contribution for Bunch Davies vacuum and  $\alpha$  vacuum with small mass parameter ( $\nu^2 \geq 0$ ). On the other hand, in table (8) and table (9), we have mentioned the numerical estimate of the normalized Rényi entropy in absence ( $f_p^{(\alpha)} = 0$ ) and presence ( $f_p^{(\alpha)} = 10^{-7}$ ) of axionic source contribution for Bunch Davies vacuum and  $\alpha$  vacuum with large mass parameter ( $\nu^2 < 0$ ). Here numerical results from both  $\nu^2 \geq 0$  and  $\nu^2 < 0$  region suggests that the quantum entanglement is significantly larger in presence of axionic source, compared to the result obtained in absence of axionic source.

## 4 Summary

To summarize, in this paper, we have addressed the following issues:

- First we have presented the computation of entanglement entropy in de Sitter space in presence of axion with a linear source contribution in the effective potential as originating from **Type IIB** string theory. To demonstrate this we have derived the axion wave function in an open chart.
- Next using the  $\alpha$  vacuum state we have expressed the wave function in terms of creation and annihilation operators. Further applying Bogoliubov transformation on  $\alpha$  vacuum state we construct the expression for reduced density matrix.
- Further, using reduced density matrix we have derived the entanglement entropy, which is consistent with ref. [10] if we set  $\alpha = 0$ . In the  $\nu^2 < 0$  range we have derived analytical result for the entanglement entropy. Finally, we have used numerical approximations to estimate entanglement entropy with any value of  $\nu^2$ .



- We have also computed the Rényi entropy in presence of axion source. In absence of the source this result is consistent with ref. [10] in  $q \rightarrow 1$  limit. Here in  $\nu^2 < 0$  region we have provided the analytical expression for the Rényi entropy. We have also used numerical techniques to study the behaviour of Rényi entropy and largest eigenvalue of the density matrix with any value of  $\nu^2$ .
- Our result provides the necessary condition to generate non vanishing entanglement in primordial cosmology due to axion.

The future directions of this paper are appended below:

- Using the derived expression for density matrix for generalized  $\alpha$  vacua one can further compute any  $n$  point long range quantum correlation to study the implications in the context of primordial cosmology. It is expected that this result will surely helps to understand the connection between the Bell's inequality violation, quantum entanglement and primordial non-Gaussianity.
- Till now we have studied the necessary condition for generating non zero entanglement entropy in primordial cosmology. In this connection one can further compute quantum discord, , entanglement negativity etc. which play significant role to quantify long range quantum correlations without necessarily involving quantum entanglement.

## Acknowledgments

SC would like to thank Quantum Gravity and Unified Theory and Theoretical Cosmology Group, Max Planck Institute for Gravitational Physics, Albert Einstein Institute and Inter University Center for Astronomy and Astrophysics, Pune for providing the Post-Doctoral Research Fellowship. SC take this opportunity to thank sincerely to Shiraz Minwalla, Gautam Mandal and Varun Sahni for their constant support and inspiration. SC also thank the organizers of Indian String Meet 2016, Advanced String School 2017 and ST<sup>4</sup> 2017 for providing the local hospitality during the work. SC also thank IOP, CMI, SINP and IACS for providing the academic visit during the work. SP acknowledges the J. C. Bose National Fellowship for support of his research. Last but not the least, We would all like to acknowledge our debt to the people of India for their generous and steady support for research in natural sciences, especially for theoretical high energy physics, string theory and cosmology.

## References

- [1] L. Amico, R. Fazio, A. Osterloh and V. Vedral, **Entanglement in many-body systems**, *Rev. Mod. Phys.* **80** (2008) 517 [quant-ph/0703044 [QUANT-PH]].
- [2] R. Horodecki, P. Horodecki, M. Horodecki and K. Horodecki, **Quantum entanglement**, *Rev. Mod. Phys.* **81** (2009) 865 [quant-ph/0702225].
- [3] N. Laflorencie, **Quantum entanglement in condensed matter systems**, *Phys. Rept.* **646** (2016) 1 [arXiv:1512.03388 [cond-mat.str-el]].
- [4] E. Martin-Martinez and N. C. Menicucci, **Cosmological quantum entanglement**, *Class. Quant. Grav.* **29** (2012) 224003 [arXiv:1204.4918 [gr-qc]].
- [5] Y. Nambu, **Entanglement of Quantum Fluctuations in the Inflationary Universe**, *Phys. Rev. D* **78** (2008) 044023 [arXiv:0805.1471 [gr-qc]].

- [6] D. Campo and R. Parentani, [Quantum correlations in inflationary spectra and violation of bell inequalities](#), *Braz. J. Phys.* **35** (2005) 1074 [[astro-ph/0510445](#)].
- [7] Y. Nambu and Y. Ohsumi, [Classical and Quantum Correlations of Scalar Field in the Inflationary Universe](#), *Phys. Rev. D* **84** (2011) 044028 [[arXiv:1105.5212 \[gr-qc\]](#)].
- [8] G. L. Ver Steeg and N. C. Menicucci, [Entangling power of an expanding universe](#), *Phys. Rev. D* **79** (2009) 044027 [[arXiv:0711.3066 \[quant-ph\]](#)].
- [9] D. Mazur and J. S. Heyl, [Characterizing entanglement entropy produced by nonlinear scalar interactions during inflation](#), *Phys. Rev. D* **80** (2009) 023523 [[arXiv:0810.0521 \[gr-qc\]](#)].
- [10] J. Maldacena and G. L. Pimentel, [Entanglement entropy in de Sitter space](#), *JHEP* **1302** (2013) 038 [[arXiv:1210.7244 \[hep-th\]](#)].
- [11] J. Maldacena, [A model with cosmological Bell inequalities](#), *Fortsch. Phys.* **64** (2016) 10 [[arXiv:1508.01082 \[hep-th\]](#)].
- [12] S. Choudhury, S. Panda and R. Singh, [Bell violation in the Sky](#), *Eur. Phys. J. C* **77** (2017) no.2, 60 [[arXiv:1607.00237 \[hep-th\]](#)].
- [13] S. Choudhury, S. Panda and R. Singh, [Bell violation in primordial cosmology](#), *Universe* **3** (2017) no.1, 13 [[arXiv:1612.09445 \[hep-th\]](#)].
- [14] S. Choudhury and S. Panda, [Entangled de Sitter from Stringy Axionic Bell pair I: An analysis using Bunch Davies vacuum](#), [arXiv:1708.02265 \[hep-th\]](#).
- [15] S. Kanno, J. Murugan, J. P. Shock and J. Soda, [Entanglement entropy of  \$\alpha\$ -vacua in de Sitter space](#), *JHEP* **1407** (2014) 072 [[arXiv:1404.6815 \[hep-th\]](#)].
- [16] S. Kanno and J. Soda, [Infinite violation of Bell inequalities in inflation](#), [arXiv:1705.06199 \[hep-th\]](#).
- [17] S. Kanno, J. P. Shock and J. Soda, [Quantum discord in de Sitter space](#), *Phys. Rev. D* **94** (2016) no.12, 125014 [[arXiv:1608.02853 \[hep-th\]](#)].
- [18] S. Kanno, J. P. Shock and J. Soda, [Entanglement negativity in the multiverse](#), *JCAP* **1503** (2015) no.03, 015 [[arXiv:1412.2838 \[hep-th\]](#)].
- [19] S. Kanno, [Impact of quantum entanglement on spectrum of cosmological fluctuations](#), *JCAP* **1407** (2014) 029 [[arXiv:1405.7793 \[hep-th\]](#)].
- [20] W. Fischler, S. Kundu and J. F. Pedraza, [Entanglement and out-of-equilibrium dynamics in holographic models of de Sitter QFTs](#), *JHEP* **1407** (2014) 021 [[arXiv:1311.5519 \[hep-th\]](#)].
- [21] W. Fischler, P. H. Nguyen, J. F. Pedraza and W. Tangarife, [Fluctuation and dissipation in de Sitter space](#), *JHEP* **1408** (2014) 028 [[arXiv:1404.0347 \[hep-th\]](#)].
- [22] S. R. Coleman and F. De Luccia, [Gravitational Effects on and of Vacuum Decay](#), *Phys. Rev. D* **21** (1980) 3305.
- [23] J. S. Bell, [On the Einstein-Podolsky-Rosen paradox](#), *Physics* **1** (1964) 195.
- [24] M. B. Fröb, J. Garriga, S. Kanno, M. Sasaki, J. Soda, T. Tanaka and A. Vilenkin, [Schwinger effect in de Sitter space](#), *JCAP* **1404** (2014) 009 [[arXiv:1401.4137 \[hep-th\]](#)].
- [25] W. Fischler, P. H. Nguyen, J. F. Pedraza and W. Tangarife, [Holographic Schwinger effect in de Sitter space](#), *Phys. Rev. D* **91** (2015) no.8, 086015 [[arXiv:1411.1787 \[hep-th\]](#)].
- [26] S. Ryu and T. Takayanagi, [Holographic derivation of entanglement entropy from AdS/CFT](#), *Phys. Rev. Lett.* **96** (2006) 181602 [[hep-th/0603001](#)].
- [27] S. Ryu and T. Takayanagi, [Aspects of Holographic Entanglement Entropy](#), *JHEP* **0608** (2006) 045 [[hep-th/0605073](#)].
- [28] T. Nishioka, S. Ryu and T. Takayanagi, [Holographic Entanglement Entropy: An Overview](#), *J. Phys. A* **42** (2009) 504008 [[arXiv:0905.0932 \[hep-th\]](#)].

- [29] M. Rangamani and T. Takayanagi, **Holographic Entanglement Entropy**, Lect. Notes Phys. **931** (2017) [arXiv:1609.01287 [hep-th]].
- [30] V. E. Hubeny, M. Rangamani and T. Takayanagi, **A Covariant holographic entanglement entropy proposal**, JHEP **0707** (2007) 062 [arXiv:0705.0016 [hep-th]].
- [31] X. Dong, **Holographic Entanglement Entropy for General Higher Derivative Gravity**, JHEP **1401** (2014) 044 [arXiv:1310.5713 [hep-th]].
- [32] J. Camps, **Generalized entropy and higher derivative Gravity**, JHEP **1403** (2014) 070 [arXiv:1310.6659 [hep-th]].
- [33] S. Banerjee, A. Bhattacharyya, A. Kaviraj, K. Sen and A. Sinha, **Constraining gravity using entanglement in AdS/CFT**, JHEP **1405** (2014) 029 [arXiv:1401.5089 [hep-th]].
- [34] A. Bhattacharyya and M. Sharma, **On entanglement entropy functionals in higher derivative gravity theories**, JHEP **1410** (2014) 130 [arXiv:1405.3511 [hep-th]].
- [35] S. S. Pal and S. Panda, **Entanglement temperature with GaussBonnet term**, Nucl. Phys. B **898** (2015) 401 [arXiv:1507.06488 [hep-th]].
- [36] E. Mottola, **Particle Creation in de Sitter Space**, Phys. Rev. D **31** (1985) 754.
- [37] B. Allen, **Vacuum States in de Sitter Space**, Phys. Rev. D **32** (1985) 3136.
- [38] K. Goldstein and D. A. Lowe, **A Note on alpha vacua and interacting field theory in de Sitter space**, Nucl. Phys. B **669** (2003) 325 [hep-th/0302050].
- [39] J. de Boer, V. Jejjala and D. Minic, **Alpha-states in de Sitter space**, Phys. Rev. D **71** (2005) 044013 [hep-th/0406217].
- [40] R. Brunetti, K. Fredenhagen and S. Hollands, **A Remark on alpha vacua for quantum field theories on de Sitter space**, JHEP **0505** (2005) 063 [hep-th/0503022].
- [41] B. S. Kay and R. M. Wald, **Theorems on the Uniqueness and Thermal Properties of Stationary, Nonsingular, Quasifree States on Space-Times with a Bifurcate Killing Horizon**, Phys. Rept. **207** (1991) 49.
- [42] R. M. Wald, **Quantum field theory in curved space-time and black hole thermodynamics**, Chicago, USA: Univ. Pr. (1994) 205 p.
- [43] L. McAllister, E. Silverstein and A. Westphal, **Gravity Waves and Linear Inflation from Axion Monodromy**, Phys. Rev. D **82** (2010) 046003 [arXiv:0808.0706 [hep-th]].
- [44] E. Silverstein and A. Westphal, **Monodromy in the CMB: Gravity Waves and String Inflation**, Phys. Rev. D **78** (2008) 106003 [arXiv:0803.3085 [hep-th]].
- [45] L. McAllister, E. Silverstein, A. Westphal and T. Wrase, **The Powers of Monodromy**, JHEP **1409** (2014) 123 [arXiv:1405.3652 [hep-th]].
- [46] S. Panda, Y. Sumitomo and S. P. Trivedi, **Axions as Quintessence in String Theory**, Phys. Rev. D **83** (2011) 083506 [arXiv:1011.5877 [hep-th]].
- [47] S. Choudhury and S. Panda, **COSMOS- $e'$ -GTachyon from string theory**, Eur. Phys. J. C **76** (2016) no.5, 278 [arXiv:1511.05734 [hep-th]] , S. Choudhury, **COSMOS- $e'$ - soft Higgsotic attractors**, Eur. Phys. J. C **77** (2017) no.7, 469 [arXiv:1703.01750 [hep-th]] , S. Choudhury and S. Pal, **Primordial non-Gaussian features from DBI Galileon inflation**, Eur. Phys. J. C **75** (2015) no.6, 241 [arXiv:1210.4478 [hep-th]] , S. Choudhury and S. Pal, **DBI Galileon inflation in background SUGRA**, Nucl. Phys. B **874** (2013) 85 [arXiv:1208.4433 [hep-th]] , S. Choudhury and S. Pal, **Fourth level MSSM inflation from new flat directions**, JCAP **1204** (2012) 018 [arXiv:1111.3441 [hep-ph]] , S. Choudhury and S. Pal, **Brane inflation in background supergravity**, Phys. Rev. D **85** (2012) 043529 [arXiv:1102.4206 [hep-th]] , S. Choudhury, **Can Effective Field Theory of inflation generate large tensor-to-scalar ratio within RandallSundrum single braneworld?**, Nucl. Phys. B **894** (2015) 29 [arXiv:1406.7618 [hep-th]] , S. Choudhury, B. K. Pal, B. Basu and P. Bandyopadhyay, **Quantum Gravity Effect in Torsion Driven Inflation and CP violation**, JHEP **1510** (2015) 194 [arXiv:1409.6036 [hep-th]] , S. Choudhury, **Reconstructing inflationary paradigm within Effective**

- Field Theory framework, *Phys. Dark Univ.* **11** (2016) 16 [arXiv:1508.00269 [astro-ph.CO]] , S. Choudhury and A. Mazumdar, *An accurate bound on tensor-to-scalar ratio and the scale of inflation*, *Nucl. Phys. B* **882** (2014) 386 [arXiv:1306.4496 [hep-ph]] , S. Choudhury and A. Mazumdar, *Primordial blackholes and gravitational waves for an inflection-point model of inflation*, *Phys. Lett. B* **733** (2014) 270 [arXiv:1307.5119 [astro-ph.CO]] , S. Choudhury and A. Mazumdar, *Reconstructing inflationary potential from BICEP2 and running of tensor modes*, arXiv:1403.5549 [hep-th] , S. Choudhury, A. Mazumdar and E. Pukartas, *Constraining  $\mathcal{N} = 1$  supergravity inflationary framework with non-minimal Kahler operators*, *JHEP* **1404** (2014) 077 [arXiv:1402.1227 [hep-th]] , S. Choudhury, *Constraining  $\mathcal{N} = 1$  supergravity inflation with non-minimal Kahler operators using  $\delta N$  formalism*, *JHEP* **1404** (2014) 105 [arXiv:1402.1251 [hep-th]] , S. Choudhury, A. Mazumdar and S. Pal, *Low & High scale MSSM inflation, gravitational waves and constraints from Planck*, *JCAP* **1307** (2013) 041 [arXiv:1305.6398 [hep-ph]].
- [48] J. Maharana, S. Mukherji and S. Panda, *Notes on axion, inflation and graceful exit in stringy cosmology*, *Mod. Phys. Lett. A* **12** (1997) 447 [hep-th/9701115] , A. Mazumdar, S. Panda and A. Perez-Lorenzana, *Assisted inflation via tachyon condensation*, *Nucl. Phys. B* **614** (2001) 101 [hep-ph/0107058] , D. Choudhury, D. Ghoshal, D. P. Jatkar and S. Panda, *Hybrid inflation and brane - anti-brane system*, *JCAP* **0307** (2003) 009 [hep-th/0305104] , D. Choudhury, D. Ghoshal, D. P. Jatkar and S. Panda, *On the cosmological relevance of the tachyon*, *Phys. Lett. B* **544** (2002) 231 [hep-th/0204204] , P. Chingangbam, S. Panda and A. Deshamukhya, *Non-minimally coupled tachyonic inflation in warped string background*, *JHEP* **0502** (2005) 052 [hep-th/0411210] , A. Deshamukhya and S. Panda, *Warm tachyonic inflation in warped background*, *Int. J. Mod. Phys. D* **18** (2009) 2093 [arXiv:0901.0471 [hep-th]] , P. Vargas Moniz, S. Panda and J. Ward, *Higher order corrections to Heterotic M-theory inflation*, *Class. Quant. Grav.* **26** (2009) 245003 [arXiv:0907.0711 [astro-ph.CO]] , A. Ali, A. Deshamukhya, S. Panda and M. Sami, *Inflation with improved D3-brane potential and the fine tunings associated with the model*, *Eur. Phys. J. C* **71** (2011) 1672 [arXiv:1010.1407 [hep-th]] , A. Bhattacharjee, A. Deshamukhya and S. Panda, *A note on low energy effective theory of chromo-natural inflation in the light of BICEP2 results*, *Mod. Phys. Lett. A* **30** (2015) no.11, 1550040 [arXiv:1406.5858 [astro-ph.CO]] , S. Panda, M. Sami and S. Tsujikawa, *Inflation and dark energy arising from geometrical tachyons*, *Phys. Rev. D* **73** (2006) 023515 [hep-th/0510112] , S. Panda, M. Sami, S. Tsujikawa and J. Ward, *Inflation from D3-brane motion in the background of D5-branes*, *Phys. Rev. D* **73** (2006) 083512 [hep-th/0601037] , S. Panda, M. Sami and S. Tsujikawa, *Prospects of inflation in delicate D-brane cosmology*, *Phys. Rev. D* **76** (2007) 103512 [arXiv:0707.2848 [hep-th]].
- [49] D. Baumann, *TASI lectures on Inflation 2009*, arXiv:0907.5424 [hep-th], D. Baumann, A. Dymarsky, I. R. Klebanov and L. McAllister, *Towards an Explicit Model of D-brane Inflation*, *JCAP* **0801** (2008) 024 [arXiv:0706.0360 [hep-th]], D. Baumann and L. McAllister, *Advances in Inflation in String Theory*, *Ann. Rev. Nucl. Part. Sci.* **59** (2009) 67 [arXiv:0901.0265 [hep-th]], V. Assassi, D. Baumann and D. Green, *Symmetries and Loops in Inflation*, *JHEP* **1302** (2013) 151 [arXiv:1210.7792 [hep-th]], D. Baumann and L. McAllister, *Inflation and String Theory*, arXiv:1404.2601 [hep-th], D. Baumann, A. Dymarsky, S. Kachru, I. R. Klebanov and L. McAllister, *Holographic Systematics of D-brane Inflation*, *JHEP* **0903** (2009) 093 [arXiv:0808.2811 [hep-th]], H. V. Peiris, D. Baumann, B. Friedman and A. Cooray, *Phenomenology of D-Brane Inflation with General Speed of Sound*, *Phys. Rev. D* **76** (2007) 103517 [arXiv:0706.1240 [astro-ph]]. . . .
- [50] N. Agarwal, R. Bean, L. McAllister and G. Xu, *Universality in D-brane Inflation*, *JCAP* **1109** (2011) 002 [arXiv:1103.2775 [astro-ph.CO]], R. Flauger, L. McAllister, E. Pajer, A. Westphal and G. Xu, *Oscillations in the CMB from Axion Monodromy Inflation*, *JCAP* **1006** (2010) 009 [arXiv:0907.2916 [hep-th]].
- [51] S. Kanno, *A note on initial state entanglement in inflationary cosmology*, *EPL* **111** (2015) no.6, 60007 [arXiv:1507.04877 [hep-th]].
- [52] F. V. Dimitrakopoulos, L. Kabir, B. Mosk, M. Parikh and J. P. van der Schaar, *Vacua and correlators in hyperbolic de Sitter space*, *JHEP* **1506** (2015) 095 [arXiv:1502.00113 [hep-th]].
- [53] A. Aguirre, C. P. Burgess, A. Friedland and D. Nolte, *Astrophysical constraints on modifying gravity at large distances*, *Class. Quant. Grav.* **18** (2001) R223 [hep-ph/0105083].
- [54] C. G. Callan, Jr. and F. Wilczek, *On geometric entropy*, *Phys. Lett. B* **333** (1994) 55 [hep-th/9401072].
- [55] P. Svrcek and E. Witten, *Axions In String Theory*, *JHEP* **0606** (2006) 051 [hep-th/0605206].

- [56] M. Sasaki, T. Tanaka and K. Yamamoto, [Euclidean vacuum mode functions for a scalar field on open de Sitter space](#), *Phys. Rev. D* **51** (1995) 2979 [gr-qc/9412025].